Deep-water sedimentary systems and processes on the continental margin offshore NW Africa

Dissertation

zur Erlangung des Doktorgrades

der Mathematisch-Naturwissenschaftlichen Fakultät

der Christian-Albrechts-Universität zu Kiel

vorgelegt von

Wei Li

Kiel, 2017

Erster Gutachter:…………………………………….............Prof. Dr. Sebastian Krastel-Gudegast

Zweiter Gutachter:……………………….. Prof. Dr. Christian Berndt

Tag der mündlichen Prüfung:………………….. 17. Juli 2017

Zum Druck genehmigt am:………….. 17. Juli 2017

Erklärung

Hiermit erkläre ich, dass ich die vorliegende Doktorarbeit selbstständig und ohneZuhilfenahme unerlaubter Hilfsmittel angefertigt habe. Sie stellt, abgesehen von der Beratungdurch meine Betreuer, nach Inhalt und Form meine eigene Arbeit dar. Weder diese noch eineähnliche Arbeit wurde an einer anderen Abteilung oder Hochschule im Rahmen einesPrüfungsverfahrens vorgelegt, veröffentlicht oder zur Veröffentlichung vorgelegt. Fernerversichere ich, dass die Arbeit unter Einhaltung der Regeln guter wissenschaftlicher Praxisder Deutschen Forschungsgemeinschaft entstanden ist.

Kiel, den 28.Mai 2017

Wei Li

Abstract

Deep-water sedimentary systems are important components of continental margins. Deep-water sedimentary processes, including gravity-driven downslope and along-slope processes, affect the construction and erosion of continental margins. Various types of deep-water sedimentary systems have been found at the Northwest Africa continental margin, e.g., canyons, mass transport deposits, turbidites, and contourites. It is an ideal laboratory for investigating different deep-water sedimentary processes. Therefore, this thesis focuses on the investigation of deep-water sedimentary processes affecting the Northwest African margin. Two research areas along the NW African margin were chosen: the Western Saharan margin and the Moroccan margin. On the Western Saharan margin, high-resolution multibeam bathymetry, sidescan sonar, sub-bottom profiler, 2D seismic data, and sediment gravity-cores were acquired during RV Maria S. Merian-Cruise MSM11/2 in 2009 and RV Poseidon-Cruise P395 in 2010. The acquired data allowed a detailed analysis of the upper headwall area of the Sahara Slide Complex and three giant, buried sediment mounds beneath the upper headwall area. On the Moroccan margin, high-resolution multibeam bathymetry data, 2D seismic profiles, and gravity cores were collected during RV Maria S. Merian-Cruise MSM32 in 2013. One focus of this cruise was an in-depth investigation of the Agadir Slide, a mega slide on the Moroccan margin, which was not described before.

Bathymetric data collected in the source area of the Sahara Slide Complex reveal that the upper headwall area is ~35 km in width and it opens towards the northwest. Numerous morphological features have been discovered in the upper headwall area, including slide scarps, glide planes, plateaus, lobes, slide blocks, and slide debris. Sidescan sonar data provide a higher resolution image of the seafloor morphology and texture on the upper headwall area. Several acoustic terrains have been identified: undisturbed smooth seafloor, eroded smooth glide planes, sediment ridges, crown cracks, slide blocks, and basal striations. These seafloor features were generated by two types of mass movement processes: translational sliding and gravitational spreading along three glide planes at different stratigraphic depths. Volume estimation illustrates that at least 150 km^3 of sediments have been displaced, which is sufficient volume to pose a significant tsunamigenic potential, even if occurring in relatively large water depths (~2000 m). The presence of weak layers and sediment layers with high compressibility are considered as the main preconditioning factors for the formation of the slide events in the upper headwall area. The timing of the failure is constrained by dated gravity cores. The failure leading to the formation of the upper headwall area is relatively young (~2 ka), which is much younger than that derived for landslide deposits on the lower reaches of the Sahara Slide Complex, which are dated at 50-60 ka. The young age of the failure contradicts

the postulate of a stable slope offshore Northwest Africa during sea-level high stands. Such an observation suggests that submarine-landslide risk along the continental margin of Northwest Africa should be reassessed based on a robust dating of proximal and distal slope failures.

2D seismic data acquired in the upper headwall area allowed the discovery of three giant sediment mounds. These sediment mounds are perpendicular to the continental margin with a predominant SE-NW orientation separated by broad troughs. They all exhibit an elongated geometry, and are at least 24 to 37 km-long and 12 to 17 km-wide. The seismic stratigraphy was established by correlating seismic horizons with published chronostratigraphic information from DSDP Sites 139, 369 and 397. The development processes of these sediment mounds can be divided into three different stages: a) initial growth stage during the Middle Eocene, b) main growth stage during the Early Miocene and, c) maintenance stage during Middle Miocene. The mounds started to grow on a regional unconformity under the interaction of downslope turbidity currents, submarine landslides, and along-slope bottom currents. The sediment mounds finally terminated to grow at the Middle-Late Miocene boundary, indicating a major paleoceanographic change along the Northwest African margin and new depositional patterns established subsequently. The sediment mounds are therefore ideal records of the initiation, intensification, and evolution of bottom currents along the Western Saharan margin. Their inception suggests a time-period (Late Miocene to Middle Miocene) of intense deep-geostrophic activity several orders of magnitude larger than present-day conditions.

The investigations off Morocco were focused on the large-scale Agadir Slide. The Agadir Slide is located south of the Agadir Canyon at a water depth ranging from 500 m to 3500 m with an affected area of ~5500 km^2. Bathymetry data illustrate the detailed seafloor morphology of the Agadir Slide, which consists of two headwall areas and two slide fairways. The Agadir Slide enters the Agadir Canyon after passing through the Central slide fairway. The internal architecture of the Agadir Slide is examined in detail based on 2D seismic data. Volume calculations indicate that approximately 340 km^3 of sediment were accumulated downslope, twice as much as strata (~170 km^3) evacuated from the source areas of the Agadir Slide. This discrepancy points to a highly erosional behaviour of the Agadir Slide along its basal shear surfaces and sidewalls, thereby increasing the volume of the Agadir Slide deposits. Age models based on stratigraphic correlations from five gravity cores indicate an age of ~142 ka for the emplacement of the Agadir Slide. The Agadir Slide developed retrogressively in two phases. Local seismicity and fault activity related to halokinesis likely triggered the Agadir Slide. In addition, salt domes breaching the seafloor acted as major topographic barriers to sediment flow and, as a result, the Agadir Slide neither disintegrated into sediment blocks nor was transformed into turbidity currents. With an age of 142 ka the Agadir Slide cannot be the source for any of the turbidite beds in the Moroccan Turbidite System.

Zusammenfassung

Sedimentäre Tiefwassersysteme sind wichtige Bestandteile von Kontinentalhängen. Sedimentäre Tiefenwasserprozesse, wie gravitativ angetriebene, parallel und senkrecht zum Hang stattfindende Prozesse, beeinflussen den Aufbau und die Erosion von Kontinentalhängen. Verschiedene Typen von sedimentären Tiefwassersystemen können auf den Kontinentalhängen vor Nordwestafrika gefunden werden. Hierzu gehören zum Beispiel Canyons, Ablagerungen von Hangrutschungen, Turbidite und Contourite. Deshalb ist diese Region ein ausgezeichnetes Untersuchungsgebiet für die Forschung an sedimentären Tiefwassersystemen. In dieser Arbeit liegt der Untersuchungsschwerpunkt daher auf den Prozessen, die auf dem Kontinentalhang vor Nordwestafrika eine wichtige Rolle spielen. Es wurden zwei Untersuchungsgebiete auf dem nordwestafrikanischen Kontinentalhang ausgewählt: Der Kontinentalhang vor der Westsahara und der marokkanische Kontinentalhang. Während der FS Maria S. Merian-Fahrt MSM12/2 (2009) und FS Poseidon-Fahrt POS395 (2010) zum Kontinentalhang vor der Westsahara wurde ein Datensatz bestehend aus hochauflösenden Fächerecholot-, Seitensichtsonar-, Sedimentecholot-, 2D-seismischen und Sedimentschwerelot-Daten aufgezeichnet. Diese Daten ermöglichen eine detaillierte Analyse der oberen Abrisskante des Sahara-Slide-Complexes, sowie von drei riesigen verschütteten Terrainwellen unter dieser Abrisskante. Während der Forschungsfahrt MSM32 (2013) zum marokkanischen Kontinentalhang wurden zudem hochauflösende Fächerecholot- und 2D-seismische Daten aufgezeichnet, sowie Schwerelotkerne genommen. Ein Schwerpunkt dieser Forschungsfahrt war die detaillierte Untersuchung des Agadir-Slides, einer riesigen Hangrutschung auf dem marokkanischen Kontinentalhang, der zuvor noch nicht beschrieben und bearbeitet wurde.

Die bathymetrischen Daten aus dem Ursprungsbereich des Sahara-Slide-Complexes zeigen, dass die obere Abrisskante ~35 km lang und in Richtung Nordwesten einfallend ist. Eine Vielzahl an morphologischen Ausprägungen kann in der Nähe der oberen Abrisskante gefunden werden. Hierzu gehören: Hangrutschungsabrisskanten, Gleitflächen, Plateaus, Lobi, gerutschte Blöcke, sowie Geröll. Seitensichtsonaraufnahmen liefern eine höhere Auflösung der Meeresbodenmorphologie und des Aufbaus der Abrisskanten. Anhand dieser Methode wurden verschiedene akustische Fazies identifiziert. Hierzu gehören: ungestörter und glatter Meeresboden, erosiv überprägte glatte Gleitflächen, sedimentäre Rücken, Kronenbrüche, gerutschte Blöcke, sowie Grundschrammen. Alle diese Strukturen am Meeresboden wurden von zwei Prozessen der Massenumlagerung erzeugt: Blattgleitung und gravitative Meeresbodenaufweitung entlang dreier Gleitebenen in verschiedenen stratigraphischen Einheiten. Eine Volumenabschätzung zeigt, dass mindestens 150 km^3 Sediment umgelagert wurden. Obwohl die Rutschung in relativ hoher

Wassertiefe (~2000 m) stattfand, ist die Masse ausreichend, um ein signifikantes Potential für die Entstehung eines Tsunamis darzustellen. Das Auftreten von schwachen Schichten, sowie sedimentären Schichten mit einer hohen Kompressibilität, werden als die wichtigsten Vorbedingungen für das Entstehen einer Rutschung im Bereich der oberen Abrisskante angesehen. Das Alter der Rutschung wurde mit Hilfe von datierten Schwerelotkernen eingegrenzt. Hieraus ergibt sich, dass die Rutschung, die für die Bildung der oberen Abrisskante verantwortlich ist, relativ jung ist (~2 ka). Dieses Alter ist wesentlich geringer als die im distalen Bereich des Sahara-Slide-Complexes datierten Ablagerungen, die auf 50-60 ka datiert wurden. Dieses junge Alter der Rutschung widerspricht der gängigen Meinung, dass der nordwestafrikanische Kontinentalhang während eines hohen Meeresspiegelstands, wie vor 2 ka, stabil ist. Diese Beobachtung zeigt, dass das Risiko von submarinen Hangrutschungen am Kontinentalhang vor Nordwestafrika, mit der Benutzung von robusteren Datierungen im proximalen und distalen Bereich, neu bewertet werden sollte.

2D-seismische Daten, die im Bereich der oberen Abrisskante aufgezeichnet wurden, ermöglichten in dieser Region die Entdeckung von drei riesigen sedimentären Rücken. Diese sedimentären Rücken sind senkrecht zum Kontinentalhang mit einer Vorzugsrichtung von SO-NW ausgerichtet und durch breite Tröge voneinander getrennt. Die Rücken weisen eine langgestreckte Geometrie auf und sind mindestens 24 bis 37 km lang sowie 12 bis 17 km breit. Die seismische Stratigraphie wurde anhand einer Korrelation von seismischen Horizonten mit publizierten, chronostratigraphischen Informationen aus den DSDP Sites 139, 369 und 397 erstellt. Hieraus folgend kann der Entwicklungsprozess der drei Rücken in drei unterschiedliche Phasen gegliedert werden: a) Initiale Wachstumsphase während des Mittleren Eozäns, b) Hauptwachstumsphase während des Unteren Miozäns und, c) Aufrechterhaltungsphase während des Mittleren Miozäns. Die Entstehung der Rücken begann mit einer Ablagerung von Turbiditen, Hangrutschungen und hangparallelen Bodenströmungen auf einer regional ausgeprägten Diskordanz. Das Wachstum der sedimentären Rücken wurde an der Grenze zwischen Mittlerem und Oberen Miozän abgeschlossen. Dies weist auf eine grundlegende paläoozeanographische Veränderung entlang des Nordwestafrikanischen Kontinentalhangs hin und geht mit der Veränderung von Ablagerungsbedingungen in der Region einher. Diese sedimentären Rücken stellen daher ein ideales Archiv der Initiierung, Verstärkung und Entwicklung der bodennahen Strömungen entlang des Kontinentalhangs vor der Westsahara dar. Ihr Beginn im Oberen Miozän bis Mittleren Miozän deutet auf eine starke tiefe geostrophische Aktivität hin, die um einige Magnituden größer als die heute beobachteten Bedingungen ist.

Die Untersuchungen vor Marokko konzentrieren sich auf den großflächigen Agadir-Slide. Der Agadir-Slide befindet sich südlich des Agadir-Canyons in Wassertiefen zwischen 500 m und 3500

m und umfasst ein Gebiet von ~5500 km^2. Bathymetrische Daten zeigen ein detailliertes Bild der Meeresbodenmorphologie des Agadir-Slide, der aus zwei Abrisskanten und zwei Schüttungsrinnen besteht. Der Agadir-Slide geht in den Agadir-Canyon über, nachdem er durch die zentral gelegene Schüttungsrinne der Hangrutschung kanalisiert wurde. Der interne Aufbau des Agadir-Slides wurde anhand von 2D-Seismik detailliert untersucht. Volumenberechnungen deuten darauf hin, dass ca. 340 km^3 an Sedimenten hangabwärts abgelagert wurden. Dies ist doppelt so viel Material, wie ursprünglich im Herkunftsgebiet des Agadir-Slides abgebrochen ist (ca. 170 km^3). Diese Abweichung weist auf ein hoch-erosives Verhalten der Agadir-Rutschung entlang seiner basalen Scherzonen und seitlichen Abrisskanten hin, was zu der Vergrößerung der Menge an Ablagerungen des Agadir-Slides führt. Altersmodelle, die auf der stratigraphischen Korrelation von fünf Schwerelotkernen basieren, datieren das Ereignis der Agadir-Rutschung auf ca. 142 ka. Der Agadir-Slide entwickelte sich retrogressiv während zwei Phasen. Lokal auftretende Seismizität und die Aktivität von Störungszonen im Zusammenhang mit der vorhandenen Salztektonik haben wahrscheinlich den Agadir-Slide ausgelöst. Zudem agieren Salzdiapire, die durch den Meeresboden brechen, als wichtige topographische Barrieren für den Sedimenttransport. Daher desintegrierte der Agadir-Slide weder in sedimentäre Blöcke, noch wurde das Sediment in einem Trübestrom abtransportiert. Mit einem Alter von 142 ka kann der Agadir-Slide nicht als Quelle für die Turbiditablagerungen im marrokanischen Turbiditsystem angesehen werden.

Contents

1 Introduction

1.1 Motivation

Continental margins are the zones of the ocean floor separating the thin oceanic crust from thick continental crust; they consist of the continental shelf, slope, and rise. The morphology of modern oceans and marginal seas can be divided into shallow water and deep-water environments based on the water depth and on changes in the slope gradient (Fig. 1). The shallow water environment is the continental shelf, which extends from the shoreline to the shelf break. The term deep-water is used here to refer to the continental slope, rise, and basin environments that occur seaward of the shelf break in more than 200 m water depths. The continental slope is separated from the continental shelf by the shelf break, which is defined by a change in the slope gradient. The continental rise is considered as the preferential area for final deposition of terrigenous sediment that bypassed the shelf and the slope area.
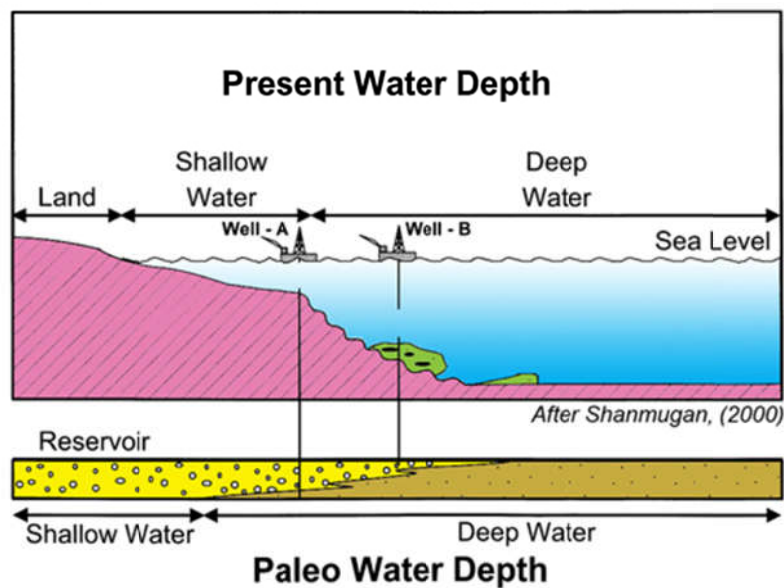
Fig.1 Shoreline crossing bathymetric profile illustrating shallow and deep water environments. The term 'deep-water' refers to bathyal water depths (>200 m) that occur seaward of the continental shelf break on the slope and basin settings. The bottom part of the figure shows the transition from coarse grained terrigenous sediments to pelagic sediments. Figure modified after Shanmugam (2000).

The understanding of deep-water sedimentary systems and processes has developed considerably after Kuenen and Migliorini's (1950) first publication on the origin of turbidity

currents and has advanced significantly in recent years (e.g., Mulder, 2011). This is largely driven by the interest of the hydrocarbon industry as their exploration on continental margins around the world has extended into increasingly deep water in order to meet the growing demand for oil and gas. The exploration and understanding of the deep oceans have been proposed as one of the principal scientific, technical and environmental challenges for the next century (Stow and Mayall, 2000). An estimated 1200 to 1300 oil and gas fields, including discoveries and producing fields, are known from the deep-water sedimentary systems in the past decades (Fig. 2). The deep-water sedimentary systems and processes are complex and they are populated by multiple products formed by a variety of processes (Fig. 3; Stow and Mayall, 2000; Stevenson et al., 2015). In general, sediment transport in deep-water environments includes gravity-driven downslope sedimentary processes, such as mass transport (i.e., slides, slumps, and debris flows) and turbidity currents, and along-slope sedimentary processes due to bottom currents. Contourites, turbidites and pelagites represent end-members in a continuum of deep-water sedimentary facies (Rebesco et al., 2014).
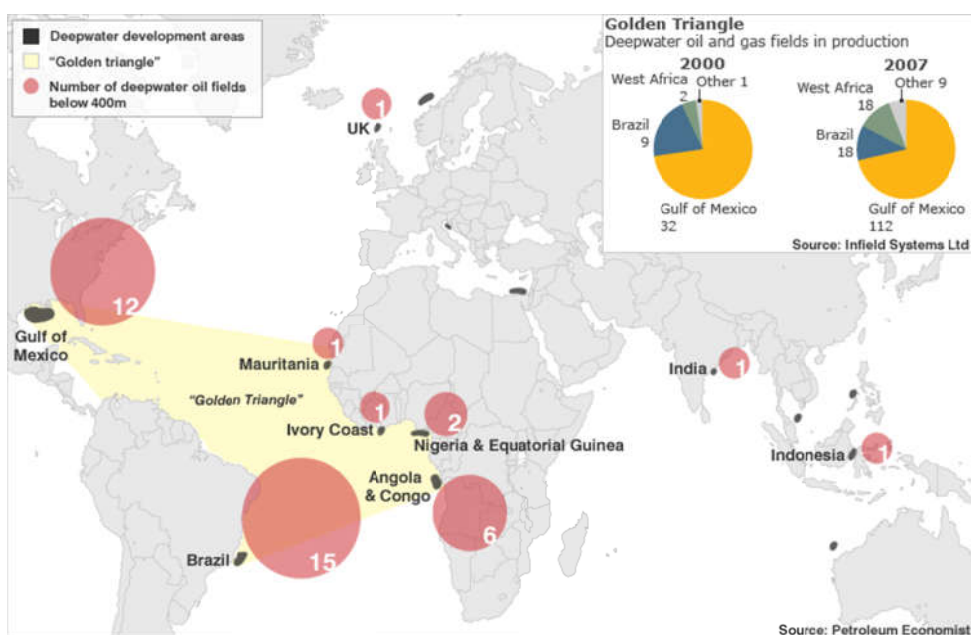
Fig.2 World map showing principal frontier areas for hydrocarbon exploration, including the main deep-water provinces (in red). Taken from http://www.bbc.co.uk/news/10298342

The investigation of deep-water systems is also important for investigating paleoclimate and marine geohazards. Contourites can be considered as ideal records of long-term variations in palaeocurrents and palaeoclimate (Hernández-Molina et al., 2006), as the deposits comprising the drifts commonly present significant lateral continuity, contain limited depositional hiatuses, and reflect high sedimentation rates (Rebesco et al., 2014). Gravity-driven sediment transport is the main process for transporting sediments from onshore sources to offshore sinks. Galy et al. (2007)

proposed that mud-rich deposits of gravity flows in the deep-water sedimentary systems may sequester globally significant volumes of organic carbon and sand-rich gravityflow deposits may form many of the World's largest oil and gas reservoirs. Gravity-driven downslope processes, e.g. submarine landslides and turbidity currents are also suggested as significant marine geohazards to seafloor infrastructures (Krastel et al., 2014). In addition, slope failures may trigger devastating tsunamis (Harbitz et al, 2014).

The knowledge on deep-water sedimentary systems and processes have benefited greatly from the recent improvements in technologies, such as the advent of high-quality 3D seismic data across a broad range of deep-water environments, (2) the recent drilling and coring of both near-surface and reservoir-level deep-water systems, and (3) the increasing utilization of multibeam bathymetry, deep-tow sidescan sonar and other imaging devices.
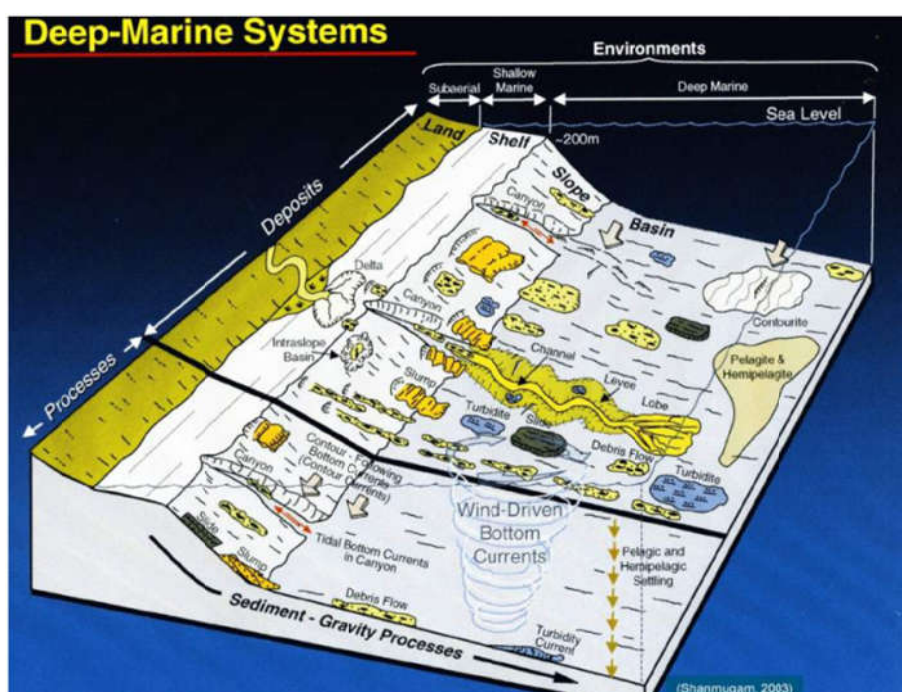
Fig.3 Schematic diagram showing complex deep-water sedimentary environments occurring at water depths than 200 m (shelf-slope break)(Shanmugam, 2000).

During the past decades intensive studies have been focused on the Northwest African continental margin and various types of deep-water sedimentary systems, e.g., canyons, mass transport deposits (MTDs), turbidites and contourites, have been discovered across the margin (Wynn et al., 2000; Krastel et al., 2012). Thus, the northwest Africa continental margin could be considered as an ideal laboratory in order to investigate deep-water sedimentary systems and processes.

1.2 Deep-water sedimentary system and processes

1.2.1 Gravity-driven downslope sedimentary processes

Gravity-driven downslope sedimentary processes comprise a range of processes from slides, slumps, cohesive debris flows to dilute turbidity currents (Fig. 4; Talling et al., 2012). They are the principal agents and mechanisms for transporting and bypassing large volumes of sediment downslope from the continent slope into the deep-marine environments (Masson et al., 2006).
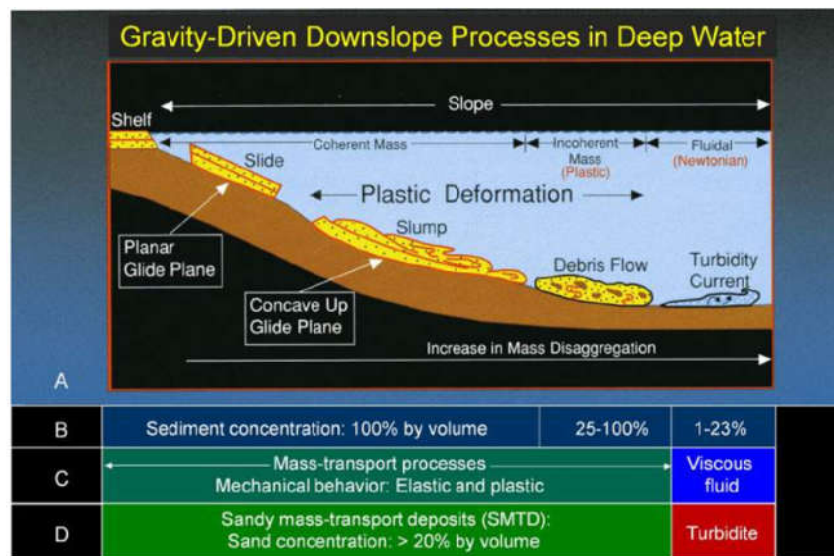
Fig.4 Schematic diagram showing four common types of gravity-driven downslope processes that transport sediment into deep-marine environments (Shanmugam, 2016).

1.2.1.1 Submarine landslides and mass-transport deposits (MTDs)

Submarine landslides are composed mainly of slides, slumps and debris flows and their deposits are termed as mass-transport deposits (MTDs) (Fig. 4; Moscardelli et al., 2006). A slide is a coherent mass of sediment that moves along a planar plane and shows almost no internal deformation. A slump is a coherent mass of sediment that moves on a concave-up glide plane and undergoes rotational movements causing internal deformation. A debris flow is a sediment flow with plastic rheology and laminar state from which deposition occurs through freezing en masse (Shanmugam, 2016).

Submarine landslides are an important mechanism in shaping continental slopes, and have been widely documented on both active and passive margins (Fig. 5; Masson et al., 2006; Krastel et al., 2014). The failed sediment moves downslope when the shear stress exceeds the shear strength

of the strata. Submarine landslides can travel hundreds of kilometers (Hampton et al., 1996). Submarine landslides represent a major geohazard not only to the oil and offshore industries but also to the marine environment and coastal facilities and they also have a tsunamigenic potential (Canals et al., 2004). They can also break telecommunication cables on the seafloor (Piper et al., 1999). The large tsunamis that devastated the North Atlantic coasts in 1755 and struck northeast Japan in 2011 both had a submarine landslide contribution (Gracia et al., 2003; Tappin et al., 2014). The Papua New Guinea tsunami occurring in 1998 resulted in the death of more than 2000 people. Tappin et al. (2001) suggested that this tsunami was triggered by a submarine landslide. A clear proof of a landslide triggered tsunami is the 1929 Grand Banks event. A tsunami struck the south coast of Newfoundland, claiming 28 lives. The landslide responsible for this tsunami destroyed 12 undersea trans-Atlantic communication cables in the landslide area (Fine et al., 2005; Piper et al., 1999). Large-scale MTDs have been proposed to have important implications for developing deep-water petroleum reservoirs and many petroleum reservoirs currently producing oil and gas are from sandy mass-transport deposits (Shanmugam et al., 2016), such as the Ormen Lange gas field inside the Storegga Slide scar, offshore Norway (Solheim et al., 2005; Bryn et al., 2005).

Fig.5 World map showing the location and distribution of mass-transport deposits (MTDs) (Moscardelli et al., 2015). Red box indicates the location of the study area of this thesis.

Many preconditioning factors have been proposed as promoting slope failures on the continental margins such as (1) overpressure due to high sedimentation rates (Laberg et al., 2002; Leynaud et al., 2009), (2) the presence of fluids and gas hydrate dissociation (Berndt et al., 2012)

and (3) the occurrence of weak layers (Baeten et al., 2014). Excess pore pressure could be generated by rapid overloading of fine-grained sediments depending on the permeability and water content in the sediment. Leynaud et al. (2007) proposed that high sedimentation rates could have been responsible for excess pore pressure building up in the Storegga area. Fluid escape features such as pockmarks, gas chimneys and pipes have been considered as indicators not only for overpressure but also for pressure release (Berndt et al., 2012). Seabed and subsurface fluid escape features have been observed at the northern Storegga slide escarpment (Hovland et al., 2005) and repeated slope failures in the Ana submarine landslide complex (Western Mediterranean Sea) have been linked to fluid migration (Berndt et al., 2012). Strain localization and creep processes on the slope could be enhanced by weak layers related to contourite drifts and rapid loading by glacial sediments (Leynaud et al., 2009). E.g., the Storegga and Traenadjupet slides occurred on the Norwegian continental along weak layers in contouritic deposits (Kvalstad et al. 2005).

A triggering mechanism is defined as the primary process that causes the necessary changes in the physical, chemical, and geotechnical properties of the soil and finally initiating the sediment failure and mass movement. Earthquakes have been considered to be the most common triggering mechanism for known historic submarine landslides (Sultan et al., 2004). Slope stability is affected by earthquakes in two ways: (1) the acceleration during the seismic ground motion affects the strata in a cyclic manner (Sultan et al., 2004); (2) the shear strength of strata may decrease due to the buildup of overpressure during an earthquake (Stigall and Dugan, 2010).

1.2.1.2 Turbidity currents and turbidites

A turbidity current is defined as a sediment flow with Newtonian rheology and turbulent state in which sediment is supported by turbulence and from which deposition occurs through suspension settling (Talling et al., 2007). It has been well documented that turbidity currents may evolve from debris flows or sediment failures (Talling et al., 2007; Hunt et al., 2013). Turbidity currents also represent a significant geohazard for submarine telecommunication cables and other seafloor infrastructures (Piper et al., 1999). The submarine landslide triggered by the 1929 Grand Banks earthquake in offshore Newfoundland, Canada evolved into a turbidity current with a speed of up to 67 km/h, which broke several submarine telegraph cables (Piper et al., 1999). Turbidites are the deposits of turbidity currents and have been defined by the Bouma Sequence (Bouma, 2000). Turbidity current events can transport extremely large volumes of sediment into the deep-water environments (Talling et al., 2007). For example, the Bed 5 event in the Moroccan Turbidite System deposited ~130 km^3 of sediment, which is more than ten times the annual sediment flux (~2×10^{13} kg) from all the world's rivers to the oceans (Mulder and Syvitski, 1995).

1.2.2 Along-slope sedimentary processes

1.2.2.1 Bottom currents, contourites and sediment drifts

Increasing amounts of work have been focused on bottom currents and the resulting deposition during the past three decades (Faugères and Stow, 1993; Hernandez-Molina et al., 2006; Rebesco et al., 2014). Bottom currents could affect continental margins worldwide on both slopes and deep continental rises. They play an important role for sediment erosion, redistribution, and preferential deposition (Stow et al., 2000; Trincardi et al., 2007). Bottom currents include thermohaline-induced bottom currents, wind-driven, tide-driven, and internal tide-driven bottom currents (Rebesco et al., 2014). Thermohaline-induced bottom currents are known as contour currents because of their tendency to follow the bathymetric contours on the continental slope and rise. In this study, we mainly focus on the thermohaline-induced bottom currents (or contour currents), which are the deep-water component of water masses that winnow, rework, and deposit sediment on the seafloor for a sustained period of time.

Bottom currents and associated processes can significantly affect the seafloor and generate various depositional and erosional features of different scales (Stow et al., 2002). The measured velocities of bottom currents usually range from 1 to 20 cm/s (Stow et al., 2002), but at some places the velocities reach up to 300 cm/s as observed at the exit of the Strait of Gibraltar (Candela, 2001). Fine to coarse sands can be eroded, transported and re-deposited by bottom currents due to their high velocities.
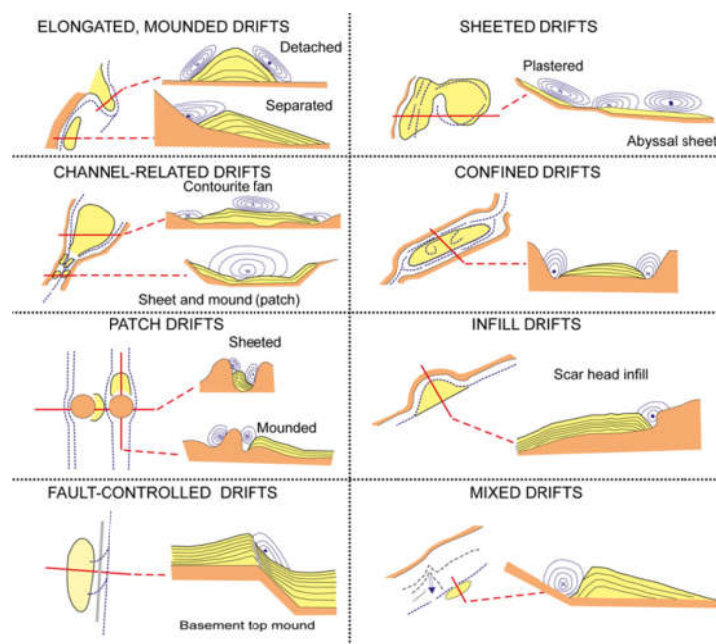
Fig.6 Different types of sediment drifts and inferred bottom-current paths (Rebesco et al., 2014).

Contourites are sediments deposited or substantially reworked by the action of bottom currents (Faugères and Stow, 1993; Stow et al., 2002; Faugères and Stow, 2008; Rebesco et al., 2014). Thick and extensive accumulations of sediments can build sediment drifts (or contourite drifts). Several different types of sediment drifts have been recognized in the ocean basins and margins (Fig. 6). These include (1) elongated, mounded drifts; (2) sheeted drifts; (3) channel-related drifts; (4) confined drifts; (5) patch drifts; (6) infill drifts; (7) fault-controlled drifts and (8) mixed drifts (Fig. 6; Stow et al., 2002; Hernández-Molina et al., 2010; Rebesco et al., 2014).
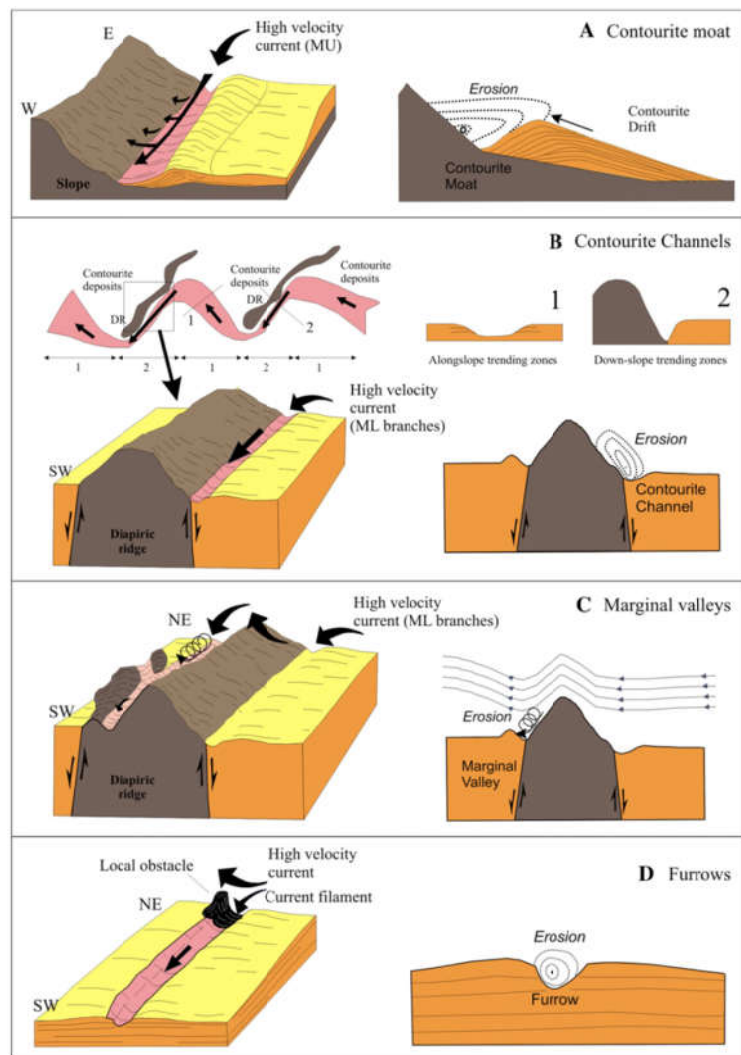
Fig.7 Interpretation of the processes involved in the origin and evolution of the erosive features (García et al., 2009).

There are mainly four types of erosive bedforms that develop in relation to the activity of

bottom currents (Fig. 7). They are contourite moats, contourite channels, marginal valleys and large isolated furrows (García et al., 2009; Hernández-Molina et al., 2006). The detection of erosional bedforms can be important for the reconstruction of bottom current velocity (Stow et al., 2009).

1.2.2.2 Significance of contourites and sediment drifts for paleoceanography and slope instability

Despite the fact that significant advances have been made in understanding bottom currents and their deposits in the past years, Rebesco et al. (2014) proposed that there still remained an urgent need to establish a sound connection between contourite deposits, basin evolution and oceanographic processes. The study on contourites and sediment drifts are of great significance for the better understanding of paleoceanography and slope instability.

The sedimentation rates in the areas affected by contourites are higher than those in the adjacent areas without contouritic influence (Rebesco et al., 2014). This results in the deposition of fairly continuous sediment records with relatively high temporal resolution. Therefore, the variability of ocean circulation patterns, current velocities and oceanographic history can be revealed from contourites. Sediment drifts can also provide paleoceanographic information on paleocurrent pathways and on changes in current energy and direction based on their geometry, internal architectures and seismic facies (Brackenridge et al., 2013).

1.2.3 Interaction of downslope and along-slope sedimentary processes

The interaction of downslope and along-slope sedimentary processes (Fig. 8) have been documented in various areas, including the Gulf of Cadiz (Brackenridge et al., 2013), the Celtic margin of the Bay of Biscay (Cunningham et al., 2005), the Cantabrian continental margin (Ercilla et al., 2008), the northeastern South China Sea margin (Gong et al., 2015), the southern Tyrrhenian Sea (Italy) (Martorelli et al., 2016), the Southern Antarctic Peninsula continental rise (McGinnis and Hayes, 1995) and the George V Land continental margin (East Antarctic) (Caburlotto et al., 2006). The interaction of turbidity currents and bottom currents can generate various sedimentary features, such as unidirectional migrating deep-water channels (Rasmussen, 1994; Gong et al., 2013), bottom-current reworked sands (Shanmugam et al., 1993; Viana et al., 1998; Gong et al. 2015) and in particular giant sediment drifts (mounds) (Rebesco et al., 2002, 2007).
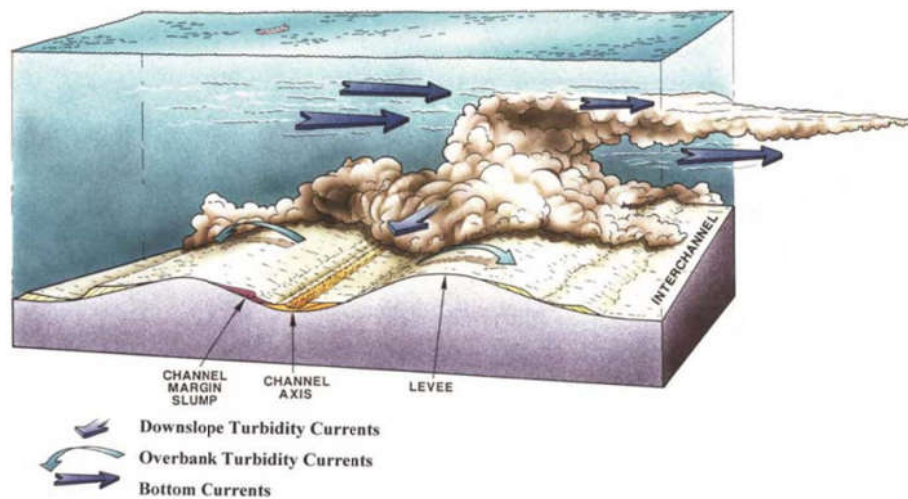
Fig.8 Conceptual model showing the spatial relationship between downslope turbidity currents and along-slope bottom currents (Shanmugam et al., 1993).

Numerous elongated sediment mounds have been identified on the Antarctic margin, such as the western Antarctic Peninsula (McGinnis and Hayes, 1995) and the Weddell Sea (Michels et al., 2001). These sediment mounds are elongated and perpendicular to the continental margin, and they are produced by the interaction of along-slope bottom water flow with downslope turbidity currents (Rebesco et al., 2007). These sediment mounds may be considered as a complete range of intermediates between two end members: the sediment drift and the channel levee (Rebesco et al., 2002). Detailed investigation of the stratigraphic development of the sediment mounds can reveal the impact of changing oceanic circulation patterns on their origin and evolution (McGinnis and Hayes, 1995; Rebesco et al., 2002).

The research on contourites and sediment drifts are also important for the analysis of slope instability and geological hazard assessment. Submarine slides in areas with fine-grained contourites have been documented on the Norwegian margin (Bryn et al., 2005). The distribution, composition and physical properties of contourites could affect the stability of submarine slopes (Solheim et al., 2005; Laberg and Camerlenghi, 2008). Weak layers (or glide planes) could be formed within the fine-grained, low-permeability, high pore-water content contourites due to the rapid sediment deposition (Laberg and Camerlenghi, 2008).

1.3 Geological setting and oceanographic setting of the continental margin off NW Africa

1.3.1 Geological setting

The Northwest African continental margin is one of the best-studied passive margins in the world. Rifting of the margin began in Late Triassic times (Davison, 2005). After Early Jurassic continental breakup between the African and North American plates, thick (>10 km) sediments were deposited during the Mesozoic and Cenozoic. The western Saharan continental slope and upper rise were shaped during the past 135 Ma from ancient paleoslopes by a number of discrete constructional and destructional phases (Seibold and Hinz, 1974). The location of the continental slope has not changed very much for the past 90 m.y. (von Rad and Wissmann, 1982). The deepwater sections of the margin consist of predominantly deep marine clastic sedimentation from the Jurassic to recent (Davison, 2005). During Late Cretaceous to Tertiary times, the continental slope has hardly prograded and the depocenter shifted to the upper rise during the Neogene.

The Northwest African margin is bordered by a flat continental shelf that is generally 40-60 km wide, although maximum shelf widths of >100 km occur off the Western Saharan coast (Fig. 9; Seibold, 1982; Wynn et al., 2000). The shelf break is observed at a water depth between 100 m and 200 m (Wynn et al., 2000). The continental slope has a width of 50-250 km beyond the shelf break, and records a slope gradient of 1-6°, with local gradients approaching 40° around areas dominated by halokinesis and salt-diapir growth (Dunlap et al., 2010). The continental slope continues into the continental rise at water depths of 1500 to 4000 m, with gradients ranging from about 1° on the lower slope/upper rise to 0.1° on the lower rise (Seibold, 1982). The continental rise is generally 100-1500 km wide, and terminates at a water depth of 4500-5400 km, beyond which lies the flat expanse of the Madeira Abyssal Plain. On this margin, earthquakes of magnitude M≥7 have rarely been recorded away from the Gulf of Cadiz (Seibold, 1982), but moderate earthquakes (4≤M≤6) are commonly observed in association with the reactivation of old weakness zones created during the opening of the Atlantic Ocean (Hayes and Rabinowitz, 1975; Pereira and Alves, 2011). The Western Sahara margin is part of the NW-African continental margin; it comprises the offshore continuation of the Aaiun-Tarfaya coastal basin (von Rad and Wissmann, 1982).
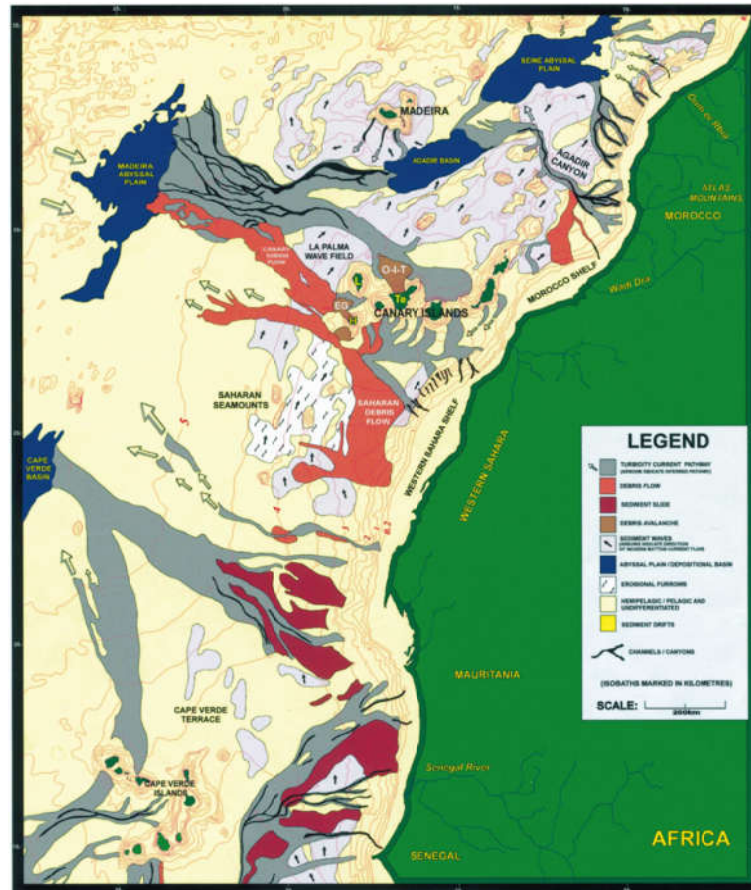
Fig.9 Deep-water sedimentary processes along the Northwest African margin, including the complex interplay between pelagic/hemipelagic sedimentation, along-slope bottom currents and downslope gravity flows (Wynn et al., 2000).

The Northwest African continental margin has been affected by complex sediment transport processes since its inception (Figs. 9 and 10; Wynn et al., 2000; Krastel et al., 2012). The NW African margin is also dissected by numerous canyons and channels, and interrupted by multiple volcanic islands and seamounts, creating a topographically complex setting that greatly influences local sedimentary processes (Fig. 9; Wynn et al., 2000). Multiple large-scale submarine landslides occurred during the Quaternary along the continental slope off NW Africa (Fig. 10; Krastel et al. 2012). The most prominent submarine landslides in the region include the Sahara Slide Complex (Gee et al., 1999; Georgiopoulou et al., 2010), the Mauritania Slide Complex (Antobreh and Krastel, 2007), the Cap Blanc Slide (Krastel et al., 2006), and the Dakar Slide (Meyer et al., 2012). The Sahara Slide Complex is one of the largest known submarine slides in the world, and affected an area of 48,000 km^2 on the northwest African slope (Embley et al., 1982). During a period of rapid sea-level rise at ~50-60 ka, high primary productivity in surface waters off Northwest Africa resulted in the accumulation of thick fine-grained pelagic/hemipelagic sediment on the continental slope (Krastel et al., 2006). Multiple slide events were interpreted to have occurred retrogressively

over ductile shaley intervals during this period (Georgiopoulou et al., 2009).
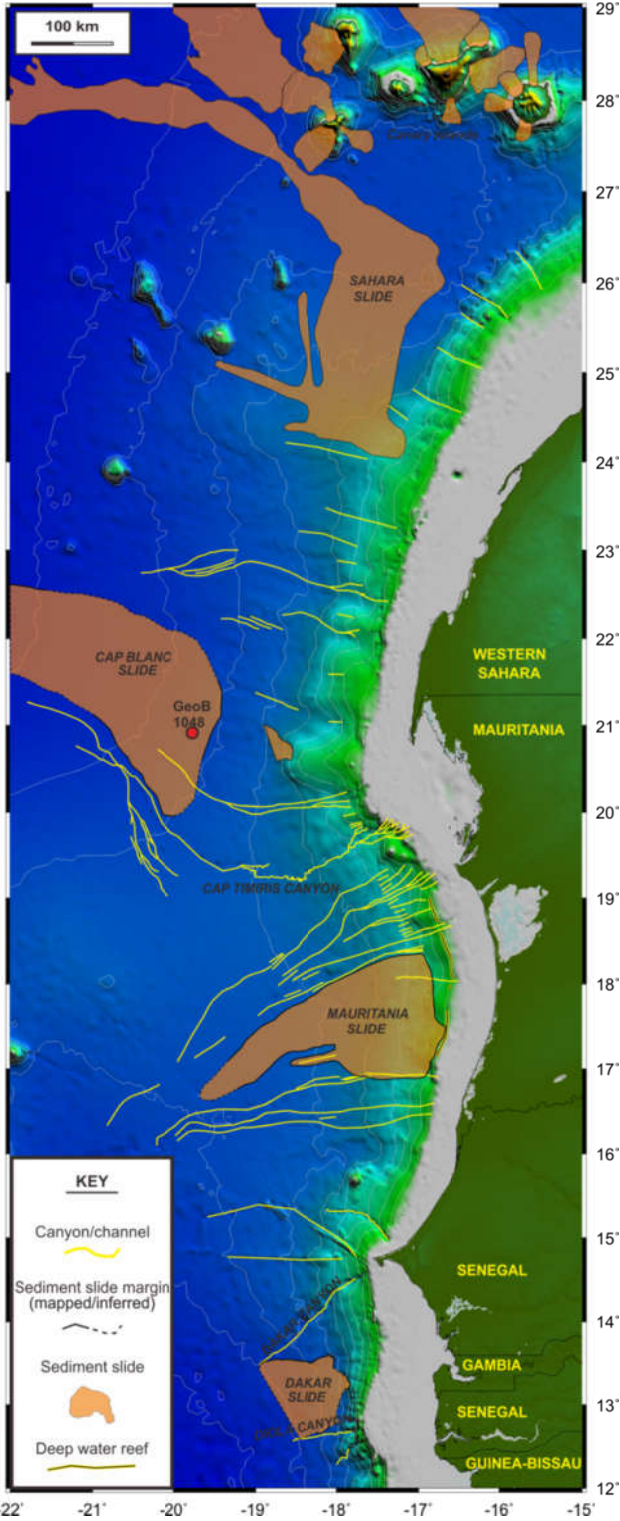
Fig.10 Map showing the distribution of the main submarine landslides on the Northwest African continental margin (modified after Krastel et al., 2012).

Most of the continental margin of Northwest Africa is now arid and records limited sediment supply by rivers, even during past glacial times (Weaver et al., 2000; Wynn et al., 2000). The margin is affected by both a seasonal and permanent oceanic upwelling system (Lange et al., 1998). Upwelling and associated high organic productivity are concentrated along the outer shelf and upper slope regions, resulting in sedimentation rates of 5 cm/ka on average, which increased to 16.5 cm/ka during the last glacial period (Bertrand et al., 1996; Weaver et al. 2000). Deep-water hemipelagic sedimentation in Northwest Africa typically consists of silts, muds, carbonate-rich marls and oozes (Weaver and Kuijpers, 1983). Wind-blown sediments transported from the Sahara Desert provide additional terrigenous sediment supply to the Northwest African continental margin (Holz et al., 2004; Henrich et al., 2008).

The Moroccan Turbidite System is located beyond 4000 m water-depth. It consists of three interlinked deep-water basins: the Agadir Basin, Seine Abyssal Plain and Madeira Abyssal Plain (Fig. 9; Wynn et al., 2002). The Agadir Basin is a large intraslope basin lying at a water depth of ~4400 m. It has an area of 22,000 km^2 and is almost flat, having a gradient of just 0.02°. The Seine Abyssal Plain is also located at a water depth of ~4400 m. The Madeira Abyssal Plain is the largest Abyssal Plain in the region, covering an area of 68,000 km^2 (Rothwell et al., 1992). It is extremely flat, with a slope of less than 0.01°, and a surface relief varying by less than 10 m. The Agadir Basin and Madeira Abyssal Plain (water depth of ~5400 m) are connected by a 600-km long network of shallow channels termed the Madeira Distributary Channel System (Masson, 1994; Wynn et al., 2000). The sedimentary fill of basins in the Moroccan Turbidite System comprises turbidites interbedded with hemipelagites (Frenz et al., 2009; Hunt et al., 2013).The largest individual flow deposits in the Moroccan Turbidite System contain sediment volumes >100 km^3, although these large-scale events are relatively infrequent with a recurrence interval of ~10,000 years (over the last 200,000 years). Provenance studies indicate that flows sourced from the Canary Islands are generated by rare volcanic flank collapses. Siliciclastic flows are interpreted to come from the area in and around upper Agadir Canyon, based upon sediment isopachs and grain-size trends (Frenz et al., 2009). The largest siliciclastic flow in the last 200,000 years was the 'Bed 5 event' (Wynn et al., 2010) which transported 130 km^3 of sediment up to 2000 km from Agadir Canyon to the southwest Madeira Abyssal Plain; this run-out distance is exceptional considering that the flow was running across flat (<0.1°) and unchannelised seafloor for more than 50% of that distance. The Bed 5 event occurred at the transition between oxygen isotope stages 4 and 3, at a time when sea level and global temperatures were rising.

1.3.2 Oceanographic setting

The present-day oceanic circulation along the Western Sahara margin is dominated by the

Canary Current, South Atlantic Central Water (SACW), North Atlantic Central Water (NACW), Mediterranean Outflow Water (MOW), North Atlantic Deep Water (NADW) and the Antarctic Bottom Water (AABW) (Sarnthein et al., 1982).

The NW African continental shelf is mainly under the influence of the south-flowing Canary Current. The Canary Current is largely linked to the atmospheric circulation along NW Africa. The Canary Current is a component of the North Atlantic Subtropical Gyre and flows southwards at the surface along the coast. Upwelling has been observed along the entire northeast Atlantic continental margin, mainly affecting the middle-outer shelf and upper continental slope down to a depth of 500 m (Sarnthein et al., 1982). Upwelling is generated by a complex interaction of the Trade Winds parallel to the coast with the Canary Current and the rotation of the Earth (Ekman transport) (Barton et al., 1998).

Upwelling waters south of 22°N are fed by the nutrient-rich South Atlantic Central Water (SACW) (Sarnthein et al., 1982). In the northern part, the upwelled water is derived from the nutrient-poorer North Atlantic Central Water (NACW), which follows the Canary Current from the north at 100-600 m water depth (Sarnthein et al., 1982). The NACW gradually veers out from the continental slope to the open sea south of 22°N. The Mediterranean Water (MW) has been traced south along the continental margin from Gibraltar to 20°N with a center of highly saline and relatively oxygen-rich water gradually sinking from 1000 m to 1500 m water depth (Knoll et al., 2002).

The North Atlantic Deep Water (NADW) is unstructured in terms of temperature, salinity, and high oxygen content (Sarnthein et al., 1982). The NADW is mainly formed by a mixture of Iceland Scotland Overflow Water, Labrador Sea Water and Lower Deep Water (van Aken, 2000). It occurs at a water depth of 1500-3800 m and flows in a southerly direction (Sarnthein et al., 1982; van Aken, 2000). The Antarctic Bottom Water (AABW) can hardly be recognized using the temperature-salinity data from the NW African continental margin, as it occurs below 3800 m and flows in a north-easterly direction (Wynn et al., 2000). Bottom currents along the margin are thought to be fairly weak at present, with current velocities generally between 1 and 6 cm/s (Sarnthein et al., 1982; Wynn et al., 2000).

1.4 Scientific objectives

The main goal of this PhD thesis is a detailed investigation of the deep-water sedimentary systems on the continental margin offshore Northwest Africa. To achieve this goal, two research areas on the NW Africa margin were selected, which are the continental margin off Western Sahara and off Morocco. High-resolution multibeam bathymetry, sidescan sonar, sub-bottom profiler, 2D seismic data and sediment gravity-cores acquired during RV Poseidon Cruise P395 in combination with bathymetric data collected during RV Maria S. Merian Data in 2011 allowed the morphological investigation of the upper headwall area of the Sahara Slide Complex and the identification of three giant sediment mounds. Multibeam bathymetry data, 2D seismic profiles, sediment echo sounder data, and gravity cores collected during RV Maria S. Cruise MSM32 allowed a detailed characterization of the Agadir Slide on the Morocco margin. These dataset were interpreted in order to address the following scientific objectives:

(1) Morphology, age and sediment dynamics of the upper headwall of the Sahara Slide Complex

Gravity-driven downslope sedimentary processes, including submarine landslides and turbidity currents are frequent and important events on the Northwest African margin, which are the dominant processes in shaping the morphology of the margin. Multiple large-scale submarine landslides occurred during the Quaternary on the Northwest African continental margin (Krastel et al. 2012). The Sahara Slide Complex is one of the largest known submarine slides in the world, and affected an area of 48,000 km^2 of the Northwest African Margin (Embley et al., 1982; Georgiopoulou et al., 2010). The distal deposits of the Sahara Slide are dated at 50-60 ka before present, which was during a period of rising sea level (Gee et al., 1999; Georgiopoulou et al., 2007). Multiple slide events were interpreted to have occurred retrogressively at this time (Georgiopoulou et al., 2007; 2009). As a result, the Sahara Slide Complex remobilised ~600 km^3 of sediments along a distance of ~900 km (Georgiopoulou et al., 2010). Reconnaissance data show that the Sahara Slide Complex is marked by the presence of two major scarps (named lower and upper headwall scarps), each up to 100 m high. Most of the published geological information on the Sahara Slide Complex has been acquired in its distal depositional part (Gee et al., 1999; 2001; Georgiopoulou et al., 2009; 2010). However, limited attention has been paid to its headwall, especially the upper headwall area, chiefly due to the lack of high-quality data on the upper continental slope of Northwest Africa. Specific questions to be addresses for the upper headwall area of the Sahara Slide complex are:

What type of morphological features can be identified in the upper headwall area? What are the ages and volumes for the slide events in the upper headwall area? What are the controlling factors for the different types of mass movements in the study area? What is the relationship between sea-level variations and the occurrence of submarine landslides? What are the implications of the timing of the slide events for the geohazard assessment along the NW Africa margin?

(2) Origin, evolution and paleoceanographic implications of giant buried sediment mounds on the Western Saharan margin (NW Africa).

Along-slope bottom currents have widely affected the Northwest African continental margin, however, large-scale sediment drifts have seldom been reported and investigated along NW Africa. Newly acquired high-resolution 2D seismic data from upper headwall area of the Sahara Slide allow us to recognise, for the first time, the presence of three giant buried sediment mounds. The identification of these sediment mounds is of great importance as they may provide an ideal opportunity to improve our understanding on the Late Cenozoic depositional and erosional processes acting along the Western Saharan margin. Analysis of these sediment mounds can also be useful in understanding ancient and modern oceanographic current patterns and, ultimately, to unravel the Cenozoic sedimentary evolution of the Western Sahara margin. In this context, the following topics will be analyzed.

What is the distribution, geometry and internal architecture of the three discovered sediment mounds? How did the three sediment mounds develop through time? What are the implications of the sediment mounds in the framework of the North Atlantic paleoceanographic evolution?

(3) Morphology, age model, evolution and implications of the Agadir Slide offshore NW Africa.

The Moroccan Turbidite System extends 1500 km from the head of the Agadir Canyon to the Madeira Abyssal Plain, and has hosted some of the largest (with volumes exceeding 150 km) landslide-triggered turbidity currents occurring in the past 200 ka (Wynn et al., 2002; Talling et al., 2007; Frenz et al., 2009). Three sources have been proposed to contribute to the Moroccan Turbidite System: (1) organic-rich siliciclastic flows sourced from the Moroccan margin (Frenz et al., 2009; Hunt et al., 2013); (2) volcaniclastic flows sourced from either the Canary Islands or Madeira (Hunt et al., 2013b), and (3) carbonate-rich flows sourced from local seamounts (Wynn et al., 2002). Most studies have been focused on the Moroccan Turbidite System for the past two decades (Wynn et al.,

2002; Frenz et al., 2009; Hunt et al., 2013; Stevenson et al., 2014). However, limited attention has been paid to its source areas, especially along the Moroccan margin from which most large-volume flows were derived. Due to the lack of geophysical data from the Moroccan margin, the shapes and sizes of the initial failures responsible for the turbidites in the Moroccan Turbidite System are largely unknown. More recently, a large-scale submarine landslide, i.e. the Agadir Slide on the Moroccan margin was mapped by means of hydroacoustic data obtained during the RV Maria S. Merian research cruise MSM32 for the first time (Krastel et al., 2016). A combination of newly acquired high-resolution multi-beam bathymetry, 2D seismic profiles and gravity cores allows a detailed analysis of the Agadir Slide in terms of its morphology, internal architecture, timing and evolution processes. The work in this thesis aims in a better understanding of the relationship between the Agadir Slide and the Moroccan Turbidite System. Specific questions include:

What are the morphological features discovered in the Agadir Slide area? What is the internal architecture of the Agadir Slide? What are the evacuated and accumulated volumes of sediments for the Agadir Slide? When did the Agadir Slide occur and how did it develop? Did the Agadir Slide evolve into a turbidity current or could it be a significant contribution to the turbidite system of the Moroccan Turbidite System?

1.5 Thesis outline

Chapter 1 provides an introduction on deep-water sedimentary systems and processes, the geological and oceanographic setting of the continental margin off NW Africa, as well as the motivation and scientific objectives of the thesis.

The manuscripts in Chapter 2-4 discuss deep-water sedimentary processes on the continental margin off NW Africa in two research areas. These manuscripts have been published, or planned for submission to international peer-reviewed journals.

Chapter 2 (Manuscript I) mainly focuses on the morphology, age and sediment dynamics of the upper headwall of the Sahara Slide Complex on the continental margin off Northwest Africa. High-resolution multibeam bathymetry, sidescan sonar, and sub-bottom profiler data were used to investigate the detailed seafloor morphology and slide processes in the upper headwall area; two gravity cores were used to constrain the timing of the failure events. The relationship between sea-level variations and the occurrence of submarine landslides is discussed. The implications of the young age of the failure are discussed in terms of a geohazard reassessment for the NW-African continental margin. This chapter is published in the journal of 'Marine Geology' as Li, W., Alves, T.M., Urlaub, M., Georgiopoulou, A., Klaucke, I., Wynn, R.B., Gross, F., Meyer, M., Repschläger, J., Berndt, C., Krastel, S., 2016. Morphology, age and sediment dynamics of the upper headwall of the Sahara Slide Complex, Northwest Africa: Evidence for a large Late Holocene failure. Marine Geology, http://dx.doi.org/10.1016/j.margeo.2016.11.013.

Chapter 3 (Manuscript II) focuses on three giant sediment mounds identified on the Western Saharan margin (NW Africa). 2D multi-channel seismic profiles along the Western Sahara margin are used to investigate the distribution, geometry and internal characters of these sediment mounds. The origin and evolution processes of the sediment mounds are discussed based on the established regional seismic stratigraphy in the study area. The paleoceanographic implications of the giant sediment mounds are discussed in the framework of the North Atlantic paleoceanographic evolution. This manuscript has been submitted to the journal 'Earth and Planetary Science Letters'.

Chapter 4 (Manuscript III) focuses on the morphology, age model and evolution of a newly identified submarine slide (Agadir Slide) on the NW African margin by using high-resolution multibeam bathymetry data, 2D seismic profiles and gravity cores. This chapter provides crucial insights on the transport dynamics and sediment-dispersal patterns of the Agadir Slide, and discusses its significance for the Moroccan Turbidite System. This manuscript will be submitted to the journal 'Geochemistry, Geophysics, Geosystems'.

Chapter 5 summarizes the main results of this PhD thesis and gives a brief outlook and open questions for future work.

References

Antobreh, A.A., Krastel, S., 2007. Mauritania Slide Complex: morphology, seismic characterisation and processes of formation. International Journal of Earth Sciences 96, 451-472.

Baeten, N.J., Laberg, J.S., Vanneste, M., Forsberg, C.F., Kvalstad, T.J., Forwick, M., Vorren, T.O., Haflidason, H., 2014. Origin of shallow submarine mass movements and their glide planes-Sedimentological and geotechnical analyses from the continental slope off northern Norway. Journal of Geophysical Research: Earth Surface 119, 2335-2360.

Barton, E.D., Arístegui, J., Tett, P., Cantón, M., García-Braun, J., Hernández-León, S., Nykjaer, L., Almeida, C., Almunia, J., Ballesteros, S., Basterretxea, G., Escánez, J., García-Weill, L., Hernández-Guerra, A., López-Laatzen, F., Molina, R., Montero, M.F., Navarro-Pérez, E., Rodríguez, J.M., van Lenning, K., Vélez, H., Wild, K., 1998. The transition zone of the Canary Current upwelling region. Progress in Oceanography 41, 455-504.

Berndt, C., Costa, S., Canals, M., Camerlenghi, A., de Mol, B., Saunders, M., 2012. Repeated slope failure linked to fluid migration: The Ana submarine landslide complex, Eivissa Channel, Western Mediterranean Sea. Earth and Planetary Science Letters 319-320, 65-74.

Bertrand, P., Shimmield, G., Martinez, P., Grousset, F., Jorissen, F., Paterne, M., Pujol, C., Bouloubassi, I., Buat Menard, P., Peypouquet, J.P., Beaufort, L., Sicre, M.A., Lallier-Verges, E., Foster, J.M., Ternois, Y., Program O.P.o.t.S., 1996. The glacial ocean productivity hypothesis: the importance of regional temporal and spatial studies. Marine Geology 130, 1-9.

Bouma, A. H., 2000, Coarse-grained and fine-grained turbidite systems as end member models: applicability and dangers: Marine and Petroleum Geology, v. 17, no. 2, p. 137-143.

Brackenridge, R.E., Hernández-Molina, F.J., Stow, D.A.V., Llave, E., 2013. A Pliocene mixed contourite–turbidite system offshore the Algarve Margin, Gulf of Cadiz: Seismic response, margin evolution and reservoir implications. Marine and Petroleum Geology 46, 36-50.

Bryn, P., Berg, K., Stoker, M.S., Haflidason, H., Solheim, A., 2005. Contourites and their relevance for mass wasting along the Mid-Norwegian Margin. Marine and Petroleum Geology 22, 85-96.

Caburlotto, A., De Santis, L., Zanolla, C., Camerlenghi, A., Dix, J.K., 2006. New insights into Quaternary glacial dynamic changes on the George V Land continental margin (East Antarctica). Quaternary Science Reviews 25, 3029-3049.

Canals, M., Lastras, G., Urgeles, R., Casamor, J.L., Mienert, J., Cattaneo, A., De Batist, M., Haflidason, H., Imbo, Y., Laberg, J.S., Locat, J., Long, D., Longva, O., Masson, D.G., Sultan, N., Trincardi, F., Bryn, P., 2004. Slope failure dynamics and impacts from seafloor and shallow sub-seafloor geophysical data: case studies from the COSTA project. Marine Geology 213, 9-72.

Candela, J., 2001.The Mediterranean water and the global circulation, in Ocean Circulation and

Climate.Observing and Modelling the Global Ocean, edited by G. Siedler, J. Church, and J. Gould, pp. 419-429, Elsevier, New York.

García, M., Hernández-Molina, F.J., Llave, E., Stow, D.A.V., León, R., Fernández-Puga, M.C., Diaz del Río, V., Somoza, L., 2009. Contourite erosive features caused by the Mediterranean Outflow Water in the Gulf of Cadiz: Quaternary tectonic and oceanographic implications. Marine Geology 257, 24-40.

Cunningham, M.J., Hodgson, S., Masson, D.G., Parson, L.M., 2005. An evaluation of along- and down-slope sediment transport processes between Goban Spur and Brenot Spur on the Celtic Margin of the Bay of Biscay. Sedimentary Geology 179, 99-116.

Davison, I., 2005. Central Atlantic margin basins of North West Africa: Geology and hydrocarbon potential (Morocco to Guinea). Journal of African Earth Sciences 43, 254-274.

Dunlap, D.B., Wood, L.J., Weisenberger, C., Jabour, H., 2010. Seismic geomorphology of offshore Morocco's east margin, Safi Haute Mer area. AAPG Bulletin 94, 615-642.

Embley, R.W., 1982. Anatomy of Some Atlantic Margin Sediment Slides and Some Comments on Ages and Mechanisms, in: Saxov, S., Nieuwenhuis, J.K. (Eds.), Marine Slides and Other Mass Movements. Springer US, Boston, MA, pp. 189-213.

Ercilla, G., Casas, D., Estrada, F., Vázquez, J.T., Iglesias, J., García, M., Gómez, M., Acosta, J., Gallart, J., Maestro-González, A., 2008.Morphosedimentary features and recent depositional architectural model of the Cantabrian continental margin. Marine Geology 247, 61-83.

Faugères, J.-C., Stow, D.A.V., 1993. Bottom-current-controlled sedimentation: a synthesis of the contourite problem. Sedimentary Geology 82, 287-297.

Faugères, J.C., Stow, D.A.V., 2008. Chapter 14 Contourite Drifts: Nature, Evolution and Controls, in: Rebesco, M., Camerlenghi, A. (Eds.), Developments in Sedimentology. Elsevier, pp. 257-288.

Fine, I.V., Rabinovich, A.B., Bornhold, B.D., Thomson, R.E., Kulikov, E.A., 2005. The Grand Banks landslide-generated tsunami of November 18, 1929: preliminary analysis and numerical modeling. Marine Geology 215, 45-57.

Frenz, M., Wynn, R.B., Georgiopoulou, A., Bender, V.B., Hough, G., Masson, D.G., Talling, P.J., Cronin, B.T., 2009.Provenance and pathways of late Quaternary turbidites in the deep-water Agadir Basin, northwest African margin. International Journal of Earth Sciences 98, 721-733.

Galy, V., France-Lanord, C., Beyssac, O., Faure, P., Kudrass, H., Palhol, F., 2007.Efficient organic carbon burial in the Bengal fan sustained by the Himalayan erosional system. Nature 450, 407-410.

Canals, M., Lastras, G., Urgeles, R., Casamor, J.L., Mienert, J., Cattaneo, A., De Batist, M., Haflidason, H., Imbo, Y., Laberg, J.S., Locat, J., Long, D., Longva, O., Masson, D.G., Sultan, N., Trincardi, F., Bryn, P., 2004. Slope failure dynamics and impacts from seafloor and shallow sub-seafloor geophysical data: case studies from the COSTA project. Marine Geology 213, 9-72.

García, M., Hernández-Molina, F.J., Llave, E., Stow, D.A.V., León, R., Fernández-Puga, M.C., Diaz del Río, V.,

Somoza, L., 2009. Contourite erosive features caused by the Mediterranean Outflow Water in the Gulf of Cadiz: Quaternary tectonic and oceanographic implications. Marine Geology 257, 24-40.

Gee, M.J.R., Masson, D.G., Watts, A.B., Allen, P.A., 1999. The Saharan debris flow: an insight into the mechanics of long runout submarine debris flows. Sedimentology 46, 317-335.

Gee, M.J.R., Masson, D.G., Watts, A.B., Mitchell, N.C., 2001. Passage of debris flows and turbidity currents through a topographic constriction: seafloor erosion and deflection of flow pathways. Sedimentology 48, 1389-1409.Geist, E.L., Lynett, P.J., Chaytor, J.D., 2009.Hydrodynamic modeling of tsunamis from the Currituck landslide. Marine Geology 264, 41-52.

Georgiopoulou, A., Masson, D.G., Wynn, R.B., Krastel, S., 2010. Sahara Slide: age, initiation and processes of a giant submarine slide. Geochemistry, Geophysics, Geosystems 11, 1-22.

Georgiopoulou, A., Wynn, R.B., Masson, D.G., Frenz, M., 2009.Linked turbidite–debrite resulting from recent Sahara Slide headwall reactivation. Marine and Petroleum Geology 26, 2021-2031.

Gong, C., Wang, Y., Xu, S., Pickering, K.T., Peng, X., Li, W., Yan, Q., 2015. The northeastern South China Sea margin created by the combined action of down-slope and along-slope processes: Processes, products and implications for exploration and paleoceanography. Marine and Petroleum Geology 64, 233-249.

Gong, C., Wang, Y., Zhu, W., Li, W., Xu, Q., 2013.Upper Miocene to Quaternary unidirectionally migrating deep-water channels in the Pearl River Mouth Basin, northern South China Sea. AAPG Bulletin 97, 285-308.

Gracia, E., Danobeitia, J.J., PARSIFAL Team, 2003. Mapping active faults offshore Portugal (368N–388N): implications for seismic hazard assessment along the southwest Iberian margin. Geology 31 (1), 83– 86.

Hampton, M.A., Lee, H.J., Locat, J., 1996. Submarine landslides. Reviews of Geophysics 34, 33-59.

Harbitz, C.B., Vholt, F.L., Bungum, H., 2014. Submarine landslide tsunamis: how extreme and how likely? Natural Hazards 72(3), 1341-1374.

Hayes, D.E., Rabinowitz, P.D., 1975. Mesozoic magnetic lineations and the magnetic quiet zone off northwest Africa. Earth and Planetary Science Letters 28, 105-115.

Henrich, R., Hanebuth, T.J.J., Krastel, S., Neubert, N., Wynn, R.B., 2008. Architecture and sediment dynamics of the Mauritania Slide Complex. Marine and Petroleum Geology 25, 17-33.

Hernández-Molina, F.J., Llave, E., Stow, D.A.V., García, M., Somoza, L., Vázquez, J.T., Lobo, F.J., Maestro, A., Díaz del Río, V., León, R., Medialdea, T., Gardner, J., 2006. The contourite depositional system of the Gulf of Cádiz: A sedimentary model related to the bottom current activity of the Mediterranean outflow water and its interaction with the continental margin. Deep Sea Research Part II: Topical Studies in Oceanography 53, 1420-1463.

Hernández-Molina, F.J., Paterlini, M., Somoza, L., Violante, R., Arecco, M.A., de Isasi, M., Rebesco, M., Uenzelmann-Neben, G., Neben, S., Marshall, P., 2010.Giant mounded drifts in the Argentine Continental Margin: Origins, and global implications for the history of thermohaline circulation. Marine and Petroleum Geology 27, 1508-1530.

Holz, C., Stuut, J.b.W., Henrich, R., 2004. Terrigenous sedimentation processes along the continental margin off NW Africa: implications from grain-size analysis of seabed sediments. Sedimentology 51, 1145-1154.

Hovland, M., Svensen, H., Forsberg, C.F., Johansen, H., Fichler, C., Fosså, J.H., Jonsson, R., Rueslåtten, H., 2005. Complex pockmarks with carbonate-ridges off mid-Norway: Products of sediment degassing. Marine Geology 218, 191-206.

Hunt, J.E., Wynn, R.B., Talling, P.J., Masson, D.G., 2013. Frequency and timing of landslide-triggered turbidity currents within the Agadir Basin, offshore NW Africa: Are there associations with climate change, sea level change and slope sedimentation rates? Marine Geology 346, 274-291.

Knoll, M., Hernández-Guerra, A., Lenz, B., López Laatzen, F., Machín, F., Müller, T.J., Siedler, G., 2002. The Eastern Boundary Current system between the Canary Islands and the African Coast. Deep Sea Research Part II: Topical Studies in Oceanography 49, 3427-3440.

Krastel, S., Behmann, J.-H., Völker, D., Stipp, M., Berndt, C., Urgeles, R., Chaytor, J., Huhn, K., Strasser, M., Harbitz, C.B., 2014.Submarine mass movements and their consequences.6th International Symposium. Advances in Natural and Technological Research 37, pp 683.

Krastel, S., Wynn, R.B., Feldens, P., Schürer, A., Böttner, C., Stevenson, C., Cartigny, M.J.B., Hühnerbach, V., Unverricht, D., 2016. Flow Behaviour of a Giant Landslide and Debris Flow Entering Agadir Canyon, NW Africa, in: Lamarche, G., Mountjoy, J., Bull, S., Hubble, T., Krastel, S., Lane, E., Micallef, A., Moscardelli, L., Mueller, C., Pecher, I., Woelz, S. (Eds.), Submarine Mass Movements and their Consequences: 7th International Symposium. Springer International Publishing, Cham, pp. 145-154.

Krastel, S., Wynn, R.B., Georgiopoulou, A., Geersen, J., Henrich, R., Meyer, M., Schwenk, T., 2012.Large-Scale Mass Wasting on the Northwest African Continental Margin: Some General Implications for Mass Wasting on Passive Continental Margins. 189-199.

Krastel, S., Wynn, R.B., Hanebuth, T.J.J., Henrich, R., Holz, C., Meggers, H., Kuhlmann, H., Georgiopoulou, A., Schulz, H.D., 2006.Mapping of seabed morphology and shallow sediment structure of the Mauritania continental margin, Northwest Africa: some implications for geohazard potential. Norwegian Journal of Geology 86, 163-176.

Kuenen, Ph. H., Migliorini, C.I., 1950. Turbidity currents as a cause of graded bedding. Journal of Geology, 58, 91-127.

Kvalstad, T.J., Andresen, L., Forsberg, C.F., Berg, K., Bryn, P., Wangen, M., 2005.The Storegga slide: evaluation of triggering sources and slide mechanics. Marine and Petroleum Geology 22, 245-256.

Laberg, J.S., Camerlenghi, A., 2008. The Significance of Contourites for Submarine Slope Stability, in: Rebesco, M., Camerlenghi, A. (Eds.), Developments in Sedimentology. Elsevier, pp. 537-556.

Laberg, J., Vorren, T., Mienert, J., Bryn, P., Lien, R., 2002. The Trænadjupet Slide: a large slope failure affecting the continental margin of Norway 4,000 years ago. Geo-Marine Letters 22, 19-24.

Lange, C.B., Romero, O.E., Wefer, G., Gabric, A.J., 1998. Offshore influence of coastal upwelling off Mauritania,

NW Africa, as recorded by diatoms in sediment traps at 2195 m water depth. Deep Sea Research Part I: Oceanographic Research Papers 45, 985-1013.

Leynaud, D., Mienert, J., Vanneste, M., 2009.Submarine mass movements on glaciated and non-glaciated European continental margins: A review of triggering mechanisms and preconditions to failure. Marine and Petroleum Geology 26, 618-632.

Leynaud, D., Sultan, N., Mienert, J., 2007. The role of sedimentation rate and permeability in the slope stability of the formerly glaciated Norwegian continental margin: the Storegga slide model. Landslides 4, 297-309.

Masson, D.G., 1994. Late Quaternary turbidity current pathways to the Madeira Abyssal Plain and some constraints on turbidity current mechanisms. Basin Research 6, 17-33.

Martorelli, E., Bosman, A., Casalbore, D., Falcini, F., 2016. Interaction of down-slope and along-slope processes off Capo Vaticano (southern Tyrrhenian Sea, Italy), with particular reference to contourite-related landslides. Marine Geology 378, 43-55.

Masson, D.G., Harbitz, C.B., Wynn, R.B., Pedersen, G., Lovholt, F., 2006. Submarine landslides: processes, triggers and hazard prediction. Philosophical transactions.Series A, Mathematical, physical, and engineering sciences 364, 2009-2039.

McGinnis, J.P., Hayes, D.E., 1995. The Roles of Downslope and Along-Slope Depositional Processes: Southern Antarctic Peninsula Continental Rise, Geology and Seismic Stratigraphy of the Antarctic Margin. American Geophysical Union, pp. 141-156.

Meyer, M., Geersen, J., Krastel, S., Schwenk, T., Winkelmann, D., 2012. Dakar Slide Offshore Senegal, NW-Africa: Interaction of Stacked Giant Mass Wasting Events and Canyon Evolution, in: Yamada, Y., Kawamura, K., Ikehara, K., Ogawa, Y., Urgeles, R., Mosher, D., Chaytor, J., Strasser, M. (Eds.), Submarine Mass Movements and Their Consequences. Springer Netherlands, pp. 177-188.

Michels, K.H., Rogenhagen, J., Kuhn, G., 2001. Recognition of contour-current influence in mixed contourite-turbidite sequences of the western Weddell Sea, Antarctica. Marine Geophysical Researches 22, 465-485.

Moscardelli, L., Wood, L., Mann, P., 2006. Mass-transport complexes and associated processes in the offshore area of Trinidad and Venezuela. AAPG Bulletin 90, 1059-1088.

Moscardelli, L., Wood, L., 2015. Morphometry of mass-transport deposits as a predictive tool.Geological Society of America Bulletin.

Mulder, T., 2011. Gravity Processes and Deposits on Continental Slope, Rise and Abyssal Plains, in: Heiko, H., Thierry, M. (Eds.), Developments in Sedimentology. Elsevier, pp. 25-148.

Mulder, T., Syvitski, J.P.M., 1995.Turbidity currents generated at river mouths during exceptional discharges into the world oceans. Journal of Geology 103, 285-299.

Pereira, R., Alves, T.M., 2011. Margin segmentation prior to continental break-up: A seismic–stratigraphic record of multiphased rifting in the North Atlantic (Southwest Iberia). Tectonophysics 505, 17-34.

Piper, D.J.W., Cochonat, P., Morrison, M.L., 1999. The sequence of events around the epicentre of the 1929 Grand Banks earthquake: initiation of debris flows and turbidity current inferred from sidescan sonar. Sedimentology 46, 79-97.

Rasmussen, E. S., 1994, The relationship between submarine canyon fill and sea level change: An example from middle Miocene offshore Gabon, west Africa: Sedimentary Geology, v. 90, p. 61-75.

Rebesco, M., Camerlenghi, A., Volpi, V., Neagu, C., Accettella, D., Lindberg, B., Cova, A., Zgur, F., Party, M., 2007. Interaction of processes and importance of contourites: insights from the detailed morphology of sediment Drift 7, Antarctica. Geological Society, London, Special Publications 276, 95-110.

Rebesco, M., Hernández-Molina, F.J., Van Rooij, D., Wåhlin, A., 2014. Contourites and associated sediments controlled by deep-water circulation processes: State-of-the-art and future considerations. Marine Geology 352, 111-154.

Rebesco, M., Pudsey, C.J., Canals, M., Camerlenghi, A., Barker, P.F., Estrada, F., Giorgetti, A., 2002. Sediment drifts and deep-sea channel systems, Antarctic Peninsula Pacific Margin. Geological Society, London, Memoirs 22, 353-371.

Rothwell, R.G., Pearce, T.J., Weaver, P.P.E., 1992. Late Quaternary evolution of the Madeira Abyssal Plain, Canary Basin, NE Atlantic.Basin Research 4, 103-131.

Sarnthein, M., Thiede, J., Pflaumann, U., Erlenkeuser, H., Fütterer, D., Koopmann, B., Lange, H., Seibold, E., 1982. Atmospheric and Oceanic Circulation Patterns off Northwest Africa During the Past 25 Million Years, in: von Rad, U., Hinz, K., Sarnthein, M., Seibold, E. (Eds.), Geology of the Northwest African Continental Margin. Springer Berlin Heidelberg, Berlin, Heidelberg, pp. 545-604.

Seibold, E., 1982. The Northwest African Continental Margin — An Introduction, in: von Rad, U., Hinz, K., Sarnthein, M., Seibold, E. (Eds.), Geology of the Northwest African Continental Margin. Springer Berlin Heidelberg, Berlin, Heidelberg, pp. 3-20.

Seibold, E., Hinz, K., 1974. Continental Slope Construction and Destruction, West Africa, in: Burk, C.A., Drake, C.L. (Eds.), The Geology of Continental Margins. Springer Berlin Heidelberg, Berlin, Heidelberg, pp. 179-196.

Shanmugam, G., 2000. 50 years of the turbidite paradigm (1950s-1990s): deep-water processes and facies models-a critical perspective. Marine and Petroleum Geology 17, 285-342.

Shanmugam, G., 2016, Slides, Slumps, Debris Flows, Turbidity Currents, and Bottom Currents, Reference Module in Earth Systems and Environmental Sciences, Elsevier.

Shanmugam, G., Spalding, T.D., Rofheart, D.H., 1993. Traction structures in deep-marine, bottom-current-reworked sands in the Pliocene and Pleistocene, Gulf of Mexico.Geology 21, 929-932.

Solheim, A., Berg, K., Forsberg, C.F., Bryn, P., 2005. The Storegga Slide complex: repetitive large scale sliding with similar cause and development. Marine and Petroleum Geology 22, 97-107.

Stevenson, C.J., Jackson, C.A.-L., Hodgson, D.M., Hubbard, S.M., Eggenhuisen, J.T., 2015.Deep-Water Sediment

Bypass. Journal of Sedimentary Research 85, 1058-1081.

Stevenson, C.J., Talling, P.J., Sumner, E.J., Masson, D.G., Frenz, M., Wynn, R.B., 2014. On how thin submarine flows transported large volumes of sand for hundreds of kilometres across a flat basin plain without eroding the sea floor. Sedimentology 61, 1982-2019.

Stigall, J., Dugan, B., 2010. Overpressure and earthquake initiated slope failure in the Ursa region, northern Gulf of Mexico. Journal of Geophysical Research: Solid Earth 115, B04101.

Stow, D.A.V., Faugères, J.-C., Howe, J.A., Pudsey, C.J., Viana, A.R., 2002. Bottom currents, contourites and deep-sea sediment drifts: current state-of-the-art. Geological Society, London, Memoirs 22, 7-20.

Stow, D.A.V., Hernández-Molina, F.J., Llave, E., Sayago-Gil, M., Díaz del Río, V., Branson, A., 2009. Bedform-velocity matrix: The estimation of bottom current velocity from bedform observations. Geology 37, 327-330.

Stow, D.A.V., Mayall, M., 2000. Deep-water sedimentary systems: New models for the 21st century. Marine and Petroleum Geology 17, 125-135.

Sultan, N., Cochonat, P., Canals, M., Cattaneo, A., Dennielou, B., Haflidason, H., Laberg, J.S., Long, D., Mienert, J., Trincardi, F., Urgeles, R., Vorren, T.O., Wilson, C., 2004. Triggering mechanisms of slope instability processes and sediment failures on continental margins: a geotechnical approach. Marine Geology 213, 291-321.

Talling, P.J., Amy, L.A., Wynn, R.B., 2007. New insight into the evolution of large-volume turbidity currents: comparison of turbidite shape and previous modelling results. Sedimentology 54, 737-769.

Talling, P.J., Masson, D.G., Sumner, E.J., Malgesini, G., 2012. Subaqueous sediment density flows: Depositional processes and deposit types. Sedimentology 59, 1937-2003.

Tappin, D. R., Grilli, S. T., Harris, J. C., Geller, R. J., Masterlark, T., Kirby, J. T., Shi, F., Ma, G., Thingbaijam, K. K. S., and Mai, P. M., 2014. Did a submarine landslide contribute to the 2011 Tohoku tsunami? Marine Geology, v. 357, p. 344-361.

Tappin, D.R., Watts, P., McMurtry, G.M., Lafoy, Y., Matsumoto, T., 2001. The Sissano, Papua New Guinea tsunami of July 1998: Offshore evidence on the source mechanism. Marine Geology 175, 1-23.

Trincardi, F., Verdicchio, G., Miserocchi, S., 2007.Seafloor evidence for the interaction between cascading and along-slope bottom water masses. Journal of Geophysical Research: Earth Surface 112, 1-11.

van Aken, H.M., 2000. The hydrography of the mid-latitude northeast Atlantic Ocean: I: The deep water masses. Deep Sea Research Part I: Oceanographic Research Papers 47, 757-788.

Viana, A.R., Faugères, J.-C., 1998. Upper slope sand deposits: the example of Campos Basin, a latest Pleistocene-Holocene record of the interaction between alongslope and downslope currents. Geological Society, London, Special Publications 129, 287-316.

von Rad, U., Wissmann, G., 1982. Cretaceous-Cenozoic History of the West Saharan Continental Margin (NW Africa): Development, Destruction and Gravitational Sedimentation, in: von Rad, U., Hinz, K., Sarnthein, M.,

Seibold, E. (Eds.), Geology of the Northwest African Continental Margin. Springer Berlin Heidelberg, Berlin, Heidelberg, pp. 106-131.

Weaver, P.P.E., Kuijpers, A., 1983. Climatic control of turbidite deposition on the Madeira Abyssal Plain. Nature 306, 360-363.

Weaver, P.P.E., Wynn, R.B., Kenyon, N.H., Evans, J., 2000.Continental margin sedimentation, with special reference to the north-east Atlantic margin. Sedimentology 47, 239-256.

Wynn, R.B., Masson, D.G., Stow, D.A.v., Weaver, P.P.E., 2000. The Northwest African slope apron: a modern analogue for deep-water systems with complex seafloor topography. Marine and Petroleum Geology 17, 253-265.

Wynn, R.B., Talling, P.J., Masson, D.G., Stevenson, C.J., Cronin, B.T., Le Bas., T.P., 2010. Investigating the timing, processes and deposits of one the World's largest submarine gravity flows: the 'Bed 5 event' off northwest Africa. In Mosher, D.C., Moscardelli, L., Shipp, C., Chaytor, J.D., Baxter, D.P., Lee, H.J. and Urgeles, R. (eds) Submarine mass movements and their consequences: Advances in Natural and Technological Hazards Research 28, Springer, 463-474.

Wynn, R.B., Weaver, P.P.E., Masson, D.G., Stow, D.A.V., 2002. Turbidite depositional architecture across three interconnected deep-water basins on the north-west African margin. Sedimentology 49, 669-695.

2 Manuscript I

Morphology, age and sediment dynamics of the upper headwall of the Sahara Slide Complex, Northwest Africa: Evidence for a large Late Holocene failure

Wei Li[a]*, Tiago M. Alves[b], Morelia Urlaub[c],Aggeliki Georgiopoulou[d],Ingo Klaucke[c], Russell B. Wynn[e], Felix Gross[a],Mathias Meyer[c],Janne Repschläger[a], Christian Berndt[c], Sebastian Krastel[a]

[a]Institute of Geosciences, University of Kiel, Kiel 24118, Germany

[b] 3D Seismic Lab, School of Earth and Ocean Sciences, Cardiff University, Main Building, Park Place, Cardiff, CF10 3AT, United Kingdom

[c]GEOMAR Helmholtz Centre for Ocean Research Kiel, 24148 Kiel, Germany

[d]UCD School of Earth Sciences, University College Dublin, Belfield, Dublin 4, Ireland

[e]National Oceanography Centre, European Way, Southampton, Hampshire SO14 3ZH, United Kingdom

*Correspondence to: Wei Li (li@geophysik.uni-kiel.de)

Abstract

The Sahara Slide Complex in Northwest Africa is a giant submarine landslide with an estimated run-out length of ~ 900 km. We present newly acquired high-resolution multibeam bathymetry, sidescan sonar, and sub-bottom profiler data to investigate the seafloor morphology, sediment dynamics and the timing of formation of the upper headwall area of the Sahara Slide Complex.The data reveal a ~35 km-wide upper headwall opening towards the northwest with multiple slide scarps, glide planes,plateaus, lobes, slide blocks and slide debris. The slide scarps in the study area are formed by retrogressive failure events, which resulted in two types of mass movements, translational sliding and spreading. Three different glide planes (GP I, II, and III) can be distinguished approximately 100 m, 50 m and 20 m below the seafloor. These glide planes are widespread and suggest failure along pronounced, continuous weak layers.Our new data suggest an age of only about 2 ka for the failure of the upper headwall area, a date much younger than derived for the landslide deposits on the lower reaches of the Sahara Slide Complex, which are dated at 50-60 ka. The young age of the failure contradicts the postulate of a stable slope off Northwest Africa during times of relative stable sea-level highstands. Such an observation suggests that submarine-landslide risk along the continental margin of Northwest Africa should be reassessed based on a robust dating of proximal and distal slope failures.

1 Introduction

Submarine landslides are a widespread phenomenon documented in multiple geological settings such as tectonically active margins, passive continental margins and volcanic islands (Masson et al., 2006; Moernaut and De Batist, 2011; Krastel et al., 2014; Lamarche et al., 2016). Submarine landslides transport large volumes of sediments into deeper continental slope and abyssal areas, and some present sufficient density and speed to pose important hazards to anthropogenic structures in shallower water (Lo Iacono et al., 2012). Submarine landslides have in the past generated tsunamis causing widespread damage to coastal communities (Harbitz et al., 2014). In addition, turbidity currents generated by submarine landslides are one of the most important near-seafloor geohazards, as they can potentially damage deep-water equipment and engineering infrastructure such as pipelines and communication lines (Piper and Aksu, 1987; Masson et al., 2006; Talling et al., 2014). Hence, the recognition of submarine landslides on continental margins is important to: a) the recognition of areas prone to slope instability on modern continental slopes, b) the investigation of possible triggers of slope instability, and c) the investigation of the global causes of submarine landsliding such as eustasy, tectonics, and climatic events (Vanneste et al., 2014). Other factors that have been proposed to trigger submarine landslides at a local scale include high sedimentation rates (Leynaud et al., 2007; Li et al., 2014), excess pore pressure (Berndt et al., 2012), gas hydrate dissociation (Sultan et al., 2004) and earthquakes (Sultan et al., 2004; Zhao et al., 2015).

In Northwest Africa, multiple large-scale submarine landslides have occurred during the Quaternary (Krastel et al. 2012). The most prominent submarine landslides in the region include the Sahara Slide Complex (Embley, 1982; Gee et al., 1999; Georgiopoulou et al., 2010), the Mauritania Slide Complex (Antobreh and Krastel, 2007; Henrich et al. 2008; Förster et al. 2010), the Cap Blanc Slide (Krastel et al., 2006) and the Dakar Slide (Meyer et al., 2012). The Sahara Slide Complex is one of the largest known submarine slides in the world, and affected an area of 48,000 km^2 of the Northwest African Margin (Embley et al., 1982; Fig. 1). During a period of rapid sea-level rise at ~50-60 ka, high primary productivity in surface waters offshore Northwest Africa resulted in the accumulation of fine-grained pelagic/hemipelagic sediment on the continental slope (Bertrand et al., 1996; Krastel et al., 2006). Multiple slide events were interpreted to have occurred retrogressively at this time (Georgiopoulou et al., 2007; 2009). As a result, the Sahara Slide Complex remobilised ~600 km^3 of sediments along a distance of ~900 km (Georgiopoulou et al., 2010). The slide eroded and entrained a volcaniclastic layer when passing close to the Canary Islands, generating a two-phase debris flow; a lower volcaniclastic debris-flow phase and an upper pelagic debrite (Gee et al., 1999; Georgiopoulou et al, 2010). The long runout-distance of the flow

was explained by retaining excess pore pressure in the lower volcaniclastic debris flow phase, which acted as a lubricating carpet for the overlying relatively impermeable pelagic debris flow phase (Gee et al., 1999; Georgiopoulou et al., 2010).
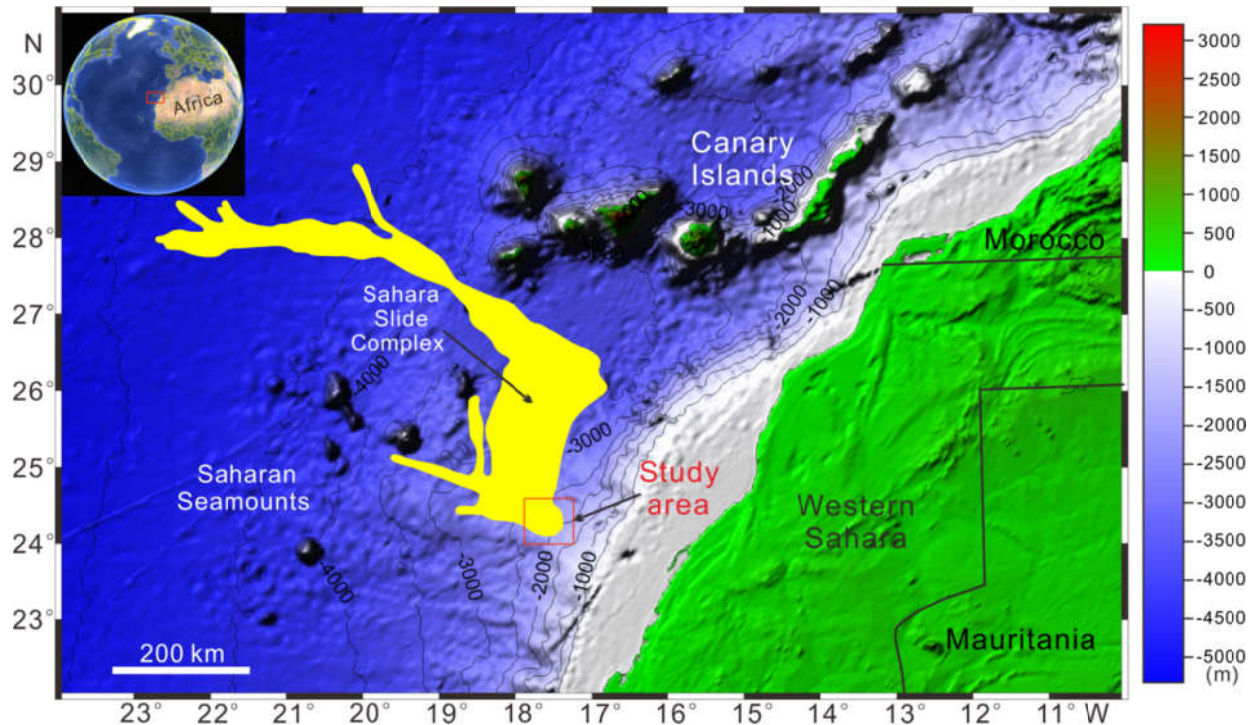
Fig. 1 Combined bathymetric and topographic map highlighting the distribution of the Sahara Slide Complex, which is marked in yellow (modified after Wynn et al., 2000; Georgiopoulou et al., 2010). Key bathymetric and structural features include the Saharan Seamounts to the west of the Sahara Slide, and the Canary Islands to the north of the study area. The red box represents the precise location of the study area. Bathymetric contours are shown as black solid lines with intervals of 1000 m.

Most of the published geological information on the Sahara Slide Complex has been acquired in its distal depositional part (Gee et al., 1999; 2001; Georgiopoulou et al., 2009; 2010). However, limited attention has been paid to its headwall, chiefly due to the lack of high-quality data on the upper continental slope of Northwest Africa. Reconnaissance data show that the Sahara Slide Complex is marked by the presence of two major scarps (named lower and upper headwall scarps), each up to 100 m high (Fig. 2). Sparse seismic lines suggested stacked landslide deposits (Georgiopoulou et al., 2010; Krastel et al., 2012).
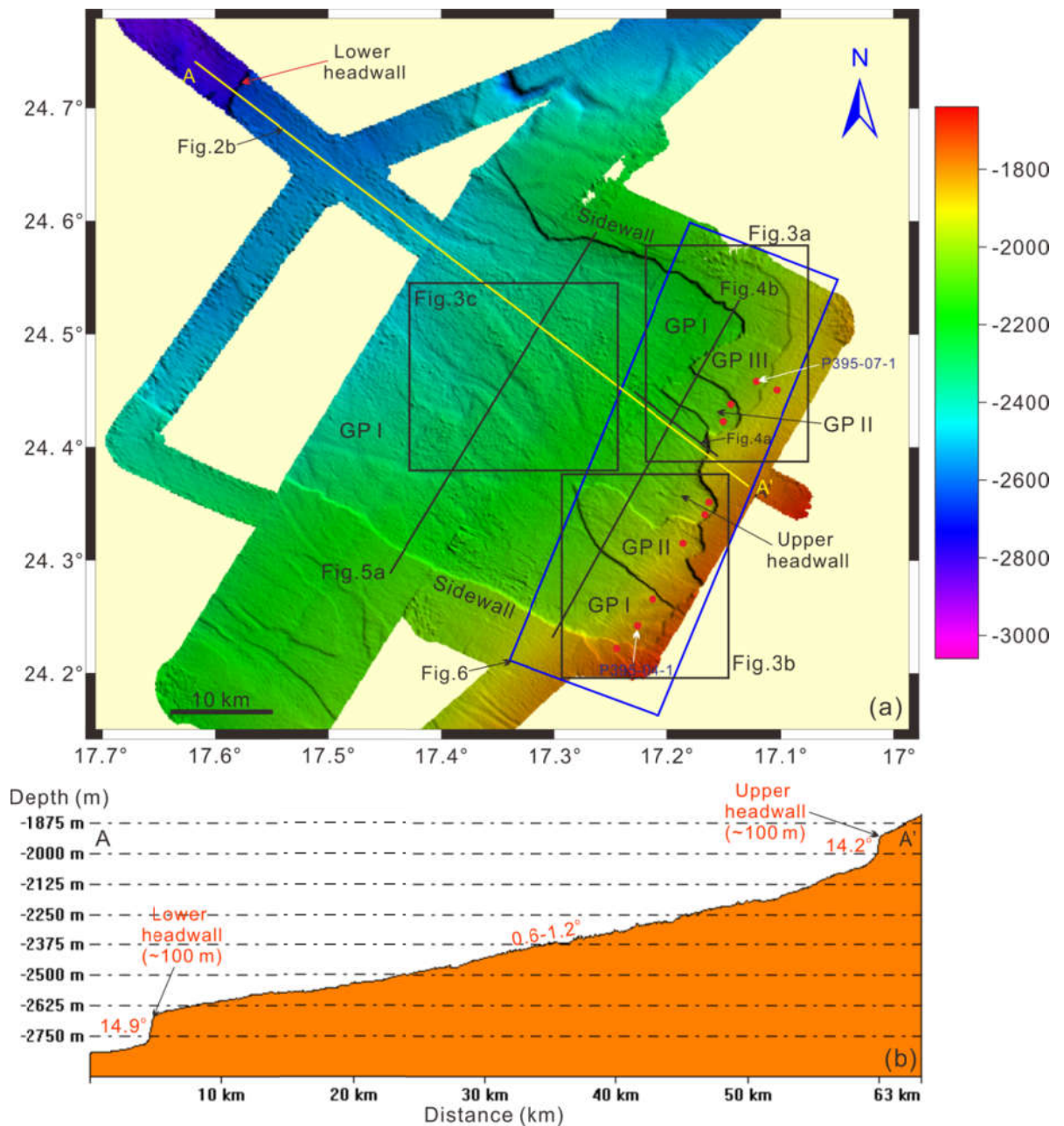
Fig. 2 (a) Multibeam bathymetric map of the headwall of the Sahara Slide Complex. The map highlights the presence of a complex headwall and associated sidewall scarps. The black boxes show the locations of the illuminated perspective views in Fig. 3. Interpreted sidescan sonar mosaics are outlined by the blue box (see detail in Fig. 6). The black solid lines indicate the Parasound profiles used in this study (Figs. 4a, b and 5a). Contours are shown at intervals of 200 m. The red circles represent the locations of sediment cores acquired during Cruise P395. (b) Profile A-A' (see location in Fig. 2a) illustrates the locations of the upper and lower headwall; each one with a height of ~100 m.

In this manuscript, we present a combination of new high-resolution multibeam bathymetry, sidescan sonar, sub-bottom profiler, and sediment gravity-core data from the upper headwall of the

Sahara Slide Complex. This manuscript presents the first detailed morphological analysis of the upper headwall of the Sahara Slide Complex, so we:

a) Determine the distribution, relative timing and estimated volumes of the different slide events in order to reconstruct the evolution of the upper headwall;

b) Analyse the different types of mass movements that occurred in the investigated area;

c) Discuss the timing of slope failures;

d) Assess the hazards related to the failure of the upper headwall.

The study contributes to the wider discussion about the stability of continental margins during the present-day relative sea-level high stand (e.g., Owen et al., 2007; Lee; 2009; Smith et al., 2013). We show that it is crucial to investigate both landslide deposits and the failure area in order to reconstruct the evolution of submarine slide complexes.

2 Geological setting

The Northwest African continental margin is one of the best-studied passive margins in the world. On this margin, earthquakes of magnitude M≥7 have rarely been recorded away from the Gulf of Cadiz (Seibold, 1982), but moderate earthquakes (4≤M≤6) are commonly observed in association with the reactivation of old weakness zones created during the opening of the Atlantic Ocean (Hayes and Rabinowitz, 1975; Pereira and Alves, 2011). The width of the continental shelf of Northwest Africa is generally 40-60 km, reaching a maximum width of more than 100 km offshore Western Sahara (Fig. 1). The shelf break is observed at a water depth between 100 m and 200 m (Fig. 1; Wynn et al., 2000). The continental slope dips 1° to 6° from a depth of 200 to 1500 metres, while the continental rise is less than 1° beyond a depth of 4000 m. The Northwest African continental margin has been affected by complex sediment transport processes since its inception (Wynn et al., 2000; Krastel et al., 2012).

Most of the continental margin of Northwest Africa is now arid and records limited sediment supply by rivers, even during past glacial times (Weaver et al., 2000; Wynn et al., 2000). The margin is affected by both a seasonal and permanent oceanic upwelling system (Lange et al., 1998). Upwelling and associated high organic productivity are concentrated along the outer shelf and upper slope regions, resulting in sedimentation rates of 5 cm/ka on average, which increased to 16.5 cm/ka during the last glacial period (Bertrand et al., 1996; Weaver et al. 2000). Deep-water hemipelagic sedimentation in Northwest Africa typically consists of silts, muds, carbonate-rich marls and oozes (Weaver and Kuijpers, 1983). Wind-blown sediments transported from the Sahara Desert provide additional terrigenous sediment supply to the Northwest African continental margin (Holz et al., 2004; Henrich et al., 2008).

3 Data and methods

The dataset used in this study consists of deep-towed sidescan sonar, multibeam bathymetry and gravity cores collected at the upper headwall of the Sahara Slide Complex (Fig. 2a). Sub-bottom profiler data mounted on the sidescan sonar and a hull-mounted Parasound system were also interpreted in this work.

3.1 Acoustic data

The bulk of multibeam bathymetric data were collected during Cruise MSM11/2 (Bickert and cruise participants, 2011) using a hull-mounted Kongsberg Simrad system EM120. The nominal sonar frequency of this system is 12 kHz with an angular coverage sector of up to 150°. A total of 191 beams were recorded for each ping. The data were gridded at 50 m; vertical resolution is in the range of 5 -10 m. Sidescan sonar data were acquired during Cruise P395 using an EdgeTech DTS-1 sonar (Krastel and cruise participants, 2011). This sidescan sonar system was towed around 100 m above the seafloor and it worked with an operating frequency centered at 75 kHz; swath range per side was 750 m. The 75 kHz signal has a bandwidth of 7.5 kHz with a pulse length of 14 ms. Horizontal resolution after processing is 1 m, which enables the identification of complex morphological and sedimentary features based on the observed variations in backscatter (Golbeck, 2010).

Deep-towed sub-bottom profiler data were collected with the sidescan sonar mosaic during cruise P395. The profiler operated with chirp based frequencies ranging from 2 kHz and 10 kHz, for a 20 ms pulse length. These frequencies provide a penetration depth of up to 30 m and a vertical resolution of a few decimeters (Golbeck, 2010). Parasound sub-bottom seismic profiles acquired during RV Meteor M58/1 and RV Maria S. Merian MSM11/2expeditions complete the geophysical dataset utilised in this work. The Parasound system DS3 (Atlas Hydrographic®) is a hull-mounted parametric sub-bottom profiler with an opening angle of only 4°. The selected frequency was 4 kHz, providing a sub-meter vertical resolution for strata below the seafloor.

3.2 Gravity cores and dating

Sediment cores were collected in the upper headwall of the Sahara Slide by utilising a standard gravity corer equipped with a 5-m barrel. In total, 10 gravity cores were acquired in the upper headwall, nine (9) from the landslide area and one (1) from undisturbed sediments above the headwall area (Fig. 2a). A sample for dating the undisturbed drape on top of landslide deposits was taken from Core P395-07-1 (24°27,36' N, 17°08,18' W) collected at a water depth of 2132 m (Figs.

2a). The sample was taken 3 cm below the seafloor (bsf), which is the interval of the first hemipelagites that drape the debris deposits. No other cores included sufficient undisturbed sediment drape for dating on top of the landslide deposits. Remnants of brownish Holocene sediments were found in a few core liners, suggesting that some undisturbed sediment drape was lost during core recovery, but we do not have any indication of a loss of more than 10 cm of surface sediments. As we were not able to date the Holocene drape in any other gravity core, we took an additional sample from Core P395-04-1 (24°14,70' N, 17°13,40' W) for our datings. Core P395-04-01 was collected at a water depth of 1930 m(Fig. 2a). The sample in the core was taken in 5 cm bsf in a clast remobilized together with the slide deposits. Hence this sample provides a maximum age of the failure.

Accelerated Mass Spectrometry (AMS) ^{14}C-age dating was applied on monospecific samples of the planktonic foraminifera *Globigerinoides ruber* (w) and it was carried out by the ^{14}C-age Leibniz-Laboratory of Kiel University, Germany. The conventional ^{14}C age was calculated according to Stuiver and Polach (1977) method. A ^{13}C correction for isotopic fractionation was applied to the method based on the ^{13}C/^{12}C ratio measured by the AMS-system simultaneously with the ^{14}C/^{12}C ratio. The Calib 7.1 software, in combination with the Marine13 calibration curve, was used to calibrate the radiocarbon age (Stuiver and Reimer, 1986; Reimer et al. 2013). A reservoir age of ±500 years was assumed for the calibration of the radiocarbon age (e.g., Mangerud and Gulliksen, 1975).

To estimate the age of the Sahara Slide we follow the method in Urlaub et al. (2013). We consider the location of the sample to date (vertical distance to the top of the landslide) as the main uncertainty in our analyses, and we do not take into account the measurement error of the ^{14}C AMS method. The sample in Core P395-07-1 was obtained very close (1 cm above) to the slide deposits, i.e. comprising the first 'background' hemipelagites deposited after the slide event. The age of the slide is calculated as the radiocarbon age of the sample + D_{sf}/SR, where D_{sf} is the distance from the sample location to the upper surface of the slide deposit, and SR is the sedimentation rate (Urlaub et al., 2013).

4 Results

The failure area of the Sahara Slide Complex consists of two major headwalls, which are called lower and upper headwalls in the following sections. Each of the headwall scarps has height of about 100 m (Fig. 2b). The upper headwall is found at a water depth of about 2000 m, while the lower headwall is located ~50 km downslope at a water depth of ~2700 m. In this paper we focus on the upper headwall, as only sparse data are available from the lower headwall.
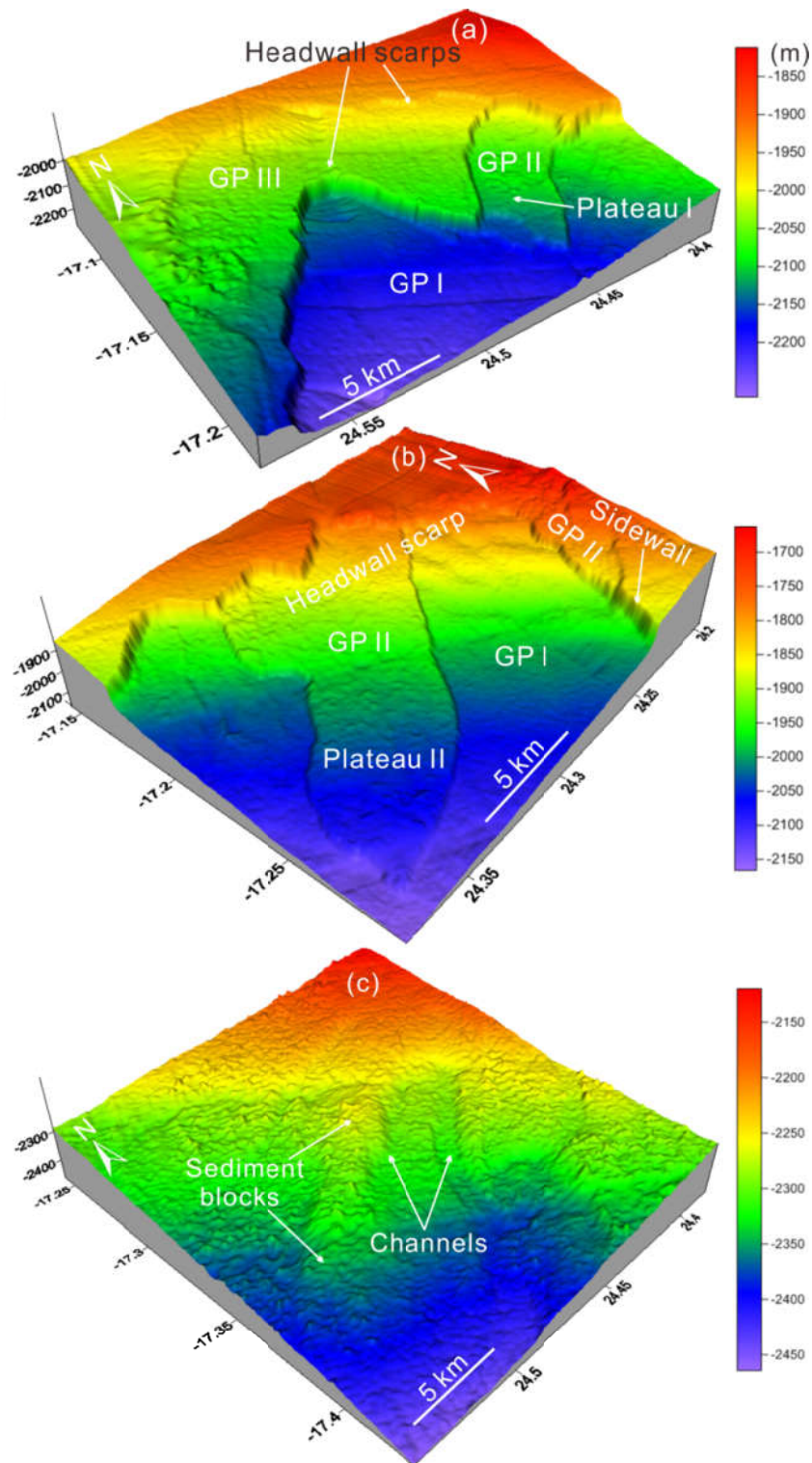
4.1 Morphology of the upper headwall

The upper headwall of the Sahara Slide Complex has an average width of ~35 km and is U-shaped, facing the northwest (Fig. 2a). Several morphological features, including slide scarps, glide planes, plateaus, slide lobes and slide blocks can be identified on the acoustic data (Figs. 2 to 5). In the following sub-sections, we will describe the morphology of the main seafloor features.

4.1.1 Slide scarps

The bathymetric data show significant sediment evacuation from the Sahara Slide Complex's headwall, with well-exposed scarps (Figs. 3a and 3b). The upper headwall is located at water depths between 1800 m and 2100 m, where slope gradients range from 4° to 23° (Fig. 2a). The height of the headwall scarps ranges from 20 m to 100 m. Two sidewall scarps show a SE-NW direction. Sidewall scarps are steep with gradients of 7°-18° and have heights of 47 m to 86 m, cutting into stratified deposits (Figs. 2a, 4b and 5b).

4.1.2 Glide planes

Three glide planes rooted at different stratigraphic depths, but all parallel to stratigraphy, are observed on both bathymetric and Parasound data (Figs. 3a, b and 4b). These glide planes, GP I, GP II and GP III, are respectively located ~100 m, ~50 m and ~20 m below a relatively undisturbed seafloor (Fig. 4b). The three glide planes are separated by steep scarps and seem to be planar, with only a few undulations observed in the study area (Figs. 3a and b). On the Parasound profiles, a thin layer (~10-15 m) of slide deposits characterised by chaotic reflections is separated by glide planes from the underlying strata (Figs. 4a, b, 5b and c).

Fig. 3 Three-dimensional (3D) perspective of the upper headwall of the Sahara Slide. See Fig. 2 for location of the 3D views. (a) Northeastern part of the upper headwall showing key morphological features including headwall scarps, glide planes (GPI, GPII and GP III) and Plateau I. (b) Southeastern part of the upper headwall showing headwall scraps, sidewall scarps and glide planes (GPI, GPII and GP III). (c) Central part of the upper headwall showing multiple sediment blocks and erosive channels.

4.1.3 Plateaus

Two large plateaus are identified in the central part of the study area; Plateau I and Plateau II (Figs. 2, 3a and b). Plateau I is located in the northeastern part of the study area. It has an average length of 7 km and an average width of 4 km. Plateau II is located in the southeastern part of the study area, showing an average length of 14 km and an average width of 6 km. The height of Plateaus I and II is approximately 30 m above the level of GP I.The morphology of both plateaus reveals the presence of several slide blocks (Figs. 3a and b).
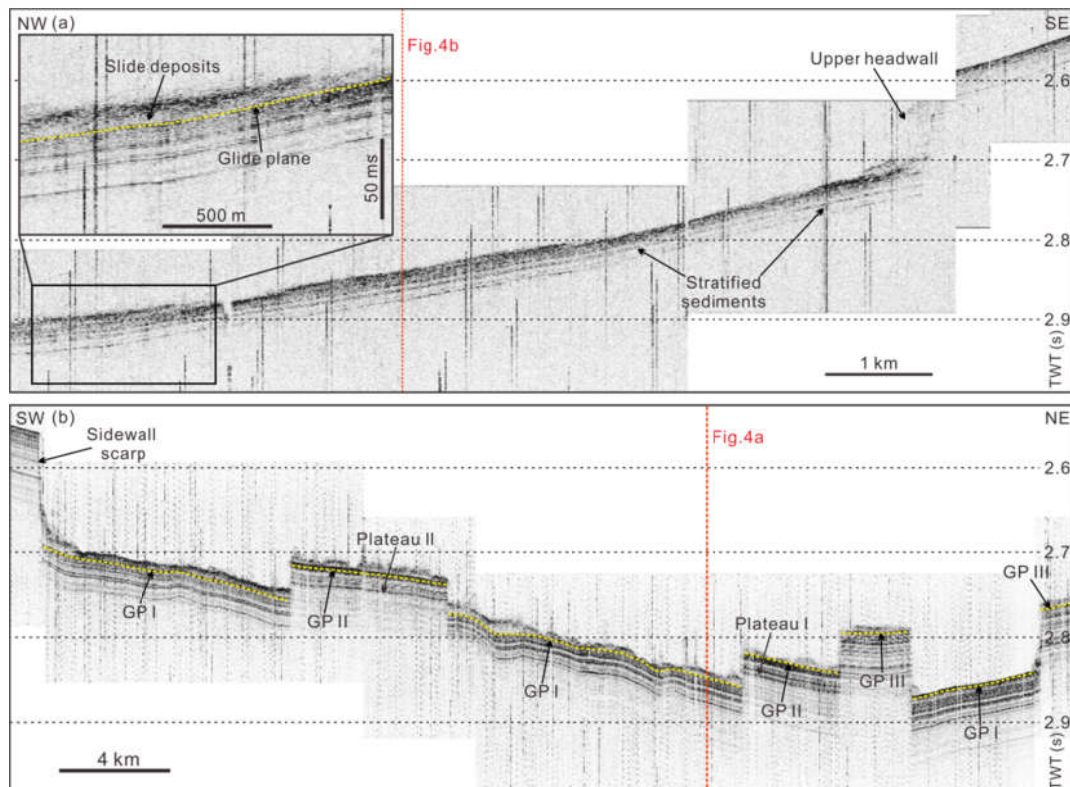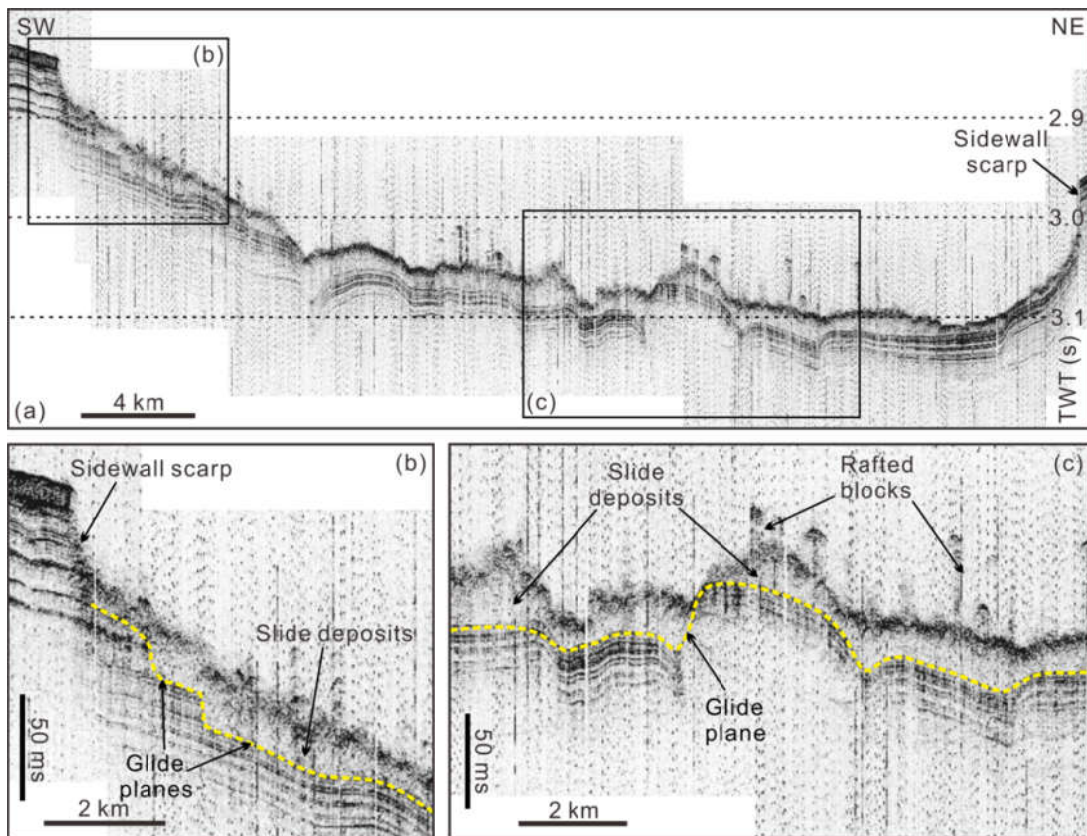

Fig. 4 (a) Parasound profile crossing the upper headwall towards the distal part of the Sahara Slide. The zoomed section reveals stratified sediments separated by a glide plane from slide deposits above. (b) Along-slope Parasound profile crossing the upper headwall showing a sidewall scarp, and Plateaus I and II. Three different glide planes (GP I, II and III) are highlighted in the figure by a yellow dashed line. The locations of the profiles are shown in Fig. 2.

4.1.4 Slide lobes

Slide lobes as defined based on data from the Storegga Slide (Haflidason et al., 2004) are individual or group of mass movements. Two slide lobes are visible in the upper headwall on the sidescan sonar mosaic (Fig. 6). One lobe is located to the south of the headwall, whereas a second lobe is located on the northwestern part of Plateau I.

Fig. 5 (a) Parasound profile crossing the distal part of the upper headwall of the Sahara Slide Complex, along the continental slope. The profile shows well-developed sidewall scarps and numerous slide blocks. (b) Zoomed section imaging slide deposits over two distinct glide planes. The yellow dashed line highlights the position of the glide plane. (c) Zoomed section revealing the slide deposits and the underlying undulated glide plane. Location of profile is shown in Fig. 2.

4.1.5 Hummocky topography with slide blocks

Slide blocks are widespread in the upper headwall and particularly found above GPI and GP II (Fig. 3). The deposits show a characteristic hummocky geometry especially in lower half of GP I (Fig. 3c). In contrast, the shallowest part of the GP I area is relatively smooth (Figs. 3a and b). The slide blocks can also be identified from Parasound profiles crossing the deeper part of GP I (Fig. 5c). The diameter of the imaged blocks reaches a maximum of 500 m and a maximum height of 35 m (Fig. 3c).

4.2 Acoustic facies

Sidescan sonar data provide a detailed image of seafloor morphology and texture in the upper headwall of the Sahara Slide Complex (Figs. 6 and 7). Based on observed variations in backscatter character, we defined four different types of acoustic facies.
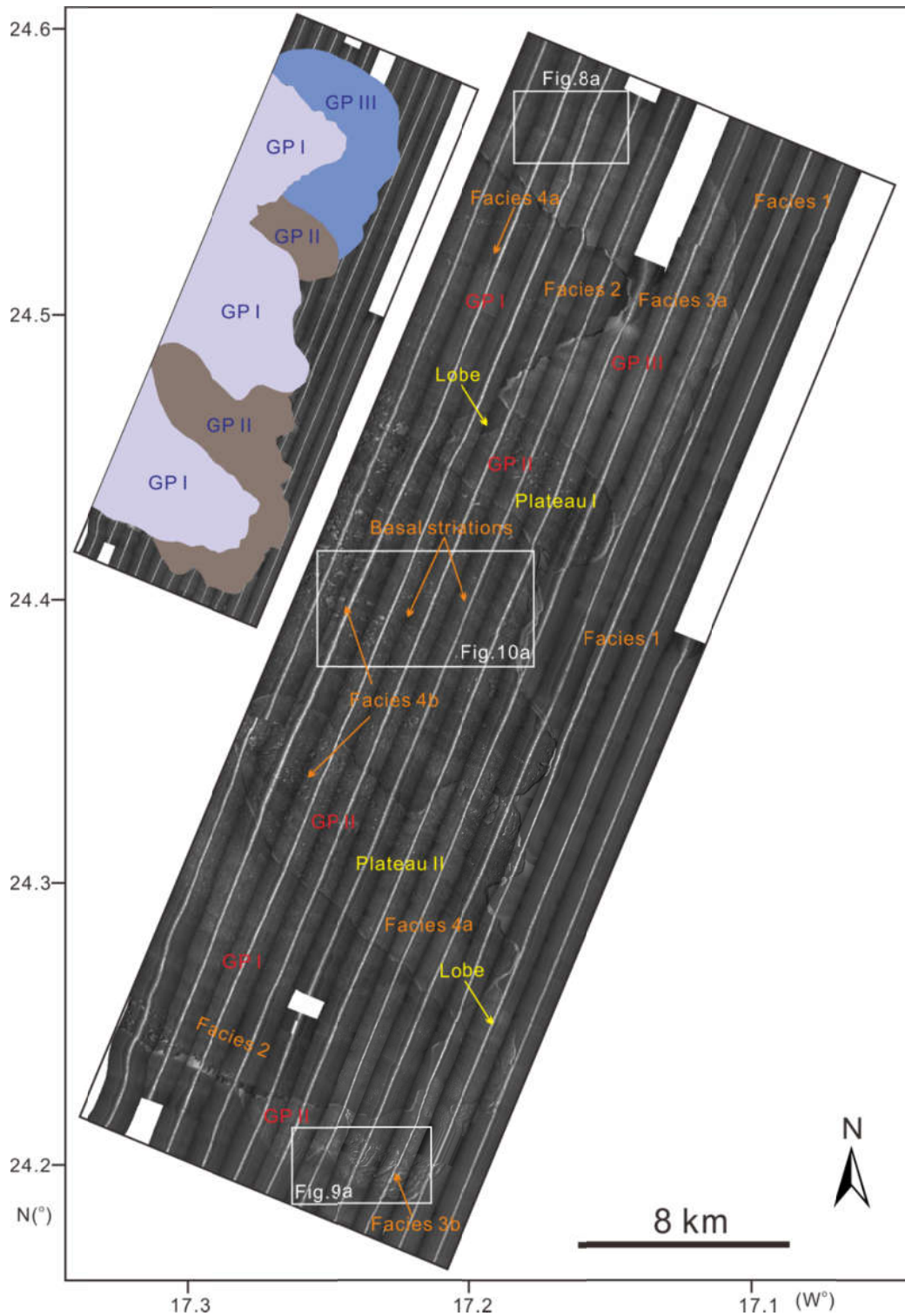
Fig. 6 Sidescan sonar mosaic on the upper headwall of the Sahara Slide Complex. Dark colors represent areas of high backscatter. Four different acoustic facies,two lobes and plateau I, II are indicated in the mosaic. The white boxes highlight the zoomed sections in Figs. 8a, 9a and 10a. The inset figure shows the distribution of the three glide planes (GP I, II and III).

4.2.1 Facies 1: Smooth, medium backscattering seafloor

Facies 1 is characterised by homogenous, medium backscatter values (Figs. 6 and 8a). Facies 1 is located in regions of undisturbed slope strata, upslope of imaged headwall scarps (Fig. 7), where stratified slope sediments are imaged on sub-bottom profiler data (Figs. 6 and 8b). We interpret these areas as comprising undisturbed fine-grained hemipelagites.

4.2.2 Facies 2: Medium to high backscattering seafloor with slight variations in backscatter

Facies 2 is characterised by a smooth, medium to high backscatter seafloor, with small variations in backscatter strength. It mainly occurs on GP I and II (Figs. 6 and 7). Facies 2 is interpreted to be associated with the presence of smooth glide planes over which sediments were evacuated. Minor variations in backscatter strength indicate the presence of thin slide deposits. Sub-bottom profile data crossing Facies 2also shows the seafloor as a relatively smooth, regular surface (Fig. 4a).

4.2.3 Facies 3: Sediment ridges and crown cracks

Facies 3 shows alternating high and low backscatter values, which highlight the presence of elongated topographical highs that are oriented parallel to the headwall (Figs. 8a and 9a). These elongated features are irregular and of variable sizes, and their length varies from a few tens of meters to several kilometers. Most of these elongated features are observed aboveGP II and GP III in the southeastern and northeastern parts of the upper headwall, respectively (Figs. 6 and 7).
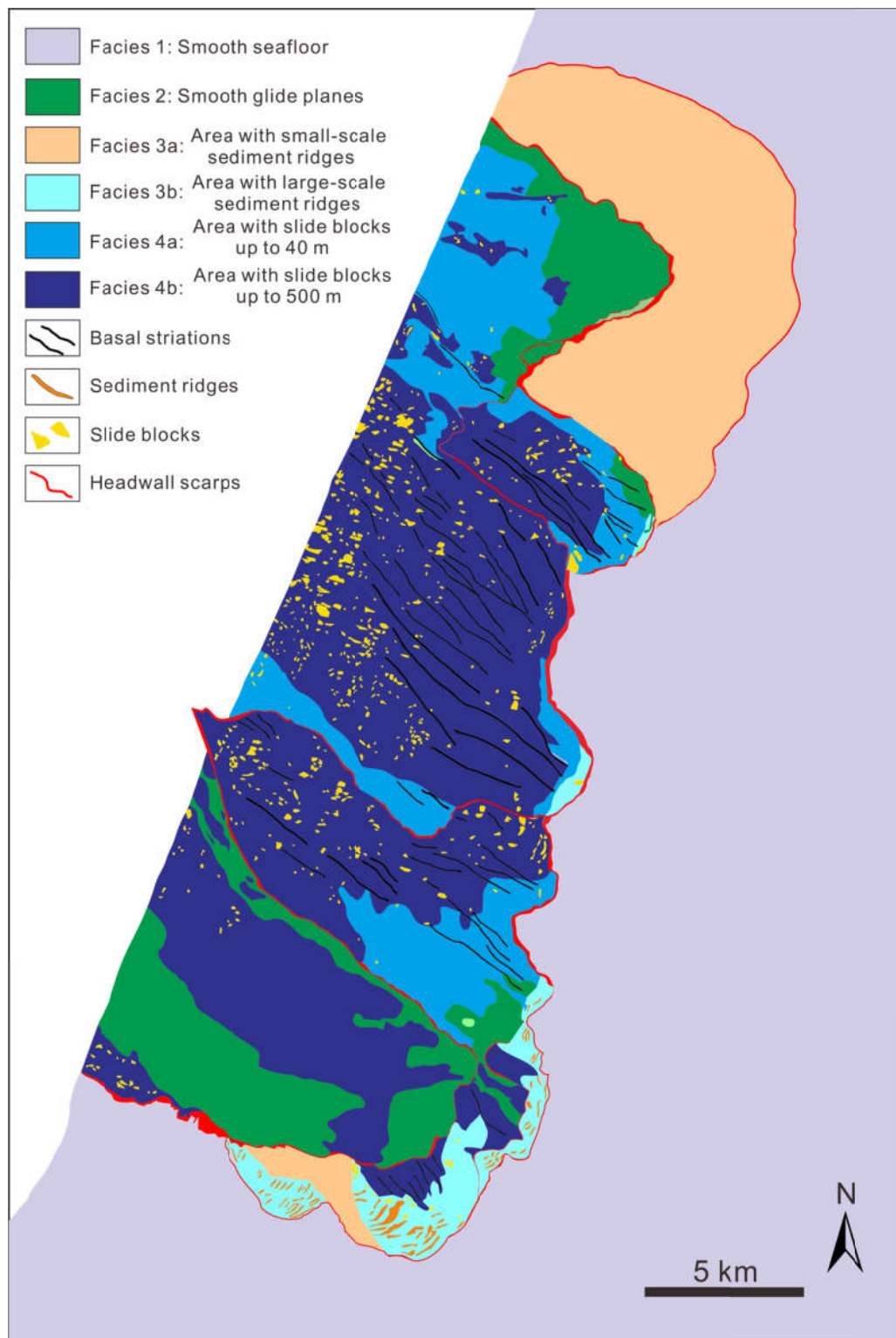
Fig. 7 Interpretation of the sidescan sonar data in Fig. 6 highlighting the distribution of four acoustic facies in the upper headwall of Sahara Slide Complex. See text for details.

Facies 3 comprises sediment ridges based on their distribution and morphology. Their orientation is parallel to the headwall. The dimension of sediment ridges to the northeast is relatively small when compared to the region to the southeast of the upper headwall (Figs. 8a and

9a). Sediment ridges can be more than 1 km in length to the southeast of the upper headwall (Fig. 9a). Thus, Facies 3can be further divided into two sub-facies 3a and 3b, based on the dimensions of sediment ridges. Facies 3a represents the area with small-scale (<500 m in length) sediment ridges and Facies 3b indicates the area with large-scale (>1 km in length) sediment ridges.The sediment ridges show a closer spacing in the areas nearest to the headwall, while their sizes and spacing increases downslope (Fig. 9a).

Crown cracks are visible in undisturbed strata behind the upper headwall (Figs. 8a and 9b). A secondary crown crack is identified ~430 m away from the headwall to the southeast (Fig. 9a). It has a length of 545 m and a width of 51 m (Fig. 9b).

4.2.4 Facies 4: Slide blocks and basal striae

Facies 4 is observed over GP I and GP II (Figs. 6 and 7). Slide blocks are imaged as high backscatter areas with shadow zones and are widespread over GP I and GP II (Figs. 6 and 10a). The size of the slide blocks varies greatly, ranging from 500-m long features to smaller blocks <40 m in length. Blocks of Facies 4 are identified in sub-bottom profiler data as a hummocky seafloor (Fig. 10b). Facies 4 can be further subdivided into Facies 4a, areas dominated by small slide blocks <40 m, and Facies 4b, areas dominated by large slide blocks>40 m.
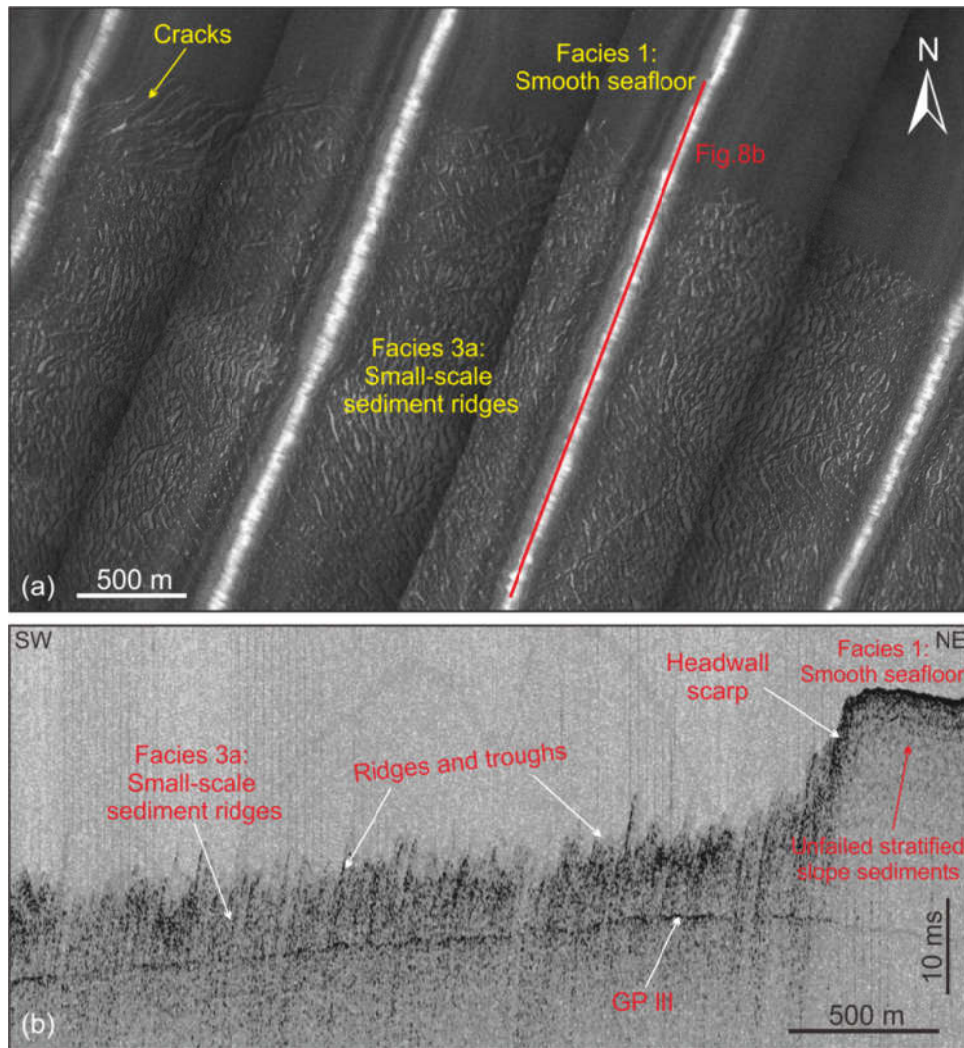
Fig. 8 (a) Sidescan sonar data of the northern part of the upper headwall showing acoustic Facies 1 and 3a. Dark colors represent areas of high backscatter. See Fig. 6 for location of the mosaic. Multiple cracks are observed near the headwall. (b) Sub-bottom profile revealing the morphology of ridges and troughs. A high-amplitude reflection represents GP III.

Facies 4 also includes striations, which are elongate areas (stripes) of smooth backscatter. Slide blocks are usually found at the end of these striations (Fig. 6). Usually the striations show slightly higher backscatter values compared to background strata(Figs. 6 and10a). The striations are interpreted as load casts formed by moving slide blocks because major blocks are found at their downslope terminations. The moving blocks eroded the glide plane through large distances to form the elongate basal striations. The NW-SE orientation of these basal striations suggests a predominant direction of mass movement to the northwest, away from the headwall (Fig. 10a), which is consistent with the direction of the maximum slope gradient.

55

4.3 Volume estimation of the mass movements

Estimates of the affected area and volume of strata involved in mass movements are critical for the assessment of their tsunamigenic potential (Watts et al., 2005). The hazard potential usually increases with the volume of the mass movements as the magnitude of tsunamis that were generated by landslides is mainly controlled by the size, initial acceleration, maximum velocity and pathway of the displaced mass movements (Harbitz et al., 2006).

As the interpreted bathymetry data do not provide full coverage of the upper headwall, we can only provide an estimate of 1700 km^2 for the area of the landslide scar enclosed by the upper headwall area (Fig. 2a). GP I has an area of 1485 km^2. GP II covers a total area of 130 km^2, including Plateau I with 25 km^2, Plateau II with 75 km^2 and the area affected by large-scale sediment ridges with 30 km^2. GP III has an area of 85 km^2 in the northeastern part affected by small-scale sediment ridges. The total volume of remobilized strata in the upper headwall is ~150 km^3. The volumes of removed sediment on GP I, II and III are approximately 140 km^3, 7 km^3 and 3 km^3, respectively. The calculated volume of missing sediments over GP I and II is reasonably accurate because bathymetric data fully cover this area, although we cannot be sure on the pre-failure morphology. The volume of missing sediments above GP I is a minimum estimate because the bathymetry indicates that the evacuation zone continues further downslope, beyond the limit of our data coverage.

4.4 Timing of the mass movements

In total, ten gravity cores were taken in the headwall area. Nine of the ten cores were taken in the landslide area (Fig. 2a). They all contain debrite deposits dominated by clasts (Fig. 11). Gravity core P395-07-1 shows a distinct thin (~4 cm) sedimentary drape on top of the underlying debris (Fig. 11). The core did not reach the glide plane. The sedimentary drape contains well-oxidised sediment (beige-pink foraminifera-bearing mud). No drape being thick enough for dating (>2cm) was identified in any other core targeting the landslide deposits. As described in the method section, we assume the loss of no more than 10 cm of surface sediments occurred at any point in our coring.
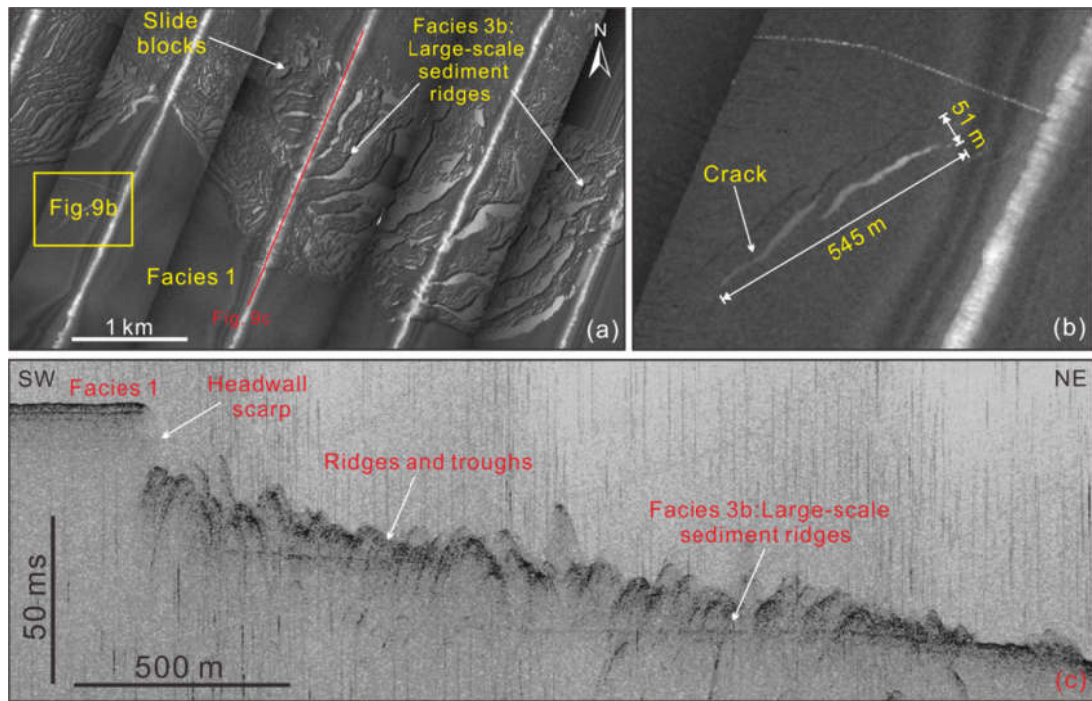
Fig. 9 (a) Sidescan sonar data of the southern part of the upper headwall showing the morphology of large-scale sediment ridges. A crown crack is identified in stratified (slope) sediments south of the headwall scarp. Dark colors represent areas of high backscatter. See Fig. 6 for location of sidescan sonar mosaic. (b) Zoomed section showing the morphology of the crown crack located south of the headwall. The crown crack has a length of ~ 550 m and a width of ~50 m. (c) Sub-bottom profile illustrating ridges, troughs and the headwall of the Sahara Slide Complex.

A sample for dating the undisturbed drape on top of the landslide deposits were taken at 3 cm bsf in Core P395-07-1, which is about 1 cm above the slide deposits (Fig. 11). The measured age for this sample is 1840 ± 23 years BP (Table 1). This age is not representing the failure age but a minimum age. A common procedure for calculating the failure age is to add the time needed for the deposition of the undisturbed deposits between the top of the landslide deposits and the sample location used for dating. Sedimentation rate is needed for this approach. The sample in Core P395-07-1 is taken only about 1 cm above the slide deposits. If we assume that the top of the core represents the seafloor and the sample is 3 cm bsf, we calculate a sedimentation rate of only ~1.63 cm/ka assuming a constant sedimentation rate. A value of ~1.63 cm/ka for the sedimentation rate is significantly lower than documented in previous studies from nearby areas (~5 cm/ka on average after, Bertrand et al., 1996; Weaver et al. 2000; Georgiopoulou et al., 2009). The most likely explanation for this discrepancy is that surface sediments were lost during gravity coring (as stated above). Using sedimentation rates of 1.63 cm/ka and 5 cm/ka, age corrections would be 0.6 ka and 0.2 ka, respectively, following the approach described in the method section. As a result, the corrected age of the slide deposits at the location of Core P395-07-1 is ~2.24±0.2 ka. We are aware

that a single date may not represent the age of the entire failure. However, we point out that cores beneath the headwall are available at various locations (Fig. 2a), and none of these additional cores shows an undisturbed drape thick enough to allow a reliable dating of the Sahara Slide Complex. Even considering a loss of about 10 cm of surface sediments, an age of ~ 2ka for the failure would still be estimated by assuming a sedimentation rate of 5 cm/ka. The missing drape may indicate an even younger age.

Sample	Sample Description	Conventional Age	Calendar Age
1	P395-04-01, 5 cm bsf	5365 ± 25 BP	6172 ± 78 BP
2	P395-07-01, 3 cm bsf	1880 ± 20 BP	1840 ± 23 BP

Table 1 AMS ^{14}C ages of samples in sediment cores P395-04-1 and P395-07-1.

In order to support a young age of the failure, we dated one clast being part of the debrite deposits in core P395-04-1. The age of this clast is 6172 ± 78 years BP (Fig. 11, Tab. 1). This clast provides a maximum age for the slide event on GP I because it comprises disrupted slope material deposited prior to the failure. Hence, this date also suggests a young age of the failure.

In summary, we consider the entire failure of the upper headwall area of the Sahara Slide to have occurred in Late Holocene times. This age contrasts to the estimate of ~50-60 ka revealed in previous studies for the distal Sahara Slide deposits (Gee et al, 1999; Georgiopoulou et al., 2010).

5 Discussion

5.1 Types of mass movements at the headwall of the Sahara Slide Complex

Differences in morphology in the GP I, II and III areas indicate distinct mass-movement types(e.g. Micallef et al., 2007; Baeten et al., 2013) (Figs. 3 and 6). The elongate ridges and troughs indicate widespread extension, leading to gravitational spreading. Gravitational spreading has a characteristic morphology, with repetitive ridges and troughs oriented parallel to scarps and perpendicular to the direction of mass movement (Micallef et al., 2007; Baeten et al., 2013). Gravitational spreading is a common and pervasive type of mass movement, which has been identified (among other areas) in the Ormen Lange area of the Storegga Slide (Kvalstad et al., 2005; Micallef et al., 2007), the Hinlopen Slide area (Vanneste et al., 2006), the St. Pierre Slope (Piper et al., 1999), the continental slope offshore Mauritania (Krastel et al., 2007), and at an outcrop in SE Crete (Alves and Lourenço, 2010; Alves, 2015). At the upper headwall of the Sahara Slide Complex, the morphology of flat-topped glide planes, with no or very little debris remaining on them, and internal architecture showing glide planes parallel to the stratigraphy, reveal that translational sliding also took place which commonly occurs along a planar failure surface, with little rotation or backward tilting(Varnes, 1978). Translational slides often disintegrate into debris flows (Piper et al., 1999). This is also observed for the Sahara Slide Complex, where elongated ridges are disintegrated downslope into blocks of decreasing size, leading to full transformation into debris flow and turbidity currents (Georgiopoulou et al., 2009). Many submarine landslides identified on continental margins are translational in nature and are developed retrogressively in multiple episodes of slope failure, e.g. the Hinlopen Slide on the Arctic Ocean margin (Vanneste et al., 2006), the Mauritania Slide Complex on the Northwest African continental margin (Krastel et al., 2007) and Storegga Slide on the Norwegian continental margin (Haflidason et al., 2004). We believe similar processes took place in the Sahara Slide Complex.

Gravitational spreading occurred mainly in the northeastern (along GP III) and southeastern (along GP II) parts of the upper headwall, where multiple sediment ridges are observed. The size of sediment ridges vary between GP II and III, with ridges being smaller on GP III compared to GP II (Figs. 8a and 9a). Due to the lack of deeper sediment samples, we cannot address the specific reasons for these differences. The scale of the sediment ridges has been proposed to be controlled by several factors including gravitationally induced stress, angle of internal friction of the sediment, pore pressure escape, and basal friction (Micallef et al., 2007).
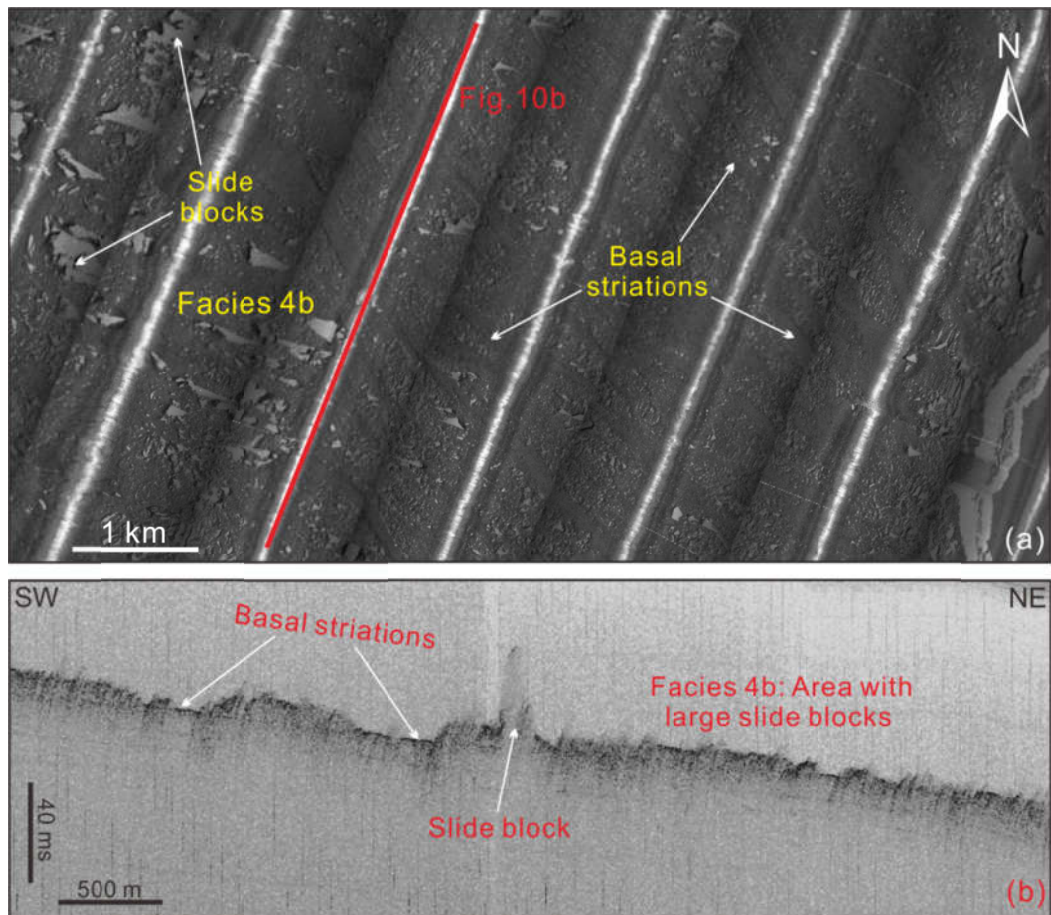
Fig. 10 (a) Sidescan sonar data of the central part of the study area, downslope from the upper headwall, showing multiple slide blocks and striae. Prominent isolated blocks are located at the termination of the striae. Dark colors represent areas of high backscatter. See Fig. 6 for location of the image (b) Sub-bottom profile showing the striae referred to in the text, which are surrounded by blocky deposits.

Translational sliding occurred in the central part of the slide scar on GP I, and on two large plateaus along GP II (Figs. 6 and 7).GP I and II are located at two different stratigraphic levels, but present similar morphologies. Both areasare characterised bywidespread large sediment blocks and elongated striations in some places (Facies 4b, Fig. 10a), whereas other places show small blocks and thin debris deposits (Facies 4a, Fig. 10a). This observation provides robust evidence that mass movement processes on GP I and II are similar. Sediment blocks likely resulted from the disintegration of failed strata but they do not disintegrate fully as they are clearly seen as blocks in the morphological data. The striations imply bottom contact causing erosion and drag forces, suggesting that the blocks moved not very fast. This is further supported by the fact that the blocks are found relatively close to the headwall. However, full disintegration seems to occur in places (Facies 4a) suggesting a higher energy regime for these areas. Hence, the translational sliding on GP I and II may represent "fast sliding" of failed slope deposits at least in the areas where full

disintegration is taking place, while relative "slow sliding" (i.e. spreading) took place above GP III and small parts of GP II, forming detached sediment ridges. The cracks identified away the headwall to the southeast suggest the presence of sediment slabs, highlighting the preferential region for future translational sliding (Laberg et al., 2013). The presence of cracks may also indicate a permanent state of instability on the continental slope.

5.2 Evidence for multiple slope failures

The upper headwall of the Sahara Slide shows a complex morphology in bathymetric and sidescan sonar data (Figs. 2a and 6). The exposed headwall scarps and the lack of slide debris close to the headwall scarps indicate that the upper headwall has been evacuated (Fig. 2a).This complex morphologyis evidence for the formation of the upper headwall during multi-stage failure events. These events are results of two different types of mass movements that occurred in the upper headwall; translational sliding and gravitational spreading. We interpret gravitational spreading in the GPI area as a direct consequence of translational sliding further downslope due to the lack of support from removed sediments. In addition, we consider that that retrogressive failure formed the upper headwall of the Sahara Slide Complex. Retrogressive failures have been identified for many landslides including the Humboldt Slide on the northern California continental margin (Gardner et al., 1999) and the Storegga Slide on the Norwegian continental margin (Kvalstad et al., 2005).

The relationship between the upper and lower headwalls, however, remains unclear as no age data and detailed acoustic data are available for the latter region. The distal deposits of the Sahara Slide are dated at 50-60 ka (Gee et al., 1999; Georgiopoulou et al., 2010), a date much older than the age estimated for the upper headwall in this study. A plausible explanation for this discrepancy in ages is that the lower headwall may have been formed in association with the 50-60 ka failure event, whereas the upper headwall is the result of a much younger instability. Sparse sediment echo-sounder data suggest younger failures of the upper headwall compared to the lower headwall. In this case, we would consider slope failure of the upper and lower headwalls as independent events due to the long time spanning these two events. The observed distance of ~50 km between the two headwalls would also be unusually large for a retrogressive failure (e.g. Imbo et al., 2003; Locat et al., 2009; Baeten et al., 2013).

An alternative explanation is that both headwalls were formed 50-60 ka ago, and the younger failure of the upper headwall represents a phase of reactivation of this latter area. This would imply that failure of both headwalls is somewhat related, but more data is necessary to investigate this hypothesis.

5.3 Possible preconditioning factors and triggers for slope instability at the upper headwall of the Sahara Slide Complex

Various preconditioning factors have been proposed as promoting failures on continental margins, including high sedimentation rates (Leynaud et al., 2007) and the presence of weak layers (Baeten et al., 2014). Recent modeling results from Urlaub et al. (2015) suggest that sedimentation rates in the Sahara Slide area (~5 cm/ka) are insufficient to destabilise the slope. Weak layers were defined by Locat et al. (2014) as sediment layers that have lower strength compared to adjacent units, and can provide a potential focus for the development of a surface of rupture. The presence of weak layers have been considered as an important preconditioning factor for the generation of submarine landslides in several regions such as the slopes at Finneidfjord, northern Norway (L'Heureux et al., 2012) and the Mauritania Slide area (Antobreh and Krastel, 2007). Slope failure in the upper headwall of the Sahara Slide Complex occurred along three pronounced and widespread glide planes; we consider this observation as evidence for the presence of weak layers at distinct depths below the seafloor. However, we do not know the composition of these layers due to missing sediment samples.

One possibility could be the presence of sediment layers with particularly high compressibilities as it has been proposed to play a vital role for the instabilities offshore Northwest Africa (Urlaub et al., 2015). Organic-rich sediments typically have high compressibilities (Booth and Dahl, 1986; Bennett et al., 1985). In fact, the study area is affected by a strong upwelling system driven by the Northeast Trade Winds (Cropper et al., 2014), which results in high primary productivity and the deposition of organic-rich sediments. This upwelling system typically reached its maximum productivity during deglaciations (Bertrand et al., 1996), which may explain the different stratigraphic depths of the glide planes.

Our new data do not provide any information on the final trigger of the slope failure. However, we consider seismicity possibly related to the reactivation of old fracture zone or the evolution of the Canary Islands as most likely trigger. The Canary Islands and surrounded areas are presently seismically active, characterised by small and medium-size earthquakes (Ibáñez et al., 2012). The study area is ~300 km away from the Canary Islands and earthquakes associated with these same islands might be a triggering mechanism for the slide events in the upper headwall of Sahara Slide. Thus, we conclude that the presence of weak layers consisting of a particular sediment type is the main potential preconditioning factor, but the final triggering of the failures remains speculative.

5.4 Timing of the failure and implications for geohazard assessment

Several authors have discussed potential relationships between sea-level and landslide frequency (Owen et al., 2007; Lee, 2009; Leynaud et al., 2009; Urlaub et al., 2013). Based on a compilation of available ages for landslides on the Atlantic Ocean margin, Lee (2009) stated that the continental margin is relatively stable at present, partly related to the stable sea level. Only 2-3 landslides are documented during the past 5000 years; the frequency of landslide occurrence for this period is less by a factor of 1.7 to 3.5 compared to the time of sea-level rise after the last glaciation. Major landslides off Northwest Africa were also related to periods of low or rising sea level (Krastel et al., 2012). The distal deposits of the Sahara Slide are dated at 50-60 ka before present, which was during a period of rising sea level (Gee et al., 1999; Georgiopoulou et al., 2007).
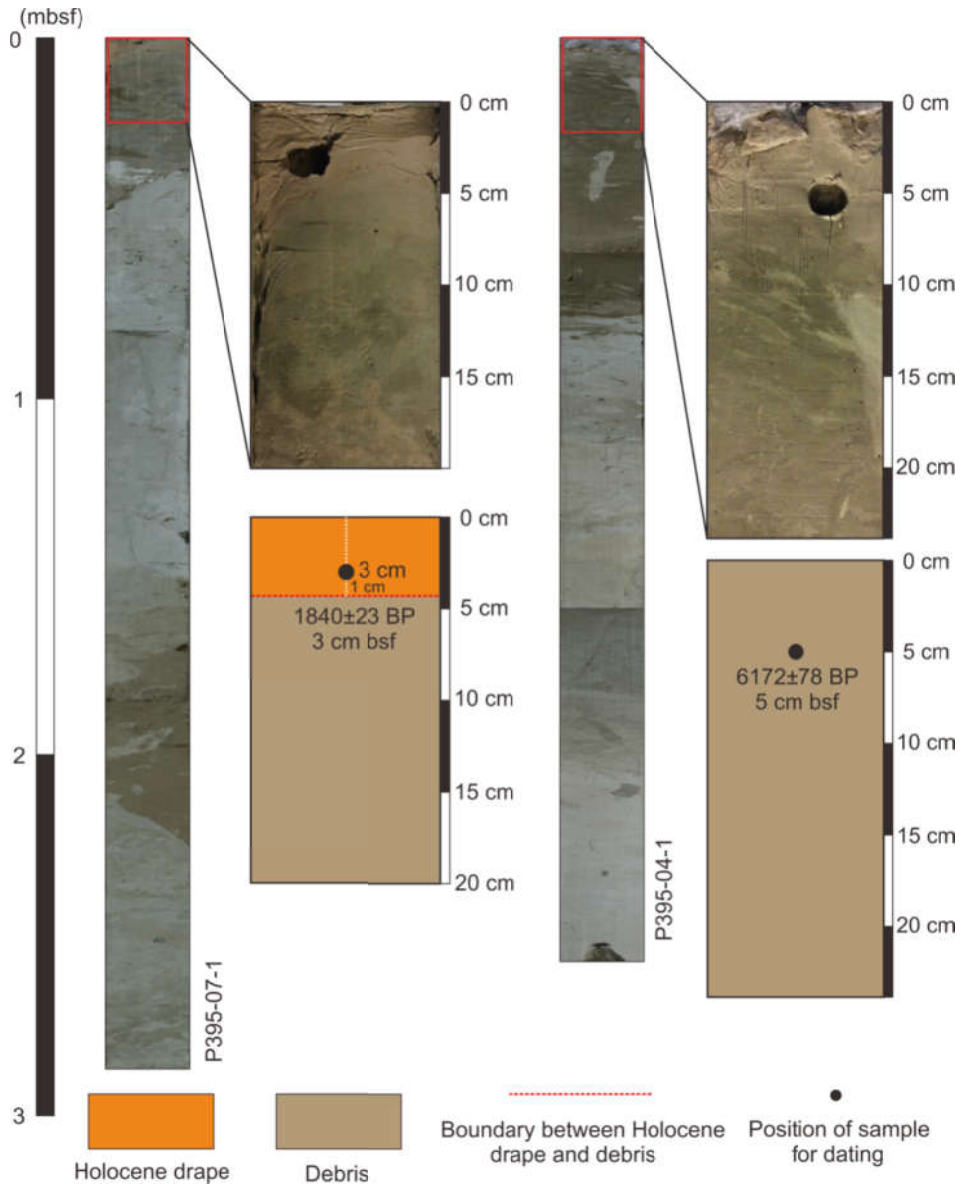
Fig. 11 Photo and schematic illustration of sediment cores P395-04-1 and P395-07-1 (see Fig. 2 for

location of cores). Black solid dots in core P395-04-1 and P395-07-1 represent the positions of AMS 14C-age dating samples in 5 and 3 cm below seafloor (bsf) with the calibrated ages. Note the distance from sample location to the boundary between Holocene drape and debris, which is ~1 cm for core P395-07-1.

A link between sea-level and landslide frequency, however, is negated by Urlaub et al. (2013) based on a statistical analysis of a global compilation of available ages for large (>1 km^3) continental margin landslides. Urlaub et al. (2013) stated that the global data set did not show statistically significant patterns, trends or clusters in landslide abundance but they note that significantly fewer events occurred in the past 6 ka. Urlaub et al. (2013) also analysed landslides at the Northwest African continental margin as subset of the global data set concluding that ages are nearly evenly distributed without any clustering or increased frequency. Our study suggests that the failure of the upper headwall of the Sahara Slide is only ~2.24±0.2 ka old. Despite the fact, that this age is only based on one dated sample, we consider the missing undisturbed drape on top of the landslide deposits at all other cores as very strong evidence for a similarly young age for the entire failure of the upper headwall area during a period of constantly high sea level. This interpretation is further supported by the occurrence of debrite deposits of a similar age up to 250 km downslope of the headwall and an associated turbidite extending for more than 700 km (Georgiopoulou et al., 2009). Georgiopoulou et al. (2009) suggest that the linked turbidite-debrite bed was formed during the recent failure of the Sahara Slide headwall.

While we consider the upper and lower headwall area of the Sahara Slide complex as independent events, the failure of the upper headwall of the Sahara Slide Complex most likely occurred in several retrogressive stages as indicated by glide planes at different levels and multiple headwalls. A retrogressive failure has large implications for the tsunamigenic potential. Tsunamigenic potential in the Sahara Slide would be larger if the slide events occurred simultaneously, compared to the case of retrogressive landslides (Harbitz et al., 2014). A key observation in the study area is that missing volumes on top of individual glide planes are large (> 100 km^3). Relatively small failures in the past have triggered significant tsunamis. In the case of the 1998 event at Papua New Guinea, Tappin et al. (2001) concluded the tsunami, which resulted in the deaths of over 2000 people, was a direct result of a slump with an estimated volume of 5-10 km^3. The 11,500-year BP BIG'95 landslide detected in the Mediterranean Sea involved a total volume of 26 km^3 (Lastras et al., 2004; Urgeles et al., 2006).Even such failures with small volume landslide deposits may cause catastrophic tsunamis based on the recent tsunami simulations (Løvholt et al., 2014). Modelling of the 165 km^3 Currituck landslide (Locat et al., 2009), also revealed potential for a devastating tsunami (Geist et al., 2009). The volumes of the removed sediments on GP I, II and III

in the upper headwall of Sahara Slide are approximately 140 km^3, 7 km^3 and 3 km^3, respectively. It is unlikely, that the failure on top of GP III occurred as a single event, but the examples above show that individual failures of the Sahara Slide complex were large enough to present a significant tsunamigenic potential, even if occurring in relatively large water depths (~2000 m) (Lo Iacono et al., 2012; Harbitz et al., 2014). In addition, Georgiopoulou et al. (2009) observed turbidite deposits up to 700 km downslope of the Sahara Slide headwall. They interpret this turbidite to have formed by recent failure of the Sahara Slide headwall; either by the near-simultaneous generation of a debris flow and turbidity current, or by entrainment of water into the debris flow leading to the generation of a turbidity current. These processes and the long run-out distance of the turbidity current suggest a relatively fast moving landslide body, high flow velocities have high tsunamigenic potential (Harbitz et al., 2006). Such an observation, in combination with the young age of the failure, calls for a reassessment of landslide hazards along the Northwest African continental margin, estimated to be low in previous studies (Lee, 2009). However, such a reassessment is beyond the scope of this manuscript.

6 Conclusions

A combination of high-resolution bathymetry, sidescan sonar, sub-bottom profiler data,and sediment cores allowed to reconstruct the failure behavior of the upper headwall of Sahara Slide Complex on the continental margin offshore Northwest Africa. The main conclusions of this study are:

(1) The upper headwall was evacuated, and several morphological elements (e.g., slide scarps, glide planes, plateaus, lobes and slide blocks) are identified on the modern seafloor. The volume of the evacuated area exceeds 150 km^3.

(2) The morphology and configuration of the upper headwall is the result of multiple failure events probably occurring mainly as spreading and translational sliding on three different glide planes retrogressively. The presence of weak layersis considered as the main preconditioning factor for instability in the Sahara Slide Complex.

(3) The slide processes on glide plane I and II record the generation of disintegrated slide blocks of different scales, indicating relatively "fast sliding". In contrast, the slide processes on glide plane III were mainly characterised by spreading resulting in widespread sediment ridges, troughs and cracks upslope (in the unfailed strata) as relative "slow sliding".

(4) The upper headwall of the Sahara Slide Complex was active (or reactivated) in the late Holocene about 2 ka BP during times of a stable sea-level high stand. The failure may be the largest of Holocene failures worldwide. The young age is an important contribution to the ongoing debate on potential relationships between sea-level and landslide frequency, as it shows that very large landslide do occur during times of a stable sea level high stand. The young age in combination with the large volume calls for a reassessment of the slope instability and the tsunamigenic potential along the margin offshore Northwest Africa and other continental margins that are considered currently stable.

(5) Crown cracks indicate the slope may not be at equilibrium and instability may still be ongoing.

Reference

Alves, T.M., 2015. Submarine slide blocks and associated soft-sediment deformation in deep-water basins: A review. Marine and Petroleum Geology 67, 262-285.

Alves, T.M., Lourenço, S.D.N., 2010. Geomorphologic features related to gravitational collapse: Submarine landsliding to lateral spreading on a Late Miocene–Quaternary slope (SE Crete, eastern Mediterranean). Geomorphology 123, 13-33.

Antobreh, A.A., Krastel, S., 2007. Mauritania Slide Complex: morphology, seismic characterisation and processes of formation. International Journal of Earth Sciences 96, 451-472.

Baeten, N.J., Laberg, J.S., Forwick, M., Vorren, T.O., Vanneste, M., Forsberg, C.F., Kvalstad, T.J., Ivanov, M., 2013. Morphology and origin of smaller-scale mass movements on the continental slope off northern Norway. Geomorphology 187, 122-134.

Baeten, N.J., Laberg, J.S., Vanneste, M., Forsberg, C.F., Kvalstad, T.J., Forwick, M., Vorren, T.O., Haflidason, H., 2014. Origin of shallow submarine mass movements and their glide planes—Sedimentological and geotechnical analyses from the continental slope off northern Norway. Journal of Geophysical Research: Earth Surface 119, 2335-2360.

Bennett, R.H., Lehman, L., Hulbert, M.H., Harvey, G.R., Bush, S.A., Forde, E.B., Crews, P., Sawyer, W.B., 1985. Interrelationships of organic carbon and submarine sediment geotechnical properties. Marine Geotechnology 6, 61-98.

Berndt, C., Costa, S., Canals, M., Camerlenghi, A., de Mol, B., Saunders, M., 2012. Repeated slope failure linked to fluid migration: The Ana submarine landslide complex, Eivissa Channel, Western Mediterranean Sea. Earth and Planetary Science Letters 319-320, 65-74.

Bertrand, P., Shimmield, G., Martinez, P., Grousset, F., Jorissen, F., Paterne, M., Pujol, C., Bouloubassi, I., Buat Menard, P., Peypouquet, J.P., Beaufort, L., Sicre, M.A., Lallier-Verges, E., Foster, J.M., Ternois, Y., Program O.P.o.t.S., 1996. The glacial ocean productivity hypothesis: the importance of regional temporal and spatial studies. Marine Geology 130, 1-9.

Bickert, T., cruise participants, 2011. Pre-Site Survey for an IODP cruise Neogene Paleoclimate and sediment transport at the continental margin of NW Africa - Cruise No. MSM11/2 - March 14 - April 09, 2009 - Dakar (Senegal) - Las Palmas (Canary Islands, Spain). MARIA S. MERIAN Berichte, MSM11/2, 53 pp., DFG-Senatskommission für Ozeanographie, DOI: 10.2312/cr_msm11_2.

Booth, J.S., Dahl, A.G., 1986. A note on the relationships between organic matter and some geotechnical properties of a marine sediment. Marine Geotechnology 6, 281-297.

Cropper, T.E., Hanna, E., Bigg, G.R., 2014.Spatial and temporal seasonal trends in coastal upwelling off Northwest Africa, 1981–2012. Deep Sea Research Part I: Oceanographic Research Papers 86, 94-111.

Embley, R.W., 1982. Anatomy of Some Atlantic Margin Sediment Slides and Some Comments on Ages and

Mechanisms, in: Saxov, S., Nieuwenhuis, J.K. (Eds.), Marine Slides and Other Mass Movements. Springer US, Boston, MA, pp. 189-213.

Förster, A., Ellis, R.G., Henrich, R., Krastel, S., Kopf, A.J., 2010. Geotechnical characterization and strain analyses of sediment in the Mauritania Slide Complex, NW-Africa. Marine and Petroleum Geology 27, 1175-1189.

Gardner, J.V., Prior, D.B., Field, M.E., 1999.Humboldt Slide — a large shear-dominated retrogressive slope failure.Marine Geology. 154, 323–338.

Gee, M.J.R., Masson, D.G., Watts, A.B., Allen, P.A., 1999. The Saharan debris flow: an insight into the mechanics of long runout submarine debris flows. Sedimentology 46, 317-335.

Gee, M.J.R., Masson, D.G., Watts, A.B., Mitchell, N.C., 2001. Passage of debris flows and turbidity currents through a topographic constriction: seafloor erosion and deflection of flow pathways. Sedimentology 48, 1389-1409.Geist, E.L., Lynett, P.J., Chaytor, J.D., 2009.Hydrodynamic modeling of tsunamis from the Currituck landslide. Marine Geology 264, 41-52.

Georgiopoulou, A., Krastel, S., Masson, D.G., Wynn, R.B., 2007. Repeated Instability Of The NW African Margin Related To Buried Landslide Scarps, in: Lykousis, V., Sakellariou, D., Locat, J. (Eds.), Submarine Mass Movements and Their Consequences: 3 International Symposium. Springer Netherlands, Dordrecht, pp. 29-36.

Georgiopoulou, A., Masson, D.G., Wynn, R.B., Krastel, S., 2010. Sahara Slide: age, initiation and processes of a giant submarine slide. Geochemistry, Geophysics, Geosystems 11, 1-22.

Georgiopoulou, A., Wynn, R.B., Masson, D.G., Frenz, M., 2009.Linked turbidite–debrite resulting from recent Sahara Slide headwall reactivation. Marine and Petroleum Geology 26, 2021-2031.

Golbeck, I., 2010. The Sahara Slide Complex.Unpublished thesis.Department of Geosciences, University of Bremen, 137 pp.

Haflidason, H., Sejrup, H.P., Nygård, A., Mienert, J., Bryn, P., Lien, R., Forsberg, C.F., Berg, K., Masson, D., 2004. The Storegga Slide: architecture, geometry and slide development. Marine Geology 213, 201-234.

Harbitz, C.B., Løvholt, F., Bungum, H., 2014. Submarine landslide tsunamis: how extreme and how likely? Natural Hazards 72, 1341-1374.

Harbitz, C.B., Løvholt, F., Pedersen, G., Masson, D.G., 2006. Mechanisms of tsunami generation by submarine landslides: a short review. Norw. J. Geol. 86, 255-264

Hayes, D.E., Rabinowitz, P.D., 1975. Mesozoic magnetic lineations and the magnetic quiet zone off northwest Africa. Earth and Planetary Science Letters 28, 105-115.

Henrich, R., Hanebuth, T.J.J., Krastel, S., Neubert, N., Wynn, R.B., 2008. Architecture and sediment dynamics of the Mauritania Slide Complex. Marine and Petroleum Geology 25, 17-33.

Holz, C., Stuut, J.b.W., Henrich, R., 2004. Terrigenous sedimentation processes along the continental margin off NW Africa: implications from grain-size analysis of seabed sediments. Sedimentology 51, 1145-1154.

Ibáñez, J.M., De Angelis, S., Díaz-Moreno, A., Hernández, P., Alguacil, G., Posadas, A., Pérez, N., 2012. Insights into the 2011–2012 submarine eruption off the coast of El Hierro (Canary Islands, Spain) from statistical analyses of earthquake activity. Geophysical Journal International 191, 659-670.

Imbo, Y., De Batist, M., Canals, M., Prieto, M.J., Baraza, J., 2003. The Gebra Slide: a submarine slide on the Trinity Peninsula Margin, Antarctica. Marine Geology 193, 235-252.

Krastel, S., Behmann, J.-H., Völker, D., Stipp, M., Berndt, C., Urgeles, R., Chaytor, J., Huhn, K., Strasser, M., Harbitz, C.B., 2014. Submarine mass movements and their consequences. 6th International Symposium. Advances in Natural and Technological Research 37, pp 683.

Krastel, S., cruise participants, 2011. FS POSEIDON Fahrtbericht/Cruise Report P395-Sahara Slide Complex, 04.02.-19.02.2010 Las Palmas - Las Palmas (Spain). IFM-GEOMAR Report, 50.IFM-GEOMAR, Kiel, 43 pp. DOI 10.3289/IFM-GEOMAR_REP_50_2011.

Krastel, S., Wynn, R.B., Georgiopoulou, A., Geersen, J., Henrich, R., Meyer, M., Schwenk, T., 2012.Large-Scale Mass Wasting on the Northwest African Continental Margin: Some General Implications for Mass Wasting on Passive Continental Margins. 189-199.

Krastel, S., Wynn, R.B., Hanebuth, T.J.J., Henrich, R., Holz, C., Meggers, H., Kuhlmann, H., Georgiopoulou, A., Schulz, H.D., 2006.Mapping of seabed morphology and shallow sediment structure of the Mauritania continental margin, Northwest Africa: some implications for geohazard potential. Norwegian Journal of Geology 86, 163-176.

Kvalstad, T.J., Andresen, L., Forsberg, C.F., Berg, K., Bryn, P., Wangen, M., 2005.The Storegga slide: evaluation of triggering sources and slide mechanics. Marine and Petroleum Geology 22, 245-256.

L'Heureux, J.-S., Longva, O., Steiner, A., Hansen, L., Vardy, M.E., Vanneste, M., Haflidason, H., Brendryen, J., Kvalstad, T.J., Forsberg, C.F., Chand, S., Kopf, A., 2012. Identification of Weak Layers and Their Role for the Stability of Slopes at Finneidfjord, Northern Norway, in: Yamada, Y., Kawamura, K., Ikehara, K., Ogawa, Y., Urgeles, R., Mosher, D., Chaytor, J., Strasser, M. (Eds.), Submarine Mass Movements and Their Consequences: 5th International Symposium. Springer Netherlands, Dordrecht, pp. 321-330.

Løvholt, F., Harbitz, C.B., Vanneste, M., Blasio, F.V., Urgeles, R., Iglesias, O., Canals, M., Lastras, G., Pedersen, G., Glimsdal, S., 2014. Modeling Potential Tsunami Generation by the BIG'95 Landslide, in: Krastel, S., Behrmann, J.-H., Völker, D., Stipp, M., Berndt, C., Urgeles, R., Chaytor, J., Huhn, K., Strasser, M., Harbitz, B.C. (Eds.), Submarine Mass Movements and Their Consequences: 6th International Symposium. Springer International Publishing, Cham, pp. 507-515.

Laberg, J.S., Baeten, N.J., Lågstad, P., Forwick, M., Vorren, T.O., 2013. Formation of a large submarine crack during the final stage of retrogressive mass wasting on the continental slope offshore northern Norway. Marine Geology 346, 73-78.

Lamarche, G., Mountjoy, J., Bull, S., Hubble, T., Krastel, S., Lane, E., Micallef, A., Moscardelli, L., Mueller, C., Pecher, I., Woelz, S., 2016. Submarine mass movements and their consequences.7th International

Symposium.Advances in Natural and Technological Research, 41, pp 621.

Lange, C.B., Romero, O.E., Wefer, G., Gabric, A.J., 1998. Offshore influence of coastal upwelling off Mauritania, NW Africa, as recorded by diatoms in sediment traps at 2195 m water depth. Deep Sea Research Part I: Oceanographic Research Papers 45, 985-1013.

Lastras, G., Canals, M., Urgeles, R., De Batist, M., Calafat, A.M., Casamor, J.L., 2004. Characterisation of the recent BIG'95 debris flow deposit on the Ebro margin, Western Mediterranean Sea, after a variety of seismic reflection data. Marine Geology 213, 235-255.

Lee, H.J., 2009. Timing and occurrence of large submarine landslides on the Atlantic Ocean Margin. Marine Geology 264, 53-64.

Leynaud, D., Mienert, J., Vanneste, M., 2009.Submarine mass movements on glaciated and non-glaciated European continental margins: A review of triggering mechanisms and preconditions to failure. Marine and Petroleum Geology 26, 618-632.

Leynaud, D., Sultan, N., Mienert, J., 2007. The role of sedimentation rate and permeability in the slope stability of the formerly glaciated Norwegian continental margin: the Storegga slide model. Landslides 4, 297-309.

Li, W., Wu, S., Völker, D., Zhao, F., Mi, L., Kopf, A., 2014. Morphology, seismic characterization and sediment dynamics of the Baiyun Slide Complex on the northern South China Sea margin. Journal of the Geological Society 171, 865-877.

Lo Iacono, C., Gràcia, E., Zaniboni, F., Pagnoni, G., Tinti, S., Bartolomé, R., Masson, D.G., Wynn, R.B., Lourenço, N., Pinto de Abreu, M., Dañobeitia, J.J., Zitellini, N., 2012. Large, deepwater slope failures: Implications for landslide-generated tsunamis. Geology 40, 931-934.

Locat, J., Lee, H., ten Brink, U.S., Twichell, D., Geist, E., Sansoucy, M., 2009. Geomorphology, stability and mobility of the Currituck slide. Marine Geology 264, 28-40.

Locat, J., Leroueil, S., Locat, A., Lee, H., 2014. Weak Layers: Their Definition and Classification from a Geotechnical Perspective, in: Krastel, S., Behrmann, J.-H., Völker, D., Stipp, M., Berndt, C., Urgeles, R., Chaytor, J., Huhn, K., Strasser, M., Harbitz, C.B. (Eds.), Submarine Mass Movements and Their Consequences. Springer International Publishing, pp. 3-12.

Mangerud, J., Gulliksen, S., 1975. Apparent radiocarbon ages of recent marine shells from Norway, Spitsbergen, and Arctic Canada. Quaternary Research 5, 263-273.Maslin, M., Owen, M., Day, S., Long, D., 2004. Linking continental-slope failures and climate change: testing the clathrate gun hypothesis. Geology 32, 53-56.

Masson, D.G., Harbitz, C.B., Wynn, R.B., Pedersen, G., Løvholt, F., 2006. Submarine landslides: processes, triggers and hazard prediction. Philosophical Transactions of the Royal Society of London A: Mathematical, Physical and Engineering Sciences 364, 2009-2039.

Meyer, M., Geersen, J., Krastel, S., Schwenk, T., Winkelmann, D., 2012. Dakar Slide Offshore Senegal, NW-Africa: Interaction of Stacked Giant Mass Wasting Events and Canyon Evolution, in: Yamada, Y., Kawamura, K., Ikehara, K., Ogawa, Y., Urgeles, R., Mosher, D., Chaytor, J., Strasser, M. (Eds.), Submarine

Mass Movements and Their Consequences. Springer Netherlands, pp. 177-188.

Micallef, A., Masson, D.G., Berndt, C., Stow, D.A.V., 2007. Morphology and mechanics of submarine spreading: A case study from the Storegga Slide. Journal of Geophysical Research: Earth Surface 112, 1-21.

Moernaut, J., De Batist, M., 2011. Frontal emplacement and mobility of sublacustrine landslides: Results from morphometric and seismostratigraphic analysis. Marine Geology 285, 29-45.

Owen, M., Day, S., Maslin, M., 2007. Late Pleistocene submarine mass movements: occurrence and causes. Quaternary Science Reviews 26, 958-978.

Pereira, R., Alves, T.M., 2011. Margin segmentation prior to continental break-up: A seismic–stratigraphic record of multiphased rifting in the North Atlantic (Southwest Iberia). Tectonophysics 505, 17-34.

Piper, D.J.W., Aksu, A.E., 1987. The source and origin of the 1929 grand banks turbidity current inferred from sediment budgets. Geo-Marine Letters 7, 177-182.

Piper, D.J.W., Cochonat, P., Morrison, M.L., 1999. The sequence of events around the epicentre of the 1929 Grand Banks earthquake: initiation of debris flows and turbidity current inferred from sidescan sonar. Sedimentology 46, 79-97.

Reimer, P.J., Bard, E., Bayliss, A., Beck, J.W., Blackwell, P.G., Bronk Ramsey, C., Grootes, P.M., Guilderson, T.P., Haflidason, H., Hajdas, I., Hatté, C., Heaton, T.J., Hoffmann, D.L., Hogg, A.G., Hughen, K.A., Kaiser, K.F., Kromer, B., Manning, S.W., Niu, M., Reimer, R.W., Richards, D.A., Scott, E.M., Southon, J.R., Staff, R.A., Turney, C.S.M., van der Plicht, J., 2013. IntCal13 and Marine13 Radiocarbon Age Calibration Curves 0–50,000 Years Cal BP.

Seibold, E., 1982. The Northwest African Continental Margin — An Introduction, in: von Rad, U., Hinz, K., Sarnthein, M., Seibold, E. (Eds.), Geology of the Northwest African Continental Margin. Springer Berlin Heidelberg, Berlin, Heidelberg, pp. 3-20.

Smith, D.E., Harrison, S., Jordan, J.T., 2013. Sea level rise and submarine mass failures on open continental margins. Quaternary Science Reviews 82, 93-103.

Stuiver, M., Polach, H. A., 1977. Reporting on 14C data. Radiocarbon 19, 355–363.

Stuiver, M., Reimer, P. J., 1986. A computer program for radiocarbon age calibration. Radiocarbon 28, 1022-1030.

Sultan, N., Cochonat, P., Canals, M., Cattaneo, A., Dennielou, B., Haflidason, H., Laberg, J.S., Long, D., Mienert, J., Trincardi, F., Urgeles, R., Vorren, T.O., Wilson, C., 2004. Triggering mechanisms of slope instability processes and sediment failures on continental margins: a geotechnical approach. Marine Geology 213, 291-321.

Talling, P., Clare, M., Urlaub, M., Pope, E., Hunt, J., Watt, S., 2014. Large Submarine Landslides on Continental Slopes: Geohazards, Methane Release, and Climate Change. Oceanography 27, 32-45.

Tappin, D.R., Watts, P., McMurtry, G.M., Lafoy, Y., Matsumoto, T., 2001. The Sissano, Papua New Guinea tsunami of July 1998 — offshore evidence on the source mechanism. Marine Geology 175, 1-23.

Urgeles, R., Leynaud, D., Lastras, G., Canals, M., Mienert, J., 2006. Back-analysis and failure mechanisms of a

large submarine slide on the ebro slope, NW Mediterranean. Marine Geology 226, 185-206.

Urlaub, M., Talling, P.J., Masson, D.G., 2013. Timing and frequency of large submarine landslides: implications for understanding triggers and future geohazard. Quaternary Science Reviews 72, 63-82.

Urlaub, M., Talling, P.J., Zervos, A., Masson, D., 2015. What causes large submarine landslides on low gradient (<2°) continental slopes with slow (~0.15 m/kyr) sediment accumulation? Journal of Geophysical Research: Solid Earth 120, 6722-6739.

Vanneste, M., Mienert, J., Bunz, S., 2006. The Hinlopen Slide: A giant, submarine slope failure on the northern Svalbard margin, Arctic Ocean. Earth and Planetary Science Letters 245, 373-388.

Vanneste, M., Sultan, N., Garziglia, S., Forsberg, C.F., L'Heureux, J.-S., 2014.Seafloor instabilities and sediment deformation processes: The need for integrated, multi-disciplinary investigations. Marine Geology 352, 183-214.

Varnes, D.J., 1978. Slope movement types and processes, in Schuster, R.L., and Krizek, R.J., eds., Landslides-Analysis and control: National Research Council, Washington, D.C., Transportation Research Board, Special Report 176, 11-33.

Watts, P., Grilli, S.T., Tappin, D.R., Fryer, G.J., 2005.Tsunami Generation by Submarine Mass Failure. II: Predictive Equations and Case Studies. Journal of Waterway, Port, Coastal, and Ocean Engineering 131, 298-310.

Weaver, P.P.E., Kuijpers, A., 1983. Climatic control of turbidite deposition on the Madeira Abyssal Plain. Nature 306, 360-363.

Weaver, P.P.E., Wynn, R.B., Kenyon, N.H., Evans, J., 2000.Continental margin sedimentation, with special reference to the north-east Atlantic margin. Sedimentology 47, 239-256.

Wynn, R.B., Masson, D.G., Stow, D.A.v., Weaver, P.P.E., 2000. The Northwest African slope apron: a modern analogue for deep-water systems with complex seafloor topography. Marine and Petroleum Geology 17, 253-265.

Zhao, F., Alves, T.M., Li, W., Wu, S., 2015. Recurrent slope failure enhancing source rock burial depth and seal unit competence in the Pearl River Mouth Basin, offshore South China Sea. Tectonophysics 643, 1-7.

3 Manuscript II

Giant buried sediment mounds on the Western Saharan margin (NW Africa): Origin, evolution and paleoceanographic implications

Wei Li[a]*, Sebastian Krastel[a], Tiago M. Alves[b], Michele Rebesco[c], Morelia Urlaub[d], Aggeliki Georgiopoulou[e], Felix Gross[a]

[a]Institute of Geosciences, University of Kiel, 24118Kiel, Germany

[b] 3D Seismic Lab, School of Earth and Ocean Sciences, Cardiff University, Main Building, Park Place, Cardiff, CF10 3AT, United Kingdom

[c] Istituto Nazionale di Oceanografia e di Geofisica Sperimentale (OGS), Borgo Grotta Gigante 42/C, Sgonico, 34010 Trieste, Italy

[d] GEOMAR Helmholtz Centre for Ocean Research Kiel, 24148 Kiel, Germany

[e]UCD School of Earth Sciences, University College Dublin, Belfield, Dublin 4, Ireland

*Correspondence to: Wei Li (li@geophysik.uni-kiel.de)

Abstract

New 2D multi-channel seismic profiles acquired along the Western Saharan margin, offshore NW Africa, reveal three giant, buried sediment mounds separated by broad troughs. These sediment mounds are 24 to 37 km-long and 12 to 17 km-wide, and show an elongated geometry and a predominant SE-NW orientation that is perpendicular to the continental margin. The sediment mounds' evolution can be divided into three different stages: a) initial growth during the Middle Eocene, b) main growth stage during the Early Miocene and, c) a maintenance stage during the Middle Miocene. Importantly, the sediment mounds were aggraded on a regional unconformity (H1) that reflects widespread canyon incision on the Western Saharan margin. After a second Oligocene erosional event, sediment aggradation on the sediment mounds was intensified in the Early Miocene under the combined effects of turbidity and contour currents. Conversely, the abandonment of the sediment mounds (Middle-Late Miocene boundary) marked a time interval of major paleoceanographic changes along NW Africa, and new depositional patterns were subsequently established. The sediment mounds are, therefore, ideal records of the initiation, intensification, and evolution of bottom currents along the Western Saharan margin. Their inception suggests a time-period of intense deep-geostrophic activity with much more energetic conditions than the ones recorded at present.

1 Introduction

Over the last few decades, a wealth of studies have focused on the interplay of sedimentary processes and their relevance for the build-up of continental margins (Rebesco et al., 2002; Hernández-Molina et al., 2006; Mulder et al., 2008; Hernández-Molina et al., 2016). Downslope and along-slope currents are, as a result, considered as the key processes shaping the architecture of continental margins, controlling the delivery of sediments to deep-ocean basins (Mulder et al., 2008). Gravity-driven, downslope sediment transport involves mass-wasting and turbidity currents on continental slopes, and both are capable of transporting material from the shelf and upper slope to the continental rise and abyssal plains (e.g. Talling et al., 2007). They can create extensive channel levee deposits and form sediment ridges or mounds (Donda et al., 2007; Rotzien et al., 2014). Along-slope processes are generated by contour-following deep-geostrophic (bottom) currents,whose role on the sedimentary evolution of continental margins is now better understood (Hernández-Molina et al., 2016).

Sediment drifts are defined as sediment bodies deposited, or significantly reworked, by the lengthy action of bottom currents (Faugères et al., 1999; Stow et al., 2002; Rebesco et al., 2014). Sediment drifts are typically composed of fine-grained, highly bioturbated mud with variable amounts of sand and silt (Stow and Faugères, 2008). They can show widths of tens of km, lengths up to hundreds of kilometers, and reliefs of 200 m to ~2000 m (e.g., sediment Drift 7 off the Antarctic Peninsula; Rebesco et al., 2002, 2007). Hence, sediment drifts can significantly influence the morphology of continental margins (Hernández-Molina et al., 2016). They can comprise ideal records of long-term variations in paleocurrents and paleoclimate (Hernández-Molina et al., 2003), as the sediment accumulated in drifts commonly present significant lateral continuity, contain limited depositional hiatuses, and reflect high sedimentation rates (Rebesco et al., 2014). When depositional hiatuses are present, they usually reflect oceanographic or tectonic changes of significance to the margin(s) on which they are identified (Alves, 2011; Gruetzner and Uenzelmann-Neben, 2016).

Sediment drifts and associated bottom currents have been widely documented along passive continental margins, such as the Gulf of Cádiz (Hernández-Molina et al., 2006, 2016), the Amundsen Sea (Uenzelmann-Neben and Gohl, 2012), and the eastern Agulhas Ridge area (Gruetzner and Uenzelmann-Neben, 2016). For instance, twelve large-scale sediment mounds separated by deep-sea channels occur west of the Antarctic Peninsula on the upper continental rise (Rebesco et al., 2002). These sediment mounds were controlled by the interaction of along-slope bottom and downslope turbidity currents (Rebesco et al., 2002, 2007). Sediment drifts have also been documented on the

Gabon continental margin (West Africa) (Séranne and Nzé Abeigne, 1999). However, despite the identification of contourites along the NW Africa margin at DSDP Site 397 and ODP Site 657 (von Rad and Arthur, 1979; Faugères et al., 1989), detailed reports of sediment drifts along the remainder of NW Africa are still sparse (Wynn et al., 2000; Krastel et al., 2012).
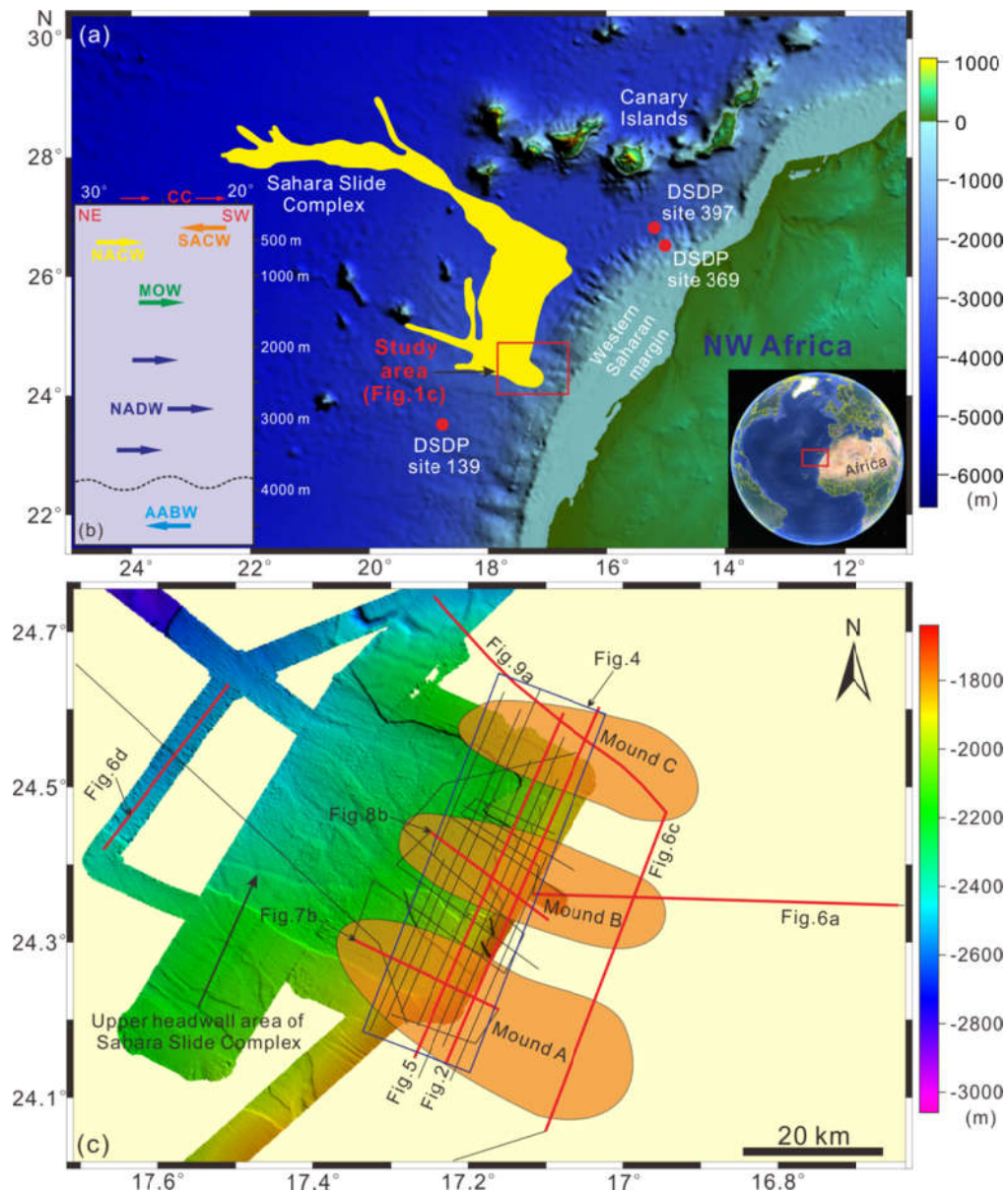

Fig.1 (a) Topographic map of the continental margin of NW Africa showing the distribution of the Sahara Slide Complex, which is marked in yellow (modified after Wynn et al., 2000 and Georgiopoulou et al., 2010) and major geomorphological features (e.g. Canary Islands). The red box represents the location of the study area. The red dots indicate the locations of the DSDP sites that are close to the study area. (b) Stratification of present-day oceanic circulations along the Western Saharan margin (modified after Sarnthein et al., 1982 and Knoll et al., 2002). The arrows indicate the directions of the oceanic circulations. CC: Canary Currents; SACW: South Atlantic Central Water;

NACW: North Atlantic Central Water; MOW: Mediterranean Outflow Water; NADW: North Atlantic Deep Water; and AABW: Antarctic Bottom Water.(c) Bathymetric map of the study area with locations of the acquired multi-channel seismic lines (marked by solid black lines). The solid red lines represent the seismic lines used in this study.

Our study area is located in the upper headwall region of the Sahara Slide Complex, on the Western Saharan margin, NW Africa (Fig. 1a). The region is largely affected by downslope gravitational processes (Georgiopoulou et al., 2010; Krastel et al., 2012; Li et al., in press). Newly acquired high-resolution 2D seismic data allowed us to recognise, for the first time, the presence of three giant buried sediment mounds (Fig. 1b). The identification of these sediment mounds provides an ideal opportunity to improve our understanding of Late Cenozoic depositional and erosional processes along the Western Saharan margin. Analysis of these sediment mounds can be useful in understanding ancient and modern oceanographic current patterns and, ultimately, to unravel the Cenozoic sedimentary evolution of NW Africa, with consequences for paleoceanography of the entire Central Atlantic Region. Hence, this paper aims to:

a) Investigate the spatial distribution, geometry and internal architecture of the interpreted sediment mounds;

b) Analyse the origin and development processes of the sediment mounds;

c) Establish the Cenozoic sedimentary evolution of the Western Saharan margin;

d) Discuss the significance of the sediment mounds in the framework of Central Atlantic paleoceanography.

2 Geological setting

2.1 Geological framework

The Northwest African margin is bordered by a flat continental shelf that is 40-60 km wide, although maximum shelf widths of >100 km occur off Western Saharan (Fig. 1a; Seibold, 1982; Wynn et al., 2000). The shelf break occurs at a water depth of 100-200 m. The Western Sahara margin comprises the offshore continuation of the Aaiun-Tarfaya coastal basin, and is now part of the mature Atlantic-type continental margin of NW Africa (von Rad and Wissmann, 1982). Rifting between NW Africa and NE America began in Late Triassic times (Davison, 2005). After Early Jurassic continental breakup between the African and North American plates, thick (>10 km) sediments were deposited on the NW African margin. The western Saharan continental slope and upper rise were shaped during the past 135 Ma from ancient paleoslopes by a number of discrete constructional and erosional phases (Seibold and Hinz, 1974). As a result, the location of the continental slope has not changed very much for the past 90 Ma. (von Rad and Wissmann, 1982). Deep-water successions predominantly consist of marine clastic intervals spanning in age from the Jurassic to Holocene (Davison, 2005). The continental slope hardly prograded from Late Cretaceous to Tertiary times and, as a result, margin depocentres shifted to the upper continental rise during the Neogene (Davison, 2005).
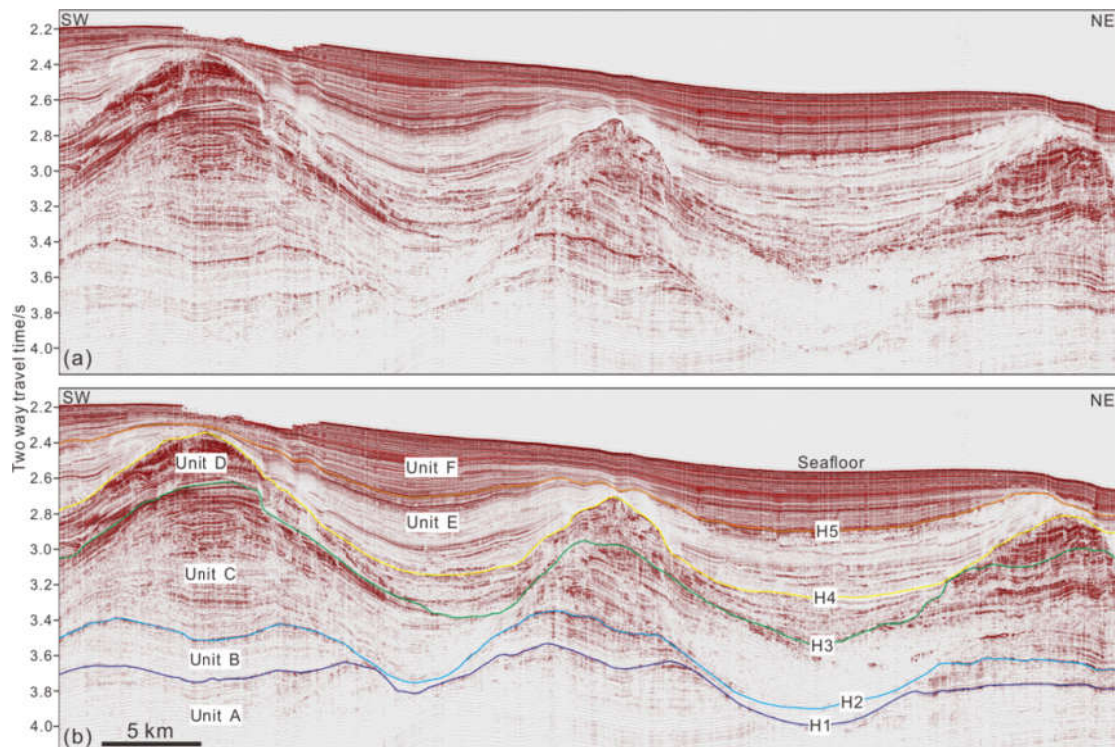
Fig.2 (a) Selected 2D seismic profile across the upper headwall region of the Sahara Slide Complex (see Fig. 1b for location) showing the seismic stratigraphy of the study area. (b) Corresponding interpretation showing the main seismic horizons (H1 to H5) and seismic units (Unit A to F).

2.2 Oceanographic framework

The present-day ocean circulation along the Western Saharan margin is dominated by the Canary Current, South Atlantic Central Water (SACW), North Atlantic Central Water (NACW), Mediterranean Outflow Water (MOW), North Atlantic Deep Water (NADW) and the Antarctic Bottom Water (AABW) (Fig. 1c; Sarnthein et al., 1982).
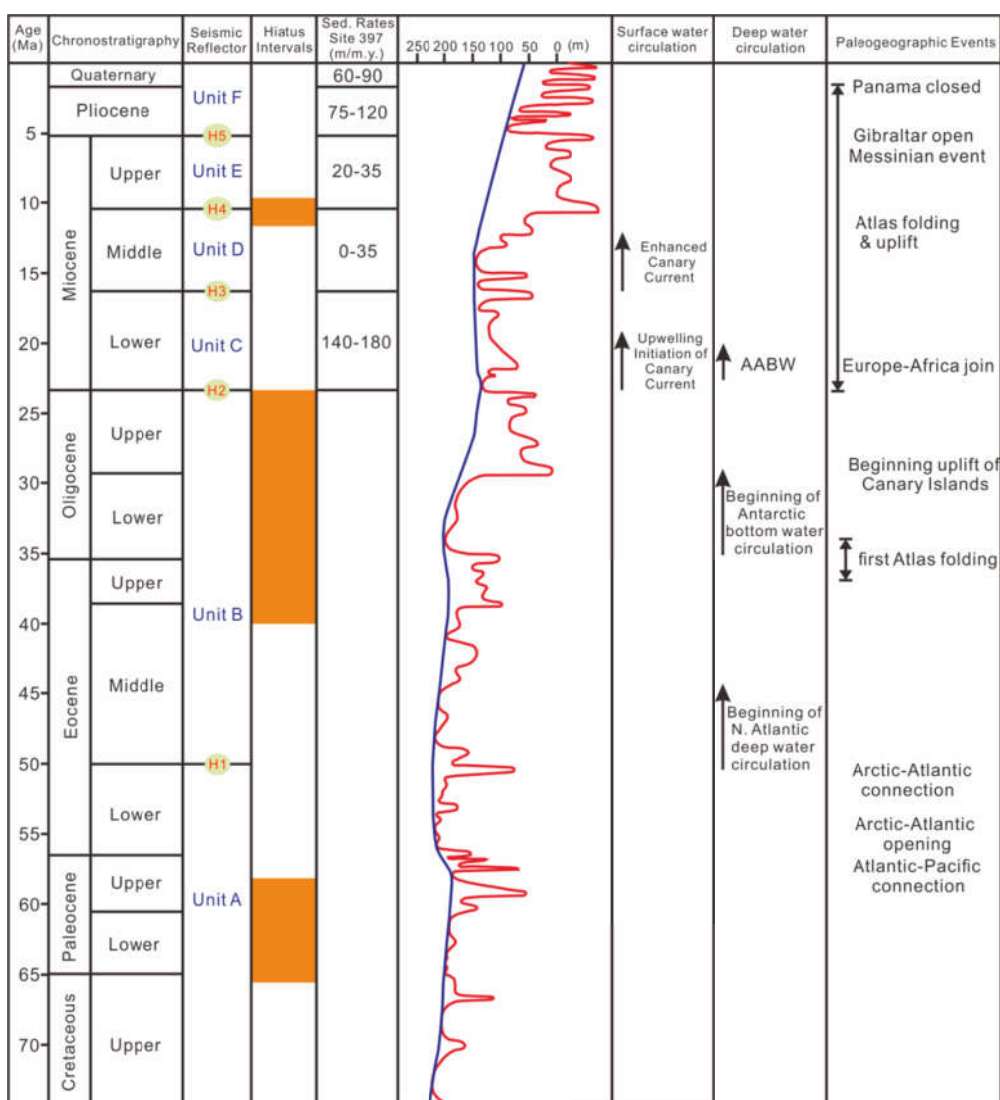

Fig.3 Stratigraphic column of the Western Saharan margin off NW Africa (modified after Arthur et al., 1979; von Rad and Wissmann, 1982; Vear, 2005). The ages of the seismic surfaces are

determined based on stratigraphic interpretation from von Rad and Wissmann et al. (1982) and chrono-stratigraphic information from nearby DSDP sites 139, 369 and 397. The orange rectangles represent depositional hiatuses. Sedimentation rates are taken from the DSDP site 397 (von Rad and Arthur, 1979). The oceanic circulations and paleogeographic events are modified after von Rad and Wissmann (1982). Eustatic sea-level curve (Haq et al., 1987) showing both short (red line) and long (blue line) term variations since the Cretaceous.

The NW African continental shelf is, at present, chiefly under the influence of the south-flowing Canary Current, a water mass that is largely linked to changes in atmospheric circulation along NW Africa. The Canary Current is a component of the North Atlantic Subtropical Gyre and flows at the surface along the coast. Upwelling occurs along the entire NW African continental margin and affects the middle-outer shelf and upper continental slope down to a depth of 500 m (Fig. 1c; Sarnthein et al., 1982). Upwelling results from complex interactions amongst the Trade Winds, which are parallel to the coast, the Canary Current, and the Earth's rotation (Ekman transport) (see Barton et al., 1998).

In the southern part of the Western Sahara margin (south of 22°N), upwelling waters are fed by the nutrient-rich South Atlantic Central Water (SACW) (Sarnthein et al., 1982). In the northern part of the same margin, upwelled water masses are derived from the nutrient-poorer North Atlantic Central Water (NACW), which follows the Canary Current from the north at 100-600 m water depth (Fig. 1c; Sarnthein et al., 1982). South of 22°N, the NACW gradually veers out from the continental slope to the open sea. In parallel, Mediterranean Outflow Water (MOW) has been traced south along the continental margin to 20°N as a center of highly saline and relatively oxygen-rich water, gradually sinking from 1000 m to 1500 m water depth (Fig. 1c; Knoll et al., 2002).

The NADW is mainly formed by a mixture of Iceland-Scotland Overflow Water, Labrador Sea Water and Lower Deep Water (van Aken, 2000). It occurs at a water depth of 1500-3800 m and flows in a southerly direction (Fig. 1c; Sarnthein et al., 1982; van Aken, 2000). The Antarctic Bottom Water (AABW) can hardly be recognised in the study area using temperature-salinity data, as it occurs below 3800 m and flows in a north-easterly direction (Fig. 1c; Wynn et al., 2000). Bottom currents along the margin are thought to be fairly weak at present, with current velocities varying between 1 and 6 cm/s (Sarnthein et al., 1982; Wynn et al., 2000).

3 Data and methods

The data set used in this study consists of multi-beam bathymetric data, 2D multi-channel seismic profiles and stratigraphic information from DSDP sites (Figs. 1a and b). The bathymetric and seismic data cover most of the upper headwall area of Sahara Slide Complex. Multi-beam bathymetry data were obtained during Cruise MSM11/2. A hull-mounted Kongsberg Simrad system EM120 was used during its acquisition. High-resolution multi-channel seismic data were acquired during Cruise P395 with the aim of investigating sedimentary structures along the continental margin of NW Africa.

Two Micro-GI gun (0.1 l each) with a main frequency of ~ 200 Hz were used as sources for the transmitting signal, and were towed about 1 m below the water surface. A 187.5 m long 120-channel digital streamer was used during data acquisition. In total, thirty-five seismic profiles were collected. Standard processing including the setup of the signal geometry, bandpass filtering, binning at 1 m, NMO-correction with a constant velocity of 1500 m/s, stacking, and time-migration. IHS Kingdom® software was used for the interpretation of the seismic data. Time-structural maps were also produced to display the geometry of the sediment mounds.
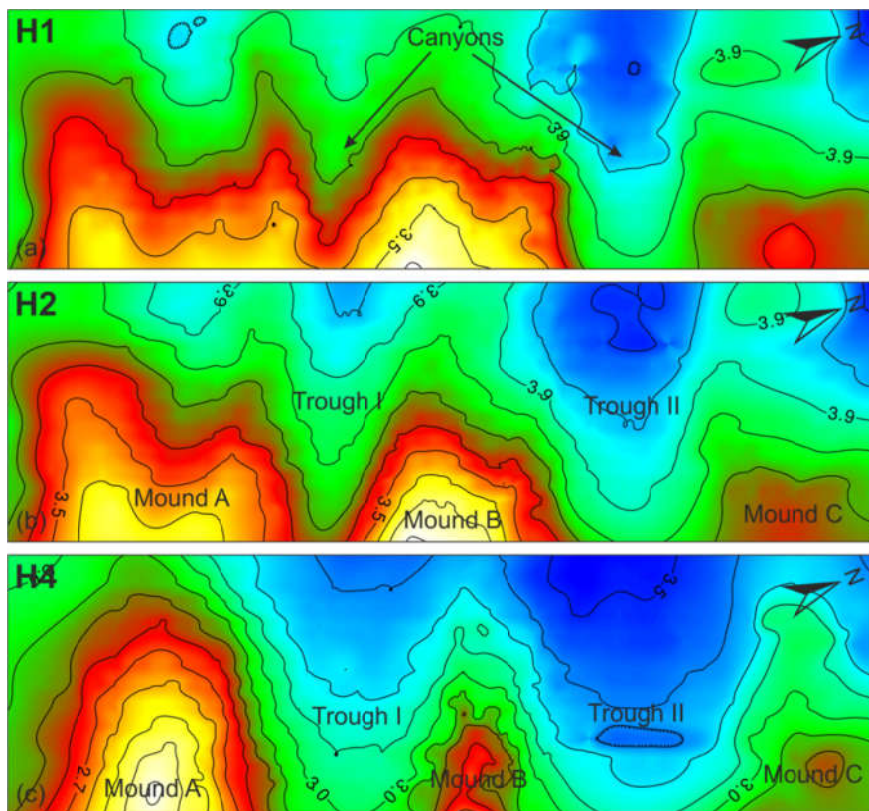

Fig.4 (a) Time structure map of the bottom surface (H1) of the sediment mounds showing the

paleotopography before the formation of the sediment mounds. Two canyons can be observed between the sediment ridges (overbank levees). (b) Time structure map of H2. (c) Time structure map of the top surface (H4) of the sediment mounds illustrating their morphology in detail. Two broad (more than 10 km in width) troughs (I and II) are identified between the sediment mounds. The contour internal is 0.1 s for these three figures.

4 Seismic stratigraphy

4.1 Seismic horizons

Five stratigraphic horizons (H1 to H5), representing regional unconformities with marked erosional truncation and onlap, can be traced throughout the study area (Figs. 2a and b). The ages of these horizons are correlated with the stratigraphic interpretation from von Rad and Wissmann et al. (1982), and chronostratigraphic information from DSDP Sites 139, 369 and 397, located in areas adjacent to the Western Saharan Margin (Fig. 3).
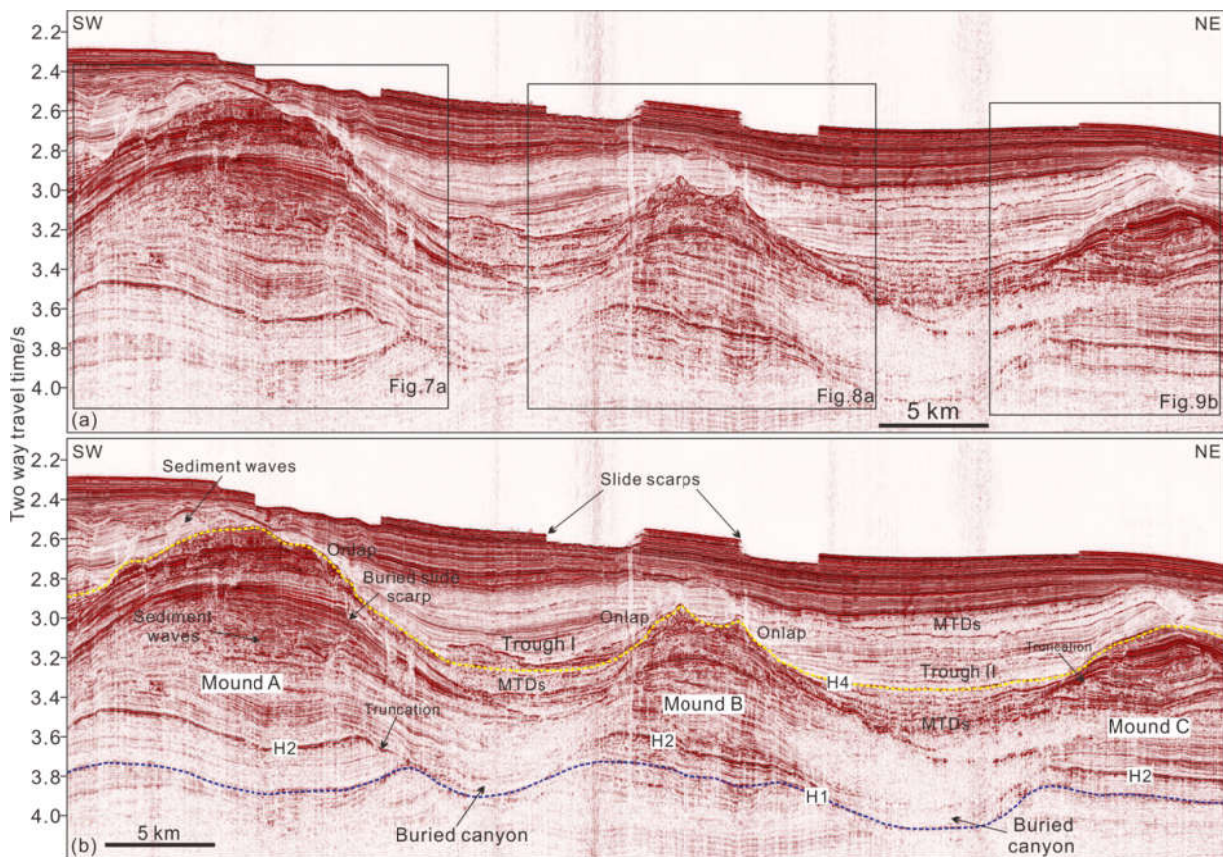

Fig.5 Two-dimensional (2D) dip-oriented seismic profile from the upper headwall region of the Sahara Slide Complex. (a) Uninterpreted seismic profile. (b) Interpreted seismic profile showing three identified sediment mounds (Mound A, B and C) separated by two broad troughs (Trough I and II). Sequence truncations and onlaps are marked. Horizon 1 (H1) and Horizon 4 (H4) represent the bottom and top surface of the sediment mounds, respectively.

Horizon H1 is the deepest identifiable erosional unconformity on our seismic profiles, and comprises a moderate- to high-amplitude, continuous reflection (Figs. 2a and b). It marks the

83

boundary between Lower and Upper Eocene strata (Fig. 3). The two-way time (TWT) depth of H1 varies from 3.4 s to 4.0 s on the time structure map, forming two elongated depressions with a NW-SE orientation (Fig. 4a). They show a U-shaped geometry on strike-oriented seismic sections (Figs. 5a and b) and can be interpreted as buried submarine canyons.

Horizon H2 forms a prominent erosional unconformity and it is characterised by a high-amplitude, continuous seismic reflection (Figs. 2a and b). It separates Oligocene from Lower Miocene strata (Fig. 3). This unconformity (H2) was interpreted as an Oligocene to Early Miocene hiatus by Hinz et al. (1974). Wissmann (1979) later confirmed that the surface does not merely represent a lithological change within Lower Miocene strata, changing from nannofossil-rich to more siliceous marls. It is, in fact, a surface of erosional truncation observed on the entire continental slope. Its TWT depth ranges from 3.3 s to 4.0 s (Fig. 4b).

Horizon H3 is an erosional, continuous, moderate- to high-amplitude seismic reflection (Fig. 2a and b). It marks the boundary between Lower and Middle Miocene strata (Fig. 3). The depth of Horizon H3 varies significantly (up to 1 s TWT) between the top of the mounds and the areas in between them. Horizon H3 crosses several buried slide scarps, which are characterised as discontinuous to chaotic low-amplitude reflections separated from continuous moderate- to high-amplitude reflections by a sharp, steep boundary (Fig. 5b).

Horizon H4 comprises a high-amplitude seismic reflection and separates Middle Miocene from Upper Miocene strata (Figs. 2a, b, 5a and b). On the time-structure map in Figure 4c, two troughs and three sediment mounds can be identified. The TWT depth of H4 changes from 2.3 s on the mounds to 3.5 s within the troughs (Fig. 4c). Horizon H4 is interpreted to be the top surface of the sediment mounds, as reflectors above onlap onto it and heal the topography created by the mounds. Multiple erosive features can be observed on this horizon.

Horizon H5 is the boundary between Upper Miocene and Pliocene strata (Fig. 3). It is recognised as a continuous, high-amplitude seismic reflection (Figs. 2a and b).

4.2 Seismic units

The horizons described in the previous section separate the seismic sections into six seismic units (Figs. 2a and b). These units are herein named as Unit A to Unit F. Unit A is bounded by Horizon H1 on its top and comprises the Late Cretaceous to Lower Eocene succession. It is mainly characterised by low-amplitude reflections that are likely due to the attenuation of the seismic signal with increasing depth. No visible faults can be observed within Unit A (Fig. 2a).

The top of Unit B corresponds to Horizon H2 and at its base coincides with H1. This unit is dominated by low to moderate amplitude, continuous seismic reflections (Figs. 2a and b). Unit B

should be Middle Eocene in age, as Upper Eocene to Oligocene strata have been eroded in our study area (von Rad and Wissmann, 1982).

Unit C comprises low-amplitude continuous reflections at its base, and semi-continuous, relatively higher amplitude reflections towards its top. Unit C is bounded by H2 and H3, and is Lower Miocene in age. Numerous sediment waves can be observed in the upper part of Unit C and exhibit continuous, moderate- to low-amplitude reflections (Figs. 2a and 5).

Unit D is bounded at its base by Horizon H3 and at its top by H4, comprising Middle Miocene strata (Fig. 2b). Unit D shows continuous, high-amplitude seismic reflections in the sediment mounds and continuous to chaotic, low- to moderate-amplitude reflections between these mounds. These latter chaotic seismic reflections can be interpreted to comprise mass-transport deposits (MTDs) based on established diagnostic criteria (e.g. Moscardelli et al., 2006). Multiple MTDs can be observed in Unit D in the downslope region (Fig. 5b).

Unit E is confined by Horizons H4 and H5 and its age spans the Late Miocene to Pliocene. Unit E shows continuous, parallel reflections of low- to moderate amplitude (Figs. 3a and b). Strata in Unit E drape and onlap the underlying Unit D.

Unit F is Pleistocene to Holocene in age. It exhibits continuous, parallel reflections of moderate to high seismic amplitude (Figs. 3a and b), which can be related to hemipelagic sediments.
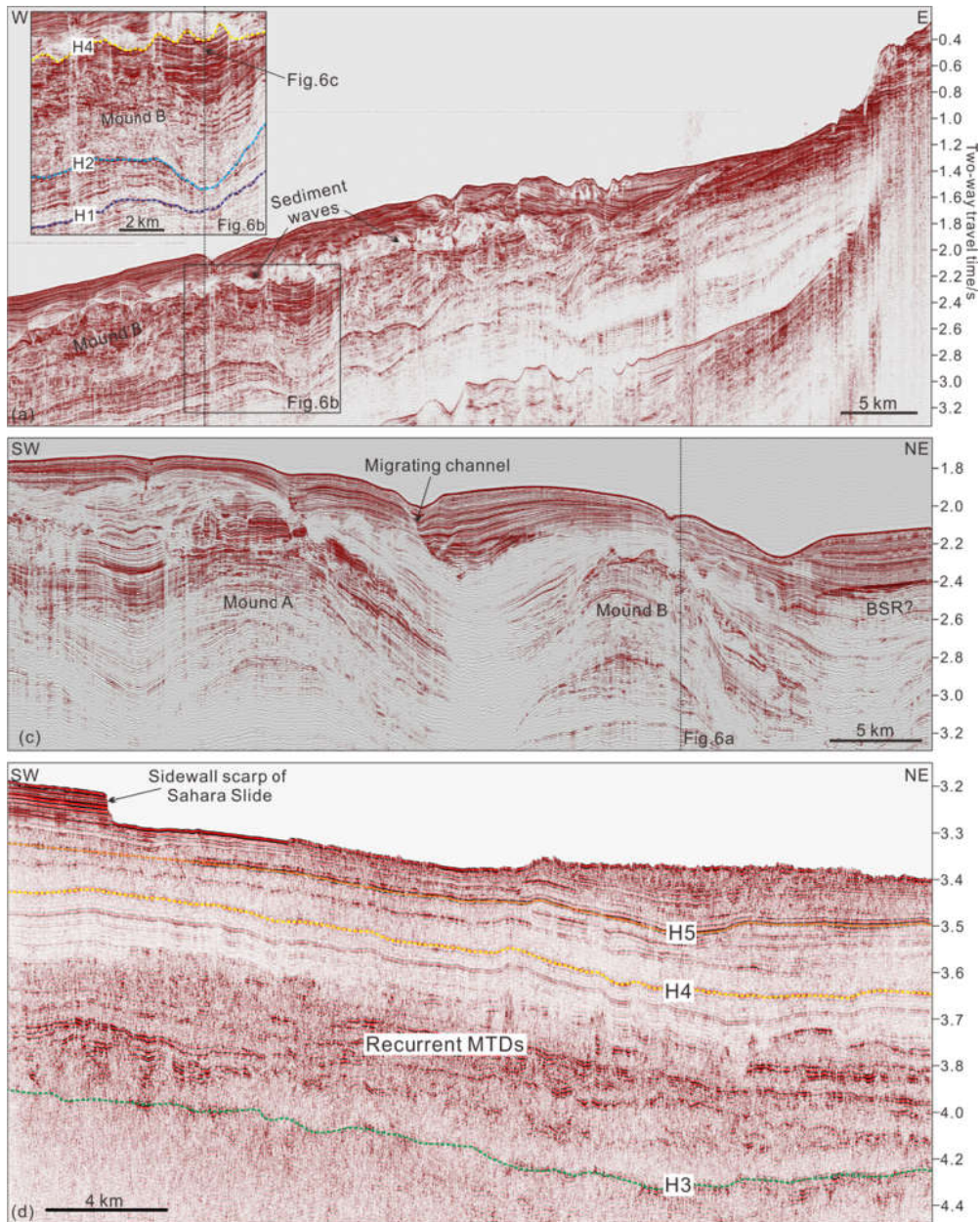
Fig.6 Two-dimensional (2D) seismic profiles showing the architecture of the West Saharan continental rise and of the sediment mounds. (a) Seismic profile across the continental slope and upper rise. The crossing with Fig. 6c is shown. (b) Zoomed profile showing the internal character of Mound B. The crossing with Fig. 6a is shown. (c) 2D seismic profile parallel to the continental margin highlighting two sediment mounds (Mounds A and B) and a SW-migrating channel. (d) Strike-oriented 2D seismic profile showing recurrent MTDs in Unit D.

5 Giant sediment mounds on the Western Sahara margin

5.1 Distribution and geometry of the sediment mounds

Seismic profiles acquired in a direction parallel to the present-day shelf edge display three sediment mounds (Figs. 2 and 5). Horizon H1 and H4 are interpreted to be the base and top of the sediment mounds and have been traced on all the seismic lines. The distribution and geometry of the sediment mounds in plan-view can be inferred from the time structure map in Fig. 4C, showing the top surface of the sediment mounds (H4). These sediment mounds (Mound A, B and C) are separated by two broad troughs, Troughs I and II, each up to 10 km wide (Fig. 4c). All three sediment mounds share common features. They are elongated in a northwest direction approximately perpendicularly to the margin (Fig. 1b). The sediment mounds decrease in height downslope until they disappear at ~2200 m water depth (about 3 s in Fig. 4). Their upslope morphology is unknown due to the absence of data (Fig. 1b). The flanks of the sediment mounds are much steeper in comparison to their internal strata. Mound A is the largest in the study area with a length of at least 37 km and a width of 17 km (Figs. 4c and 5b). Mound B is smaller than Mound A. Its length is at least 30 km and its width is ~12 km. Mound C has a length of at least 24 km and its width is ~10 km in the region covered by seismic data.

5.2 Internal character of the sediment mounds

The closely-spaced seismic grid interpreted in this work provides detailed insight into the internal character of the sediment mounds, which are remarkably different from the surrounding strata. In general, the sediment mounds are characterised by reflections of low to moderate continuity at their base, and moderate- to high-amplitude seismic reflections towards its top (Fig. 5b).The crests of the sediment mounds appear to have been eroded (Figs. 6a and b). Multiple slide scarps mark the steep flanks of the sediment mounds (Figs. 5b and 6c). The acoustic facies inside the troughs is characterised by continuous, low to moderate amplitude reflections, strikingly different from the mounds (Fig. 5b).
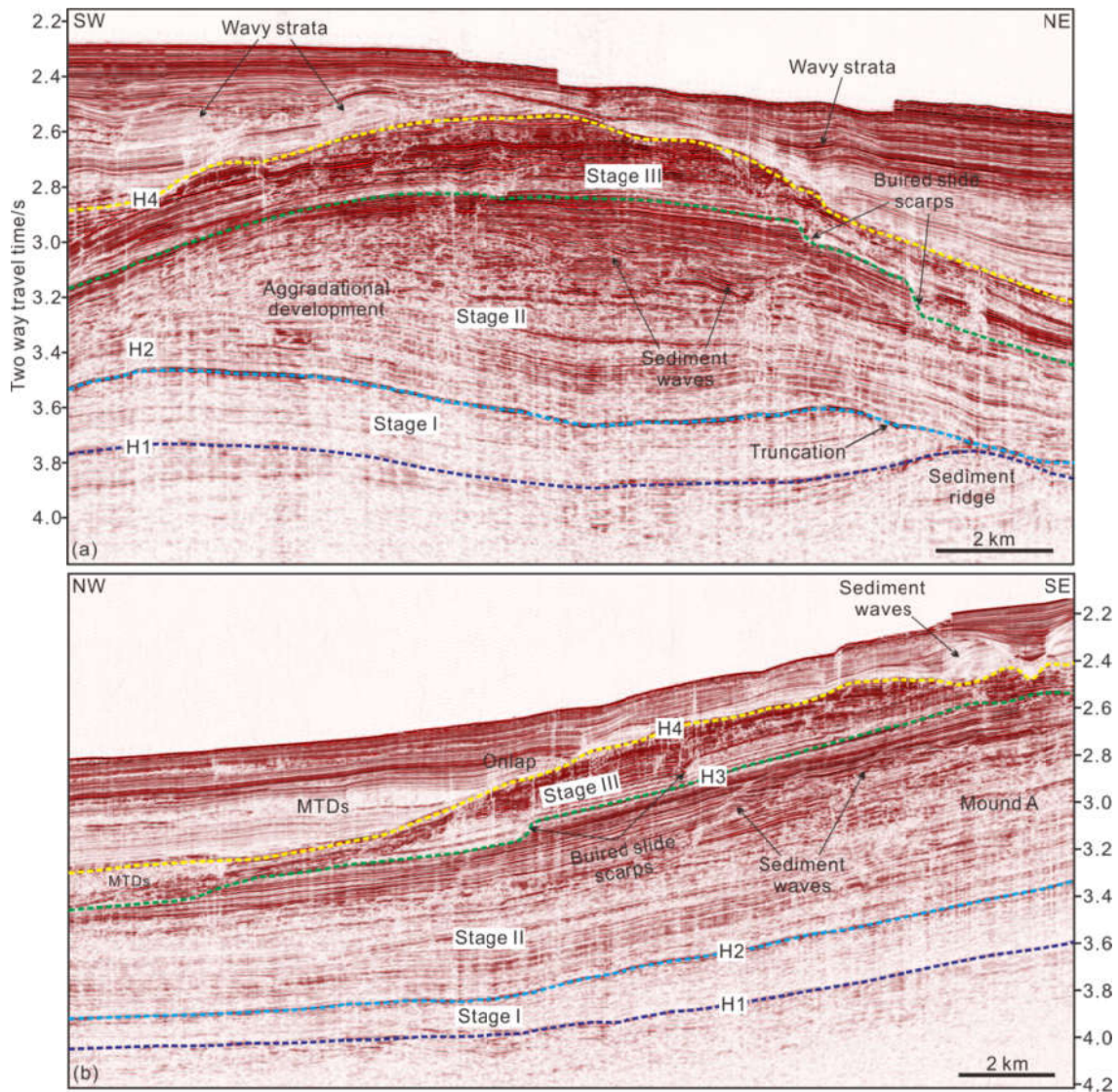
Fig.7 Two-dimensional (2D) seismic profile crossing Mound A. (a) Strike-oriented seismic profile showing the detailed internal character and development processes of Mound A (Stages I, II and III). Onlap and truncation can be identified on the flanks of the mound. Several buried slide scarps are observed within the mound. Note the wavy strata that drape the top of the mound. (b) Dip-oriented seismic profile crossing Mound A revealing the presence of slide scarps and wavy strata inside. MTDs and sediment waves are observed to drape the mound.
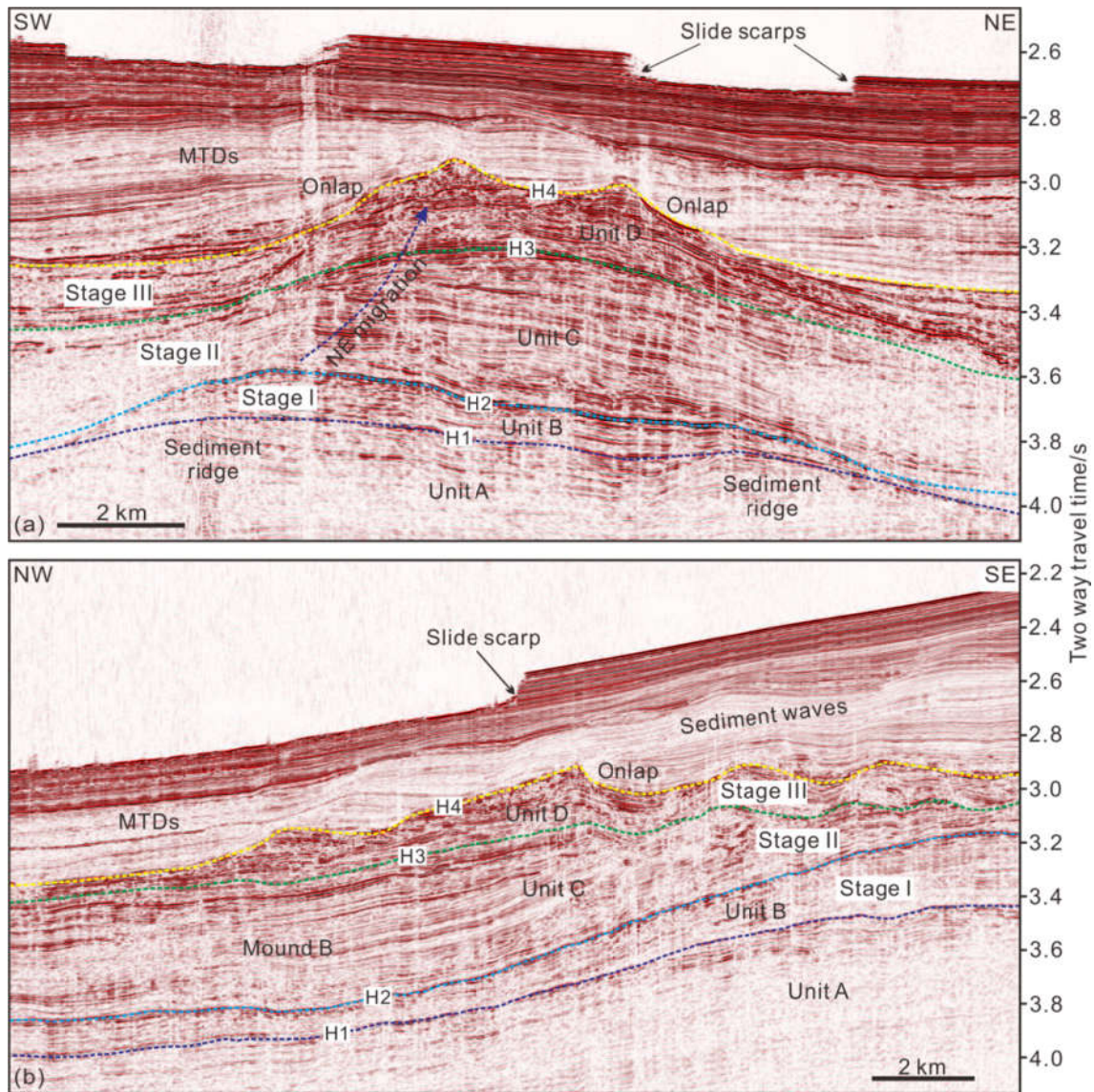
Fig.8 Two-dimensional (2D) seismic profiles crossing Mound B. (a) Strike-oriented revealing the detailed internal character and development processes of Mound B (Stages I, II and III). The crest of the mound shows a slightly NE migration trend. (b) Dip-orientedprofile showing the development processes of Mound B. Note that the top surface (H4) of the mound was eroded severely and onlaps are labeled.

The depth difference between Mound A and the nearby Trough I can reach ~800 m considering an average velocity of 2000 m/s for the strata within the sediment mounds.On the SW-NE seismic profile (Fig. 7a), Mound A seems to be slightly asymmetric and shows an aggradational stacking pattern. Mound A reaches a maximum thickness of ~1100 m at its center. Both flanks of Mound A are steep and have been unstable in the past; several buried slide scarps can be identified along its flanks at different stratigraphic depths. In addition, numerous MTDs can be seen in the troughs. In the middle and upper part of Mound A, numerous sediment waves can be distinguished. The thickness of

Mound A decreases downslope (Fig. 7b). In the downslope region, wavy strata and several mass-transport deposits (MTDs) cover the top of Mound A. They display onlap geometries over Mound A.

Mound B has an asymmetric shape in cross-section; its southwest flank is steeper than its northeast counterpart (Fig. 8a). Seismic reflections in the lower part of Mound B dip towards the northeast, and are convex in the upper part of this same mound. The development of Mound B started at H1 and exhibits a northeast migration trend. The maximum thickness of Mound B is ~900 m. However, it was likely thicker in the past if we consider the observed erosional features on its top. Sediment waves are also found within Mound B, especially in its upper part (Unit D) (Fig. 8b). MTDs are widely distributed on the top of Mound B and fill the depression flanking it.

Mound C was developed above H1. On the NW-SE seismic profile in Figs. 9a and c, Mound C thins and disappears gradually downslope. Numerous MTDs and buried slide scarps are found in the lower slope region. Seismic reflectors within Mound C terminate laterally. Several slide scarps, occurring at different depths, can be recognised on the southwest flank of Mound C. They were buried by continuous, high-amplitude strata (Fig. 9b).
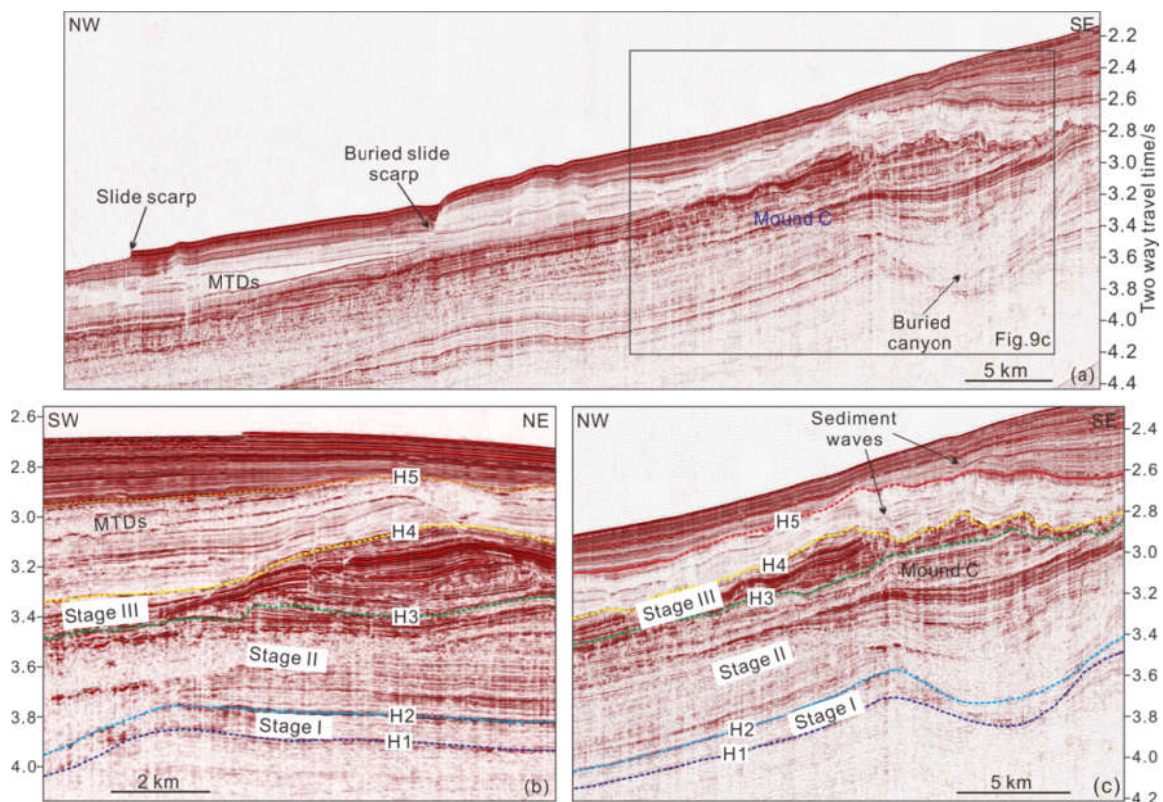

Fig.9 Two-dimensional (2D) seismic profiles crossing Mound C. (a) Dip-oriented profile. Slide scarps and MTDs are identified downslope. Note that the mound thins and disappears gradually downslope. (b) Strike- oriented seismic profile revealing the development stages of Mound C. The

main horizons are labeled. (c) Zoomed profile showing the detailed internal character and development processes (Stages I, II and III) of Mound C. Sediment waves are identified above.

6 Discussion

6.1 Genesis of the sediment mounds on the Western Sahara margin

Sediment mounds have been extensively documented around the world (Rebesco et al., 1996, 2002; Séranne and Nzé Abeigne, 1999; Donda et al., 2007; Gruetzner and Uenzelmann-Neben, 2016). The formation of sediment mounds has been attributed to a variety of processes: (a) turbidity currents (Donda et al., 2007), (b) along-slope bottom currents (Gruetzner and Uenzelmann-Neben, 2016), (c) landward bottom currents (Séranne and Nzé Abeigne, 1999), and (d) the interaction of bottom and turbidity currents (Rebesco et al., 1996). Georgiopoulou et al. (2007) interpreted the buried morphology of the sediment mounts in this paper as giant landslide scarps, but they had based their interpretation on a very small number of seismic lines that did not reveal their geometry. With our new data, we are now in a position to exclude this interpretation and examine the other four processes in order to identify those responsible for the generation of the three giant elongated sediment mounds in the Western Sahara Margin (Figs. 1b, 5a and b).

(a) Turbidity currents: A first explanation for the formation of these sediment mounds implies significant overbank sedimentation between major canyon systems. Sediment mounds have been formed by turbidity currents in overbank regions along the Wilkes Land margin (Donda et al., 2007). The buried submarine canyons observed between the sediment mounds offshore NW Africa are inferred to have been the preferential pathways for turbidity currents, mostly originated from hyperpycnal flows on the shelf or initiated by small-scale slope failures triggered on the continental slope. However, the heights of the sediment mounds reach up to 1 km (e.g. Mound A) and such large scale sediment mounds could not have been formed only by turbidity currents travelling down the submarine canyons. Due to the effect of Coriolis force, more overbank deposition should have occurred on the northeast flank of the submarine canyons, whereas less deposition should have been identified southwest of the canyons. No such asymmetry can be seen on the interpreted seismic data (Fig. 5b). In contrast, the northeastern flank of Trough I is steeper than its southwest counterpart. The size of Mound A is also larger than Mound B. Thus, the sediment mound system does not appear to have been formed by turbidity currents alone.

(b) Along-slope bottom currents: Bottom currents are known to significantly control deep-sea sedimentation, occur almost everywhere in the oceans, and are capable of building up thick and extensive sediment drifts (Hernández-Molina et al., 2006). The geometry and internal character of the sediment mounds in the study area are similar to the sediment drifts documented in the Gulf of Cádiz (Hernández-Molina et al., 2006), northern Rockall Trough (Masson et al., 2002) and the

Amundsen Sea (Uenzelmann-Neben and Gohl, 2012). In order to determine the type of the sediment drifts developed offshore NW Africa, we followed the proposed criteria of Rebesco et al. (2014). Based on the mounds' external geometry (elongated) and dimensions (at least 24 to 37 km in length and 12 to 17 km in width), they could be classified as elongate-mounded drifts (Faugères et al., 1999; Stow et al., 2002). The dimensions of elongate-mounded drifts are very variable, with lengths ranging from a few tens of kilometers to over 1000 km, length-to-width ratios from 2:1 to 10:1, and thicknesses up to several hundred meters (Faugères et al., 1999). In the literature, drift elongation is generally parallel or sub-parallel to the margin (Faugères et al., 1999). However, the sediment mounds identified in this study are all perpendicular to the continental margin, which indicate that the growth of the sediment mounds cannot be controlled by along-slope bottom currents alone.

(c) Landward bottom currents: Séranne and Nzé Abeigne (1999) identified several Oligocene-Holocene sediment drifts perpendicular to the continental margin of Gabon (West Africa). The authors explained their growth by bottom currents flowing upslope under the influence of the Coriolis force. Such landward-directed bottom currents acting on the slope were generated by the southeast Atlantic upwelling, which has been active along the southwestern Africa margin throughout the Neogene (Séranne and Nzé Abeigne, 1999). In our study area, the Canary Current has been active along NW Africa since the Early Miocene (Sarnthein et al., 1982). It is directed towards the southwest, together with divergent surface currents, via an Ekman-driven motion (Barton et al., 1998). Costal upwelling along NW Africa allows surface water masses to be replaced by upwelled deep waters, and further enhances the upward movement of deep water (e.g. Séranne and Nzé Abeigne, 1999). The upwelled water was previously suggested to be NACW (Sarnthein et al., 1982). However, the NACW is only recorded at a water depth of 100-600 m (Sarnthein et al., 1982) and is unlikely to have affected the study area, which is located at larger water depths. Therefore, though some kind of landward bottom currents are not excluded, upwelling of NACW does not appear to be responsible for creating the sediment mounds in our study area.

(d) Interaction of bottom currents and turbidity currents: Caburlotto et al. (2006) identified several sediment mounds on the George V Land (East Antarctica) that are perpendicular to the continental margin. They proposed that sediment mounds were affected by the interplay of westward-flowing contour currents and downslope turbidity currents during the Quaternary. Contour currents were thus responsible for the redistribution of the fine-grained sediment on the flanks of the sediment mounds on the continental rise. A similar interpretation for the origin of sediment mounds has been proposed for the western Antarctica Peninsula (Rebesco et al., 1996). The sediment that forms the sediment mounds chiefly originates from the fine-grained components of turbidity currents flowing on the continental slope through submarine canyons, with the bottom currents pirating the

suspended sediments and re-depositing them on the mounds (Rebesco et al., 1996). This process may well be responsible for the formation of the sediment mounds in our study area. The occurrence of sediment waves within the interpreted sediment mounds also indicates that high-energy, bottom currents were continuously sweeping the NW Africa margin during the growth phase of the sediment mounds (Figs. 7b, 8b and 9c).

6.2 Development processes and controlling factors of the sediment mounds

Based on the overall geometry, morphology, and internal seismic architecture of the sediment mounds we identify three evolutionary stages: (1) an initial growth stage (Middle Eocene), (2) a main growth stage (Early Miocene), and (3) a maintenance stage (Middle Miocene). The continental slope hardly prograded during Late Cretaceous to Eocene (von Rad and Wissmann, 1982). During late Eocene times, Paleogene and Cretaceous strata were eroded and a very large part of the Late Cretaceous to Paleogene record was removed by successive erosional episodes (von Rad and Wissmann, 1982). Slope canyon incision further occurred on the lower slope, and a regional unconformity (H1) was formed along the lower parts of the continental margin.
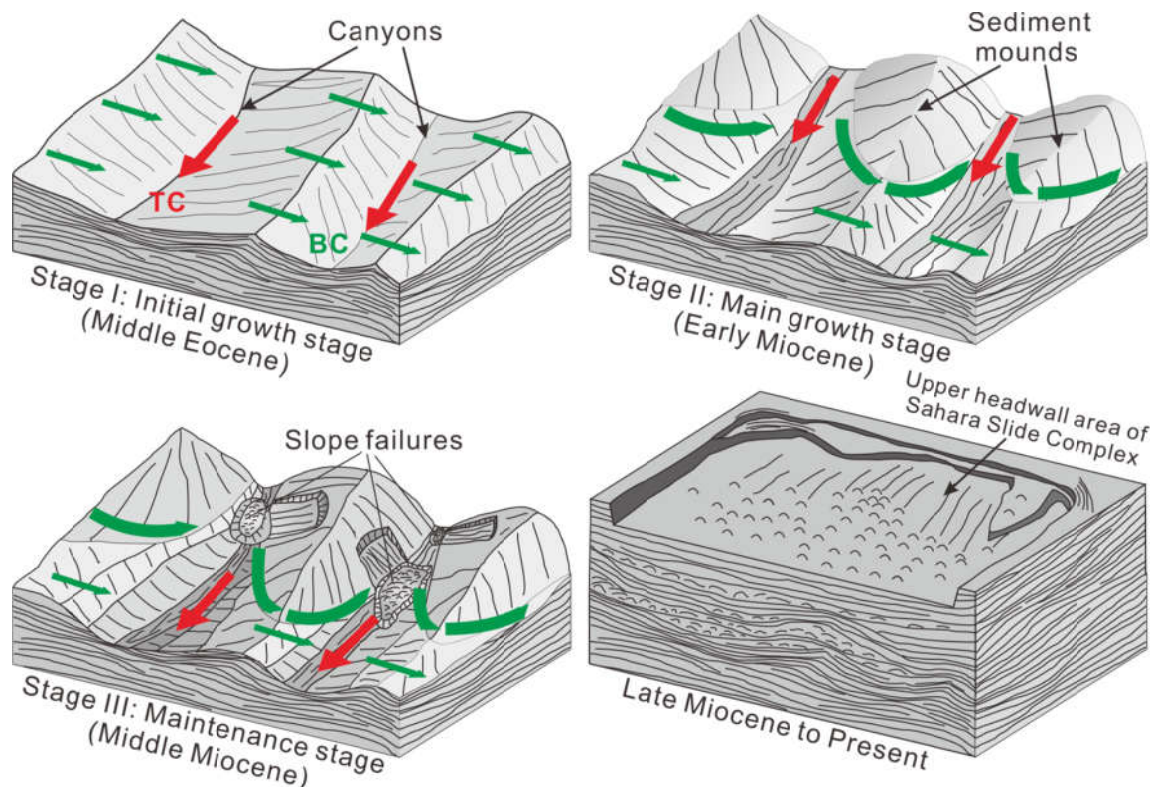

Fig.10 Three-dimensional conceptual model (based on topography of unconformity surfaces) illustrating the evolution processes of the sediment mounds (Mound A, B and C) on the Western Saharan margin. TC: Turbidity currents (Red arrows); BC: Bottom currents (Green arrows). (a) Stage

I: Initial growth stage during the Middle Eocene. The sediment mounds began to develop on an erosional unconformity (H1) (b) Stage II: Main growth stage during the Early Miocene. (c) Stage III: Maintenance stage during the Middle Miocene. Slope failure occurred frequently and resulted in the deposition of MTDs inside the troughs. (d) The sediment mounds and troughs were filled by hemipelagic sediment since Late Miocene.

(1) Stage I: Initial growth stage (Unit B, Middle Eocene)

The development of sediment mounds started after H1, following the pre-existing topography formed by canyon incision. During Stage I (Unit B) the growth of the sediment mounds appears to have resulted from a combination of turbidity and bottom current activity. The control on the location and elongation of the sediment mounds is inherited from the sediment ridges (overbank levees) produced by turbidity currents (Fig. 10a). During this stage, sediment mounds began to develop on pre-existing sediment ridges.

(2) Stage II: Main growth stage (Unit C, Early Miocene)

A major unconformity (H2) was formed by the Oligocene erosional event; slumping, turbidity currents, and submarine canyon incision took place on the continental slope (Figs. 5b and 10b). This conspicuous erosional event occurred simultaneously with a global Late Oligocene sea level drop of several hundred meters (Veil et al., 1977; von Rad and Wissmann, 1982), also recorded on the Moroccan margin, offshore West Iberia and in Mauritania and Senegal (Alves et al., 2003; Vear, 2005). Stage II (Unit C) represents the main growth stage of the sediment mounds, with the development of sediment mounds intensifying above H2 (Fig. 10b). The main growth stage of the sediment mounds may be considered as the direct evidence of enhanced oceanic circulation in the Early Miocene (Sarnthein et al., 1982). Both significant sediment supply and persistent bottom currents are considered as the key processes in the development of large sediment drifts, otherwise only erosional hiatuses and smaller drifts can be produced (Rebesco et al., 1997). The seaway between the North Atlantic and the Tethys gradually closed from the Early Miocene onwards, and Trade Winds were enhanced at this time leading to the initiation of the Canary Current (Knoll et al., 2002). The enhanced Trade Winds also resulted in increased dust (documented at DSDP Site 369) derived from the northwest Saharan fringe, with the subsequent deposition of aeolian-sand turbidites (documented in DSDP Sites 138 and 139) (Diester-Haass, 1978). During this stage, (Early Miocene) DSDP Site 397 also recorded high sedimentation rates (110-140 m/Ma) (Arthur et al., 1979). The growth of Mound B is characterised by NE migration of its crest (Fig. 8a), suggesting that bottom currents came from the northeast. Hence, along-slope bottom currents flowing from northeast to southwest must have been active during the entire stage II.

(3) Stage III: Maintenance stage (Middle Miocene)

Stage III was also affected by bottom currents (Fig. 10c). The high amplitude reflections in Unit D, especially on the top of Mound A and C, are thought to be a result of more vigorous bottom currents that were capable of redistributing coarser sediments. Slope instability processes occurred frequently on the flanks of the sediment mounds as numerous slide scarps can be identified on the flanks of the sediment mounds (Figs. 7a and 9b). Recurrent MTDs can be identified in Unit D, corresponding to the Middle Miocene strata especially in the downslope region (Fig. 6c) (Georgiopoulou et al., 2007). Seafloor failure on the steeper flanks of the sediment mounds tend to remove sediment from these areas, resulting in permanent size increments on the top (or crest) of the sediment mounds (Figs. 7a, 8a and 9b). Gravitational instability and mass-transport processes appear to relate to physical properties of contourite sediments (Laberg and Camerlenghi, 2008). In the late stage of Middle Miocene, the sediment mounds stopped growing and their top surface was eroded severely (Fig. 10d). A Middle-Late Miocene unconformity (H4) was formed and the troughs were gradually filled by MTDs from the mound failures or from further upslope (Fig. 4b).

As discussed above, bottom currents, slope failure, turbidity currents and paleotopography are suggested to be the main controlling factors for the development of the investigated sediment mounds in South Sahara. The sediment ridges produced by canyon incision and turbidity currents provided an initial paleotopography for the development of the sediment mounds. A southwesterly contour current mainly influenced the continental rise of the Western Saharan margin by waning and re-depositing the suspended sediments produced by turbidity currents and slope failures on the mounds.

6.3 The significance of giant sediment mounds in the framework of Central Atlantic paleoceanographic evolution

Seismic investigations of sediment drifts have been extensively used to unravel the Cenozoic evolution of deep-ocean circulation (Rebesco et al., 2014). The location, shape and internal architecture of sediment drifts can be used as indicators of changing pathways and intensities of bottom currents (Hernández-Molina et al., 2006; Gruetzner and Uenzelmann-Neben, 2016). The sediment mounds identified in this study may provide key information on the bottom currents responsible for their formation and host valuable data on the past ocean circulation and evolution of bottom currents along the Western Saharan margin.

Thus far, the paleoceanography and bottom current evolution along the NW African continental margin are poorly understood. In order to use our knowledge of the evolution of the sediment mounds off Western Sahara to learn about the paleoceanographic setting of this margin, we need to

identify (i) why the sediment mounds started to develop, (ii) why they stopped growing, and (iii) why the sedimentation pattern changed drastically to non-contouritic sedimentation.

On the Western Saharan margin, sediment mounds began to develop over a regional unconformity marking the Early to Middle Eocene boundary (H1). Nearly all deep-sea drill sites that have penetrated the Early to Middle Eocene boundary yield a sedimentary hiatus across it of at least 1-2 Ma duration (Aubry, 1995; Hohbein et al., 2012). Hohbein et al. (2012) suggested that this extremely widespread deep-sea hiatus was likely caused by strengthening erosion by bottom-water currents, with the Early to Middle Eocene boundary representing a time of significant reorganization of the global overturning circulation. The initial development of the sediment mounds may be in accordance with the initiation or establishment of the NADW along the NW African margin since Middle Eocene (Fig. 2).

The pronounced erosional unconformity H2 represents a hiatus of over 100 Ma and separates Middle Eocene from Early Miocene in DSDP site 397 (Arthur et al., 1979). Erosion at H2 level, which led to canyon incision, may not be related to a sea-level drop but can, instead, be associated with erosion of strong bottom currents (Arthur et al., 1979). Zachos et al. (2010) proposed that the Oligocene erosional event is a global phenomenon resulting from the formation of a large East Antarctic ice sheet and deep-water cooling. Bottom current circulation was intensified since the Early Oligocene due to the establishment of a permanent steep gradient between the glaciated south polar and the tropical regions (Kennett, 1977). Prominent unconformities caused by vigorous bottom current activities have also been documented in the southern Indian Ocean (Uenzelmann-Neben, 2001), the South Pacific (Horn and Uenzelmann-Neben, 2016) and western South Atlantic (Hernández-Molina et al., 2009).

Another important issue to consider is the cessation in growth of the interpreted sediment mounds. The top surface of the sediment mounds corresponds to the Middle to Late Miocene boundary. At this time, there is a marked sea level drop, coinciding with deposition of large amounts of turbidites at DSDP Site 397 (Arthur et al., 1979). This sea-level drop, however, might not be the main reason for the widespread erosion on the top surface of the mounds, as incising canyons or any indication of turbidity current activity are seldom observed around H4. Thiede (1979) proposed two reasons for the sudden onset of erosion near the Middle to Late Miocene boundary. The first reason considers that the western Tethyan equatorial pathways, which were important for deep-water circulation, closed near this time. In addition, an outlet for cold Norwegian Sea Overflow across the Island-Faeroe Ridge started to affect the northwest African continental margin at this time. Hiatuses caused by bottom currents have been drilled in several DSDP/ODP sites (e.g. Sites 366, 369 and 397). The erosional unconformity near the Middle to Late Miocene boundary, caused by increased bottom

currents, has also been identified on the northern Argentine slope (Preu et al., 2012). These authors attributed the enhanced bottom current erosion to a rapid global cooling after the termination of the Mid-Miocene climatic optimum. In summary, it is reasonable to propose that the widespread erosion surfaces and hiatuses are probably the result of the interplay between strong bottom currents and sea level drops.

The depositional pattern changed from erosion to sediment deposition after the Middle to Late Miocene boundary (H4). As documented at DSDP Site 397, the lithology changes from slumped pebbly mudstone and turbidite sandy mudstones and volcaniclastic sandstones to hemipelagic marly chalks and limestones with thin sand beds (Arthur et al., 1979). The Middle to Late Miocene boundary (H4) may also mark a major paleoceanographic change and a new depositional pattern along the NW African margin established after Middle to Late Miocene boundary. The change in depositional style may have been controlled by weakening of the deep-water circulation (Wynn et al., 2000). After the final closure of the Central American Seaway, the modern oceanographic regime was finally established in Late Pliocene (Bartoli et al., 2005).

7 Conclusions

New high-resolution seismic data were used to investigate the origin, evolution and paleoceanography significance of three giant, buried sediment mounds on the Western Saharan margin offshore NW Africa. The main conclusions of this study are as follows:

(1) The sediment mounds identified are perpendicular to the continental margin with a SE-NW orientation. They are at least 25 to 37 km in length and 10 to 15 km in width and up to 900 m in height.

(2) Sediment mounds began to develop in the Middle Eocene over a regional unconformity (H1), and halted at the Middle-Late Miocene boundary (H4). Their development processes can be divided into three main stages: a) an initial growth stage during the Middle Eocene, b) a main growth stage during Early Miocene and, c) a maintenance stage during Middle Miocene.

(3) The development of the sediment mounds is interpreted as the result of interactions amongst downslope turbidity currents, mass movements and along-slope bottom currents.

(4) A major paleoceanographic change occurred at the Middle to Late Miocene boundaryand, since the Late Miocene,a new depositional pattern was established along the NW Africa margin.

The study of these sediment mounds may improve our understanding on the sedimentary evolution of the Western Saharan margin. It also provides new insights into patterns of deep water circulation along the NW African margin in the context of the greater Atlantic circulation.

References

Alves, T., 2003.Cenozoic tectono-sedimentary evolution of the western Iberian margin. Marine Geology 195, 75-108.

Alves, T.M., 2010. A 3-D morphometric analysis of erosional features in a contourite drift from offshore SE Brazil. Geophysical Journal International 183, 1151-1164.

Aubry M.P., 1995, From chronology to stratigraphy: Interpreting the lower and middle Eocene stratigraphic record in the Atlantic Ocean, in Berggren W.A., et al., eds., Geochronology, time scales, and global stratigraphic correlation: SEPM (Society for Sedimentary Geology) Special Publication 54, p. 213–274.

Arthur, M.A., von Rad, U., Corford, C., McCoy, F., Sarnthein, M., 1979.Evolution and sedimentary history of the Cape Bojador continental margin, Northwestern Africa. http://dx.doi.org/10.2973/dsdp.proc.47-1.139.1979.

Bartoli, G., Sarnthein, M., Weinelt, M., Erlenkeuser, H., Garbe-Schönberg, D., Lea, D.W., 2005. Final closure of Panama and the onset of northern hemisphere glaciation. Earth and Planetary Science Letters 237, 33-44.

Barton, E.D., Arístegui, J., Tett, P., Cantón, M., García-Braun, J., Hernández-León, S., Nykjaer, L., Almeida, C., Almunia, J., Ballesteros, S., Basterretxea, G., Escánez, J., García-Weill, L., Hernández-Guerra, A., López-Laatzen, F., Molina, R., Montero, M.F., Navarro-Pérez, E., Rodríguez, J.M., van Lenning, K., Vélez, H., Wild, K., 1998. The transition zone of the Canary Current upwelling region. Progress in Oceanography 41, 455-504.

Caburlotto, A., De Santis, L., Zanolla, C., Camerlenghi, A., Dix, J.K., 2006. New insights into Quaternary glacial dynamic changes on the George V Land continental margin (East Antarctica). Quaternary Science Reviews 25, 3029-3049.

Davison, I., 2005. Central Atlantic margin basins of North West Africa: Geology and hydrocarbon potential (Morocco to Guinea). Journal of African Earth Sciences 43, 254-274.

Diester-Haass, L., 1978. Sediments as Indicators of Upwelling, in: Boje, R., Tomczak, M. (Eds.), Upwelling Ecosystems. Springer Berlin Heidelberg, Berlin, Heidelberg, pp. 261-281.

Donda, F., Brancolini, G., O'Brien, P.E., De Santis, L., Escutia, C., 2007. Sedimentary processes in the Wilkes Land margin: a record of the Cenozoic East Antarctic Ice Sheet evolution. Journal of the Geological Society 164, 243-256.

Faugères, J.C., Legigan, P., Maillet, N., Sarnthein, M., and Stein, R., 1989. Characteristics and distribution of Neogene turbidites at Site 657 (Leg 108, Cap Blanc continental rise, northwest Africa): variations in turbidite source and continental climate. In Ruddiman, W., Sarnthein, M., et al., Proc. ODP, Sci. Results, 108: College Station, TX (Ocean Drilling Program), 329-348.

Faugères, J.-C., Stow, D.A.V., Imbert, P., Viana, A., 1999. Seismic features diagnostic of contourite drifts. Marine Geology 162, 1-38.

Georgiopoulou, A., Krastel, S., Masson, D.G., Wynn, R.B., 2007. Repeated instability of the NW African margin related to buried landslide scarps, in: Lykousis, V., Sakellariou, D., Locat, J. (Eds.), Submarine Mass Movements and Their Consequences: 3 International Symposium. Springer Netherlands, Dordrecht, pp. 29-36.

Georgiopoulou, A., Masson, D.G., Wynn, R.B., Krastel, S., 2010. Sahara Slide: Age, initiation, and processes of a giant submarine slide. Geochemistry, Geophysics, Geosystems 11, 1-22.

Gruetzner, J., Uenzelmann-Neben, G., 2016.Contourite drifts as indicators of Cenozoic bottom water intensity in the eastern Agulhas Ridge area, South Atlantic. Marine Geology 378, 350-360.

Haq, B. U., Hardenbol, J., and Vail, P. R., 1987.Chronology of fluctuating sea levels since the Triassic (250 million years ago to present). Science 235, 1156-1166.

Hernández-Molina, F.J., Llave, E., Stow, D.A.V., García, M., Somoza, L., Vázquez, J.T., Lobo, F.J., Maestro, A., Díaz del Río, V., León, R., Medialdea, T., Gardner, J., 2006. The contourite depositional system of the Gulf of Cádiz: A sedimentary model related to the bottom current activity of the Mediterranean outflow water and its interaction with the continental margin. Deep Sea Research Part II: Topical Studies in Oceanography 53, 1420-1463.

Hernández-Molina, F.J., Sierro, F.J., Llave, E., Roque, C., Stow, D.A.V., Williams, T., Lofi, J., Van der Schee, M., Arnáiz, A., Ledesma, S., Rosales, C., Rodríguez-Tovar, F.J., Pardo-Igúzquiza, E., Brackenridge, R.E., 2016. Evolution of the gulf of Cádiz margin and southwest Portugal contourite depositional system: Tectonic, sedimentary and paleoceanographic implications from IODP expedition 339. Marine Geology 377, 7-39.

Hernández-Molina, J., Llave, E., Somoza, L., Fernández-Puga, M.C., Maestro, A., León, R., Medialdea, T., Barnolas, A., García, M., del Río, V.D., Fernández-Salas, L.M., Vázquez, J.T., Lobo, F., Dias, J.M.A., Rodero, J., Gardner, J., 2003. Looking for clues to paleoceanographic imprints: A diagnosis of the Gulf of Cádiz contourite depositional systems. Geology 31, 19-22.

Hohbein, M.W., Sexton, P.F., Cartwright, J.A., 2012. Onset of North Atlantic Deep Water production coincident with inception of the Cenozoic global cooling trend. Geology 40, 255-258.

Horn, M., Uenzelmann-Neben, G., 2016. The spatial extent of the Deep Western Boundary Current into the Bounty Trough: new evidence from parasound sub-bottom profiling. Marine Geophysical Research 37, 145-158.

Kennett, J.P., 1977. Cenozoic evolution of Antarctic glaciation, the circum-Antarctic Ocean, and their impact on global paleoceanography.Journal of Geophysical Research 82, 3843-3860.

Knoll, M., Hernández-Guerra, A., Lenz, B., López Laatzen, F., Machín, F., Müller, T.J., Siedler, G., 2002.The Eastern Boundary Current system between the Canary Islands and the African Coast. Deep Sea Research Part II: Topical Studies in Oceanography 49, 3427-3440.

Krastel, S., Wynn, R.B., Georgiopoulou, A., Geersen, J., Henrich, R., Meyer, M., Schwenk, T., 2012.Large-Scale Mass Wasting on the Northwest African Continental Margin: Some General Implications for Mass Wasting on Passive Continental Margins. 189-199.

Laberg, J.S., Camerlenghi, A., 2008. Chapter 25 The Significance of Contourites for Submarine Slope Stability, in: Rebesco, M., Camerlenghi, A. (Eds.), Developments in Sedimentology. Elsevier, pp. 537-556.

Li, W., Alves, T.M., Urlaub, M., Georgiopoulou, A., Klaucke, I., Wynn, R.B., Gross, F., Meyer, M., Repschläger, J., Berndt, C., Krastel, S., Morphology, age and sediment dynamics of the upper headwall of the Sahara Slide Complex, Northwest Africa: Evidence for a large Late Holocene failure. Marine Geology.

Moscardelli, L., Wood, L., Mann, P., 2006. Mass-transport complexes and associated processes in the offshore area of Trinidad and Venezuela. AAPG Bulletin 90, 1059-1088.

Mulder, T., Faugères, J.C., Gonthier, E., 2008. Chapter 21 Mixed Turbidite–Contourite Systems, in: Rebesco, M., Camerlenghi, A. (Eds.), Developments in Sedimentology. Elsevier, pp. 435-456.

Preu, B., Schwenk, T., Hernández-Molina, F.J., Violante, R., Paterlini, M., Krastel, S., Tomasini, J., Spieß, V., 2012.Sedimentary growth pattern on the northern Argentine slope: The impact of North Atlantic Deep Water on southern hemisphere slope architecture. Marine Geology 329-331, 113-125.

Rebesco, M., Camerlenghi, A., Volpi, V., Neagu, C., Accettella, D., Lindberg, B., Cova, A., Zgur, F., Party, M., 2007. Interaction of processes and importance of contourites: insights from the detailed morphology of sediment Drift 7, Antarctica. Geological Society, London, Special Publications 276, 95-110.

Rebesco, M., Hernández-Molina, F.J., Van Rooij, D., Wåhlin, A., 2014. Contourites and associated sediments controlled by deep-water circulation processes: State-of-the-art and future considerations. Marine Geology 352, 111-154.

Rebesco, M., Larter, R.D., Camerlenghi, A., Barker, P.F., 1996. Giant sediment drifts on the continental rise west of the Antarctic Peninsula. Geo-Marine Letters 16, 65-75.

Rebesco, M., Pudsey, C.J., Canals, M., Camerlenghi, A., Barker, P.F., Estrada, F., Giorgetti, A., 2002. Sediment drifts and deep-sea channel systems, Antarctic Peninsula Pacific Margin. Geological Society, London, Memoirs 22, 353-371.

Rotzien, J.R., Lowe, D.R., King, P.R., Browne, G.H., 2014. Stratigraphic architecture and evolution of a deep-water slope channel-levee and overbank apron: The Upper Miocene Upper Mount Messenger Formation, Taranaki Basin. Marine and Petroleum Geology 52, 22-41.

Séranne, M., Nzé Abeigne, C.-R., 1999. Oligocene to Holocene sediment drifts and bottom currents on the slope of Gabon continental margin (west Africa): Consequences for sedimentation and southeast Atlantic upwelling. Sedimentary Geology 128, 179-199.

Sarnthein, M., Thiede, J., Pflaumann, U., Erlenkeuser, H., Fütterer, D., Koopmann, B., Lange, H., Seibold, E., 1982. Atmospheric and Oceanic Circulation Patterns off Northwest Africa During the Past 25 Million Years, in: von Rad, U., Hinz, K., Sarnthein, M., Seibold, E. (Eds.), Geology of the Northwest African Continental Margin. Springer Berlin Heidelberg, Berlin, Heidelberg, pp. 545-604.

Seibold, E. and Fütterer, D. (1982): Sediment dynamics on the Northwest African continental margin / R. Scrutton

and M. Talwani (editors), In: The Ocean Floor : Bruce Heezen commemorative volume, (A Wiley-Interscience publication), Chichester, Wiley, ISBN: 0-471-10091-9 .

Seibold, E., Hinz, K., 1974. Continental Slope Construction and Destruction, West Africa, in: Burk, C.A., Drake, C.L. (Eds.), The Geology of Continental Margins. Springer Berlin Heidelberg, Berlin, Heidelberg, pp. 179-196.

Stow, D.A.V., Faugères, J.-C., Howe, J.A., Pudsey, C.J., Viana, A.R., 2002. Bottom currents, contourites and deep-sea sediment drifts: current state-of-the-art. Geological Society, London, Memoirs 22, 7-20.

Stow, D.A.V., Faugères, J.C., 2008. Chapter 13 Contourite Facies and the Facies Model, in: Rebesco, M., Camerlenghi, A. (Eds.), Developments in Sedimentology. Elsevier, pp. 223-256.

Talling, P.J., Wynn, R.B., Masson, D.G., Frenz, M., Cronin, B.T., Schiebel, R., Akhmetzhanov, A.M., Dallmeier-Tiessen, S., Benetti, S., Weaver, P.P.E., Georgiopoulou, A., Zuhlsdorff, C., Amy, L.A., 2007. Onset of submarine debris flow deposition far from original giant landslide. Nature 450, 541-544.

Thiede, J., 1979. History of the North Atlantic Ocean: Evolution of an Asymmetric Zonal Paleo-Environment in a Latitudinal Ocean Basin, Deep Drilling Results in the Atlantic Ocean: Continental Margins and Paleoenvironment. American Geophysical Union, pp. 275-296.

Uenzelmann-Neben, G., 2001. Seismic characteristics of sediment drifts: An example from the Agulhas Plateau, southwest Indian Ocean. Marine Geophysical Researches 22, 323-343.

Uenzelmann-Neben, G., Gohl, K., 2012.Amundsen Sea sediment drifts: Archives of modifications in oceanographic and climatic conditions. Marine Geology 299-302, 51-62.

van Aken, H.M., 2000. The hydrography of the mid-latitude northeast Atlantic Ocean: I: The deep water masses. Deep Sea Research Part I: Oceanographic Research Papers 47, 757-788.

Vear, A., 2005. Deep-water plays of the Mauritanian continental margin. Geological Society, London, Petroleum Geology Conference series 6, 1217-1232.

von Rad, U., Arthur, M.A., 1979. Geodynamic, Sedimentary and Volcanic Evolution of the Cape Bojador Continental Margin (NW Africa), Deep Drilling Results in the Atlantic Ocean: Continental Margins and Paleoenvironment. American Geophysical Union, pp. 187-203.

von Rad, U., Wissmann, G., 1982. Cretaceous-Cenozoic History of the West Saharan Continental Margin (NW Africa): Development, Destruction and Gravitational Sedimentation, in: von Rad, U., Hinz, K., Sarnthein, M., Seibold, E. (Eds.), Geology of the Northwest African Continental Margin. Springer Berlin Heidelberg, Berlin, Heidelberg, pp. 106-131.

Wynn, R.B., Masson, D.G., Stow, D.A.v., Weaver, P.P.e., 2000. The Northwest African slope apron: a modern analogue for deep-water systems with complex seafloor topography. Marine and Petroleum Geology 17, 253-265.

Zachos, J.C., McCarren, H., Murphy, B., Röhl, U., Westerhold, T., 2010. Tempo and scale of late Paleocene and

early Eocene carbon isotope cycles: Implications for the origin of hyperthermals. Earth and Planetary Science Letters 299, 242-249.

4 Manuscript III

Morphology, age model and evolution of a newly discovered Quaternary mega-slide: The Agadir Slide offshore NW Africa

Wei Li[a]*, Sebastian Krastel[a], Morelia Urlaub[b],Tiago M. Alves[c],Lisa Mehringer[d],Anke Schürer[d], Christopher J. Stevenson[e],Peter Feldens[f], Felix Gross[a],Russell B. Wynn[g]

[a]Christian-Albrechts-Universität zu Kiel, Institute of Geosciences, Otto-Hahn-Platz 1, 24118 Kiel, Germany

[b]GEOMAR Helmholtz Centre for Ocean Research Kiel, Wischhofstr. 1-3, 24148 Kiel, Germany

[c]3D Seismic Lab. School of Earth and Ocean Sciences, Cardiff University, Main Building, Park Place, Cardiff, CF10 3AT, United Kingdom

[d]Faculty of Geosciences and MARUM, Center for Marine Environmental Sciences, University of Bremen, Klagenfurter Straße, 28359 Bremen, Germany

[e]School of Earth and Environment, University of Leeds, Leeds LS2 9JT, United Kingdom

[f]Leibniz Institute for Baltic Sea Research, Warnemünde, 18119 Rostock, Germany

[g]National Oceanography Centre, European Way, Southampton, Hampshire SO14 3ZH, United Kingdom

*Correspondence to: Wei Li (li@geophysik.uni-kiel.de)

Planned submission to: **Geochemistry, Geophysics, Geosystems**

Abstract

A newly identified giant submarine landslide on the NW African margin (Agadir Slide) is investigated in terms of its morphology, internal architecture, timing and emplacement processes by using high-resolution multibeam bathymetry data, 2D seismic profiles and gravity cores. The Agadir Slide is located south of the Agadir Canyon at a water depth ranging from 500 m to 3500 m with an affected area of ~5500 km^2. The complex morphology of the Agadir Slide reveals two headwall areas and two slide fairways (Western and Central slide fairways). Volume calculations indicate that approximately 340 km^3 of sediment were accumulated downslope, twice as much as the volume (~170 km^3) evacuated from the source areas of the Agadir Slide. This discrepancy is interpreted to have resulted from volume increase due to the highly erosional behaviour of the Agadir Slide along its basal shear surfaces and sidewalls. Age models based on stratigraphic correlations from five gravity cores indicate an age of ~142 ka for the emplacement of the Agadir Slide. This work provides crucial insights on the transport dynamics and sediment-dispersal patterns of the Agadir Slide, which is inferred as having been developed retrogressively in two phases. Local seismicity and fault activity related to halokinesis likely triggered the Agadir Slide. In addition, salt domes breaching the seafloor acted as major topographic barriers to sediment flow and, as a result, the Agadir Slide neither disintegrated into sediment blocks nor was transformed into turbidity currents. With an age of 142 ka the Agadir Slide cannot be the source for any of the turbidite beds in the Moroccan Turbidite System.

1 Introduction

Submarine landslides have been the focus of intensive research in the past decades and are comprehensively documented on multiple continental margins (Hampton et al., 1996; Masson et al., 2006; Krastel et al., 2014). They comprise one of the key mechanisms transporting sediments from continental shelves and upper slope areas into deep-sea basins (Masson et al., 2006). Submarine landslides can also generate damaging tsunamis, affecting local and distal coastal communities and associated infrastructure (Tappin et al., 2014). At local scales, large-volume and fast-moving submarine landslides can disintegrate to produce turbidity currents through mixing processes with the surrounding sea water (Talling et al., 2007a; Clare et al., 2014). Turbidity currents are another flow process capable of transporting sediment over long distances to reach distal Abyssal Plains (Talling et al., 2007b). Turbidity currents can travel for hundreds of kilometres, with speeds of up to 19 m/s, to cause damage to sea floor structures such as communication cables and pipelines (Piper et al., 1999).

The NW African continental margin has been a region of slope instability in the Quaternary and some of the World's largest submarine landslides have occurred in the region for past 200 ka (Krastel et al., 2012). Some of NW Africa's submarine landslides were transformed into highly mobile turbidity currents soon after slope failure (Wynn et al., 2002), whereas others did not record such a transformation (Georgiopoulou et al., 2010). For example, the Sahara Slide offshore Western Sahara has a run-out distance of up to 900 km, and was partially disintegrated into a plastic debris flow. However, there is no evidence for its transformation into a turbidity current (Gee et al., 1999; Georgiopoulou et al., 2010). In contrast, the Moroccan Turbidite System extends 1500 km from the head of the Agadir Canyon to the Madeira Abyssal Plain, and has hosted some of the largest (with volumes exceeding 150 km) landslide-triggered turbidity currents occurring in the past 200 ka (Wynn et al., 2002; Talling et al., 2007a; Frenz et al., 2009). The Moroccan Turbidite System fills three interconnected sub-basins: the Seine Abyssal Plain, the Agadir Basin and the Madeira Abyssal Plain (Wynn et al., 2002; Fig. 1). Individual turbidite beds have been correlated across all three sub-basins by taking advantage of the excellent core recovery and the established robust geochemical and chronostratigraphic framework throughout the system (Wynn et al., 2002; Frenz et al., 2009; Hunt et al., 2013a). As a result, three sources have been proposed to contribute to the Moroccan Turbidite System: (1) organic-rich siliciclastic flows sourced from the Moroccan margin (Frenz et al., 2009; Hunt et al., 2013a); (2) volcaniclastic flows sourced from either the Canary Islands or Madeira (Hunt et al., 2013b), and (3) carbonate-rich flows sourced from local seamounts (Wynn et al., 2002).
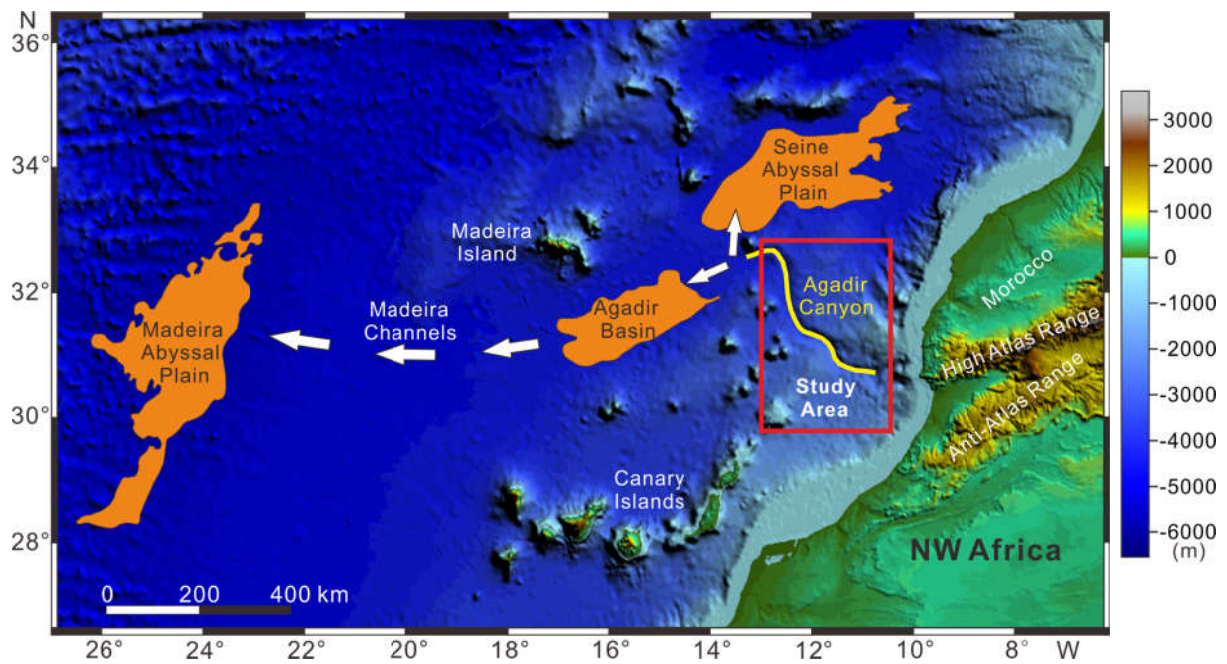
Fig.1 Combined bathymetric and topographic map showing key geomorphological features offshore Northwest African continental margin, e.g. Canary Islands and Maderia Island. The red box represents the location of the study area. The yellow curve indicates the distribution of the Agadir Canyon. The locations of the Moroccan Turbidity System (MTS), including the Seine Abyssal Plain, Agadir Basin, Madeira Channels and Madeira Abyssal Plain, from east to west, are shaded in orange.

Several studies have been focused on the Moroccan Turbidite System for the past two decades (Wynn et al., 2002; Frenz et al., 2009; Hunt et al., 2013a; Hunt et al., 2013b; Stevenson et al., 2014). However, limited attention has been paid to its source areas, especially along the Moroccan margin from which most large-volume flows were derived. Due to the lack of geophysical data from the Moroccan margin, the sources of the turbidites in the Moroccan Turbidite System are unknown. Most likely, they originated as slope failures in the Agadir Canyon region and transformed into turbidity currents but shapes and sizes of these failures are unknown. More recently, a large-scale submarine landslide, i.e. the Agadir Slide, was identified on the Moroccan margin based on hydroacoustic data obtained during the Maria S. Merian research cruise MSM32 (Krastel et al., 2016). A combination of newly acquired high-resolution multi-beam bathymetry, 2D seismic profiles and gravity cores allows us to provide the first detailed analysis of the Agadir Slide in terms of its morphology, internal architecture, timing and evolution processes. One focus of the work is to investigate the contribution of the Agadir Slide to the sedimentary succession of the Moroccan Turbidite System, thereby discuss the factors controlling flow dynamics and transformation.

Hence, the specific objectives of this paper are to:

a) Investigate the detailed seafloor morphology of the Agadir Slide;

b) Describe the internal architecture of the Agadir Slide and estimate its volume;

c) Determine the timing of the Agadir Slide in order to better understand its emplacement processes;

d) Discuss the flow behaviour of the Agadir Slide and test whether it could be a key source of the turbidites in the Moroccan Turbidite System.

2 Geological setting

2.1 The Northwest African margin

The Northwest (NW) African margin is characterised by a flat continental shelf, generally 40-60 km wide, and a shelf break at a water depth of 100 to 200 m (Seibold, 1982; Hühnerbach and Masson, 2004). The continental slope has a width of 50-250 km beyond the shelf break, and records a slope gradient of 1-6°(Fig. 2; Dunlap et al., 2010). The continental slope continues into the continental rise at water depths of 1500 to 4000 m, with gradients ranging from about 1° on the lower slope/upper rise to 0.1° on the lower rise (Seibold, 1982). The continental rise is generally 100-1500 km wide, and terminates at a water depth of 4500-5400 km, beyond which lies the flat expanse of the Madeira Abyssal Plain (Fig. 1). The NW African margin is also dissected by numerous canyons and channels, and interrupted by multiple volcanic islands and seamounts, creating a topographically complex setting that greatly influences local sedimentary processes (Wynn et al., 2000). The study area is situated on the Moroccan continental margin at water depths ranging from 30 to more than 4000 m. It includes a landslide area north of Agadir Canyon and the canyon itself. Prominent bathymetric near the study area include a group of volcanic seamounts to the west and the Canary Islands to the southwest (Fig. 1). The Agadir Canyon extends from the edge of the shelf break down to the upper continental rise, opening out into the Agadir Basin (Wynn et al., 2000; Krastel et al., 2016) (Fig. 1). It has a length of 460 km, a width ranging from 5 to 15 km and a depth of ~1 km (Wynn et al., 2000).
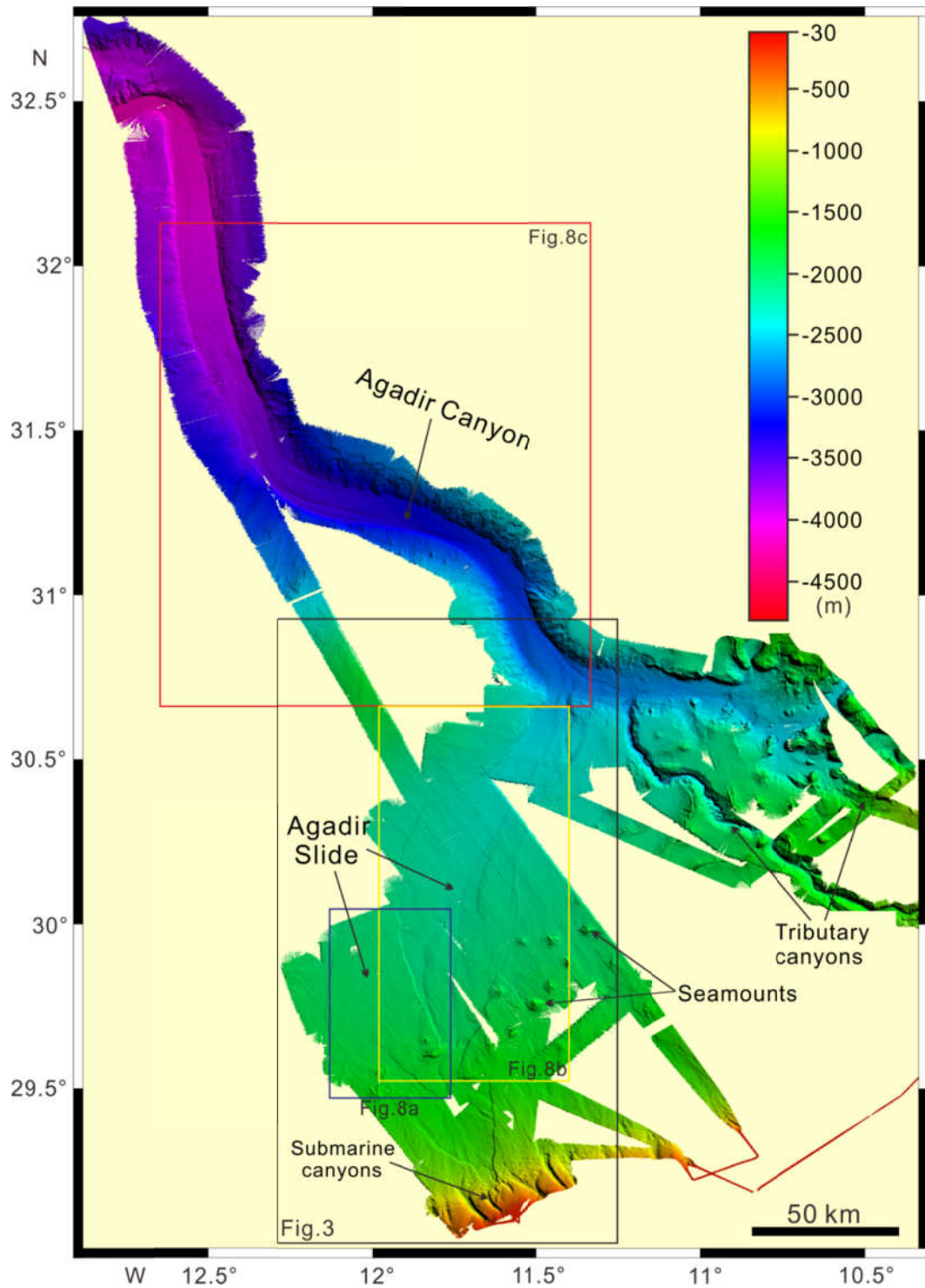
Fig.2 Multibeam bathymetric map of the study area illustrating the distribution and seafloor morphology of the Agadir Canyon and the Agadir Slide. Several tributary canyons can be identified at the head of the Agadir Canyon. The boxes with different colours represent the locations of figures used in the following sections of this work.

2.2 The Moroccan Turbidite System

The Moroccan Turbidite System (MTS) is located downslope of the study area beyond 4000 m water-depth and has a total length of 1500 km (Fig. 1). The morphology of MTS is largely controlled by the position of volcanic islands, seamounts and salt diapirs (Wynn et al., 2000). The MTS consists of three interlinked deep-water basins: the Agadir Basin, the Seine Abyssal Plain and the Madeira Abyssal Plain (Wynn et al., 2002). The Agadir Basin is a large intraslope basin lying at a water depth of ~4400 m. It has an area of 22,000 km^2 and is almost flat, having a gradient of just 0.02°. The Seine Abyssal Plain is also located at a water depth of ~4400 m. The Madeira Abyssal Plain is the largest Abyssal Plain in the region, covering an area of 68,000 km^2 (Rothwell et al., 1992). It is extremely flat, with a slope of less than 0.01°, and a surface relief varying by less than 10 m (Searle, 1987). The Agadir Basin and Madeira Abyssal Plain (water depth of ~5400 m) are connected by a 600-km long network of shallow channels termed the Madeira Distributary Channel System (Masson, 1994; Wynn et al., 2000). The sedimentary fill in these basins in the Moroccan Turbidite System shows a relatively low turbidite frequency of ~ 1 every 10,000 years (Wynn et al., 2002) and the turbidites are separated by discrete hemipelagic intervals (Frenz et al., 2009; Hunt et al., 2013a).

Fourteen turbidite beds (AB1 to AB14) have been identified in the MTS during the past 200 ka (Wynn et al. 2002; Talling et al. 2007a; Hunt et al. 2013a). The youngest turbidite in the MTS is AB1, which has been estimated to be ~1 ka (Thomson and Weaver, 1994).It was suggested to be sourced from the continental margin south of the Canary Islands and related to the recent re-activation of Sahara Slide (Frenz et al., 2009).The turbidite AB2 is mainly located in the Agadir Basin and its age is interpreted to be ~15 ka (Masson et al., 2006; Wynn and Masson, 2003). It is likely sourced from the El Golfo landslide around the western Canary Islands (Frenz et al., 2009).Both AB3 and AB11 originated on the Morocco continental margin and were transported into the Agadir Basin via the Agadir Canyon (Frenz et al., 2009). They are estimated to contain ~15-20 km^3 of sediment.Turbidites AB5 containis ~130 km^3 of sediment and it reaches a maximum thickness of ~300 cm in the proximal Agadir Basin. The AB8 is mainly distributed in the western Agadir Basin (Wynn et al., 2002) and it originated from relatively localised failure of a presorted volcaniclastic sand source (Frenz et al., 2009).AB10 occurs throughout the Agadir Basin except along the northern margin and the Agadir Canyon mouth (Frenz et al., 2009). Turbidite AB12 is the largest turbidite in the Moroccan Turbidite System and contains ~230 km^3 of sediment. It is sourced from the Morocco shelf (Frenz et al., 2009). Turbidite AB 14 is distributed in all three interlinked basins (Frenz et al., 2009). It is interpreted as being deposited at ~160 ka. The Icod landslide valley on the northeast flank of Tenerife is the likely source for volcaniclastic turbidite AB14.

3 Data and methods

The dataset used in this study was collected offshore northwest Morocco during the Maria S. Merian research cruise MSM32, in October 2013. The dataset comprises multibeam bathymetry data, 2D seismic profiles and gravity cores (Figs. 2, 3a and b).

3.1 Multibeam bathymetry data

During cruise MSM32, the hull-mounted Kongsberg Simrad system EM122 was used for accurate bathymetric mapping. The EM122 system allows an accurate bathymetric mapping down to full ocean depth (20 to 11000 m). It works with a nominal frequency of 12 kHz and an angular coverage sector of up to 150° and 864 soundings per ping. The multibeam bathymetry data cover about 13,000 km^2, from the Agadir Slide headwall area at a water depth of 600 m, down to the Agadir Canyon at a water depth of 4500 m. The multibeam data was processed by using the QPS FLEDERMAUS and MBSYSTEM software, including general quality checks (navigation, attitude data and sound velocity profiles), the generation of a CUBE surface, and the removal of spikes, especially at the overlapping parts of the individual profiles. The acquired bathymetric data were gridded for visualisation and subsequent volume calculations. A 30 m×30 m grid of the bathymetry was generated and stored in geographic coordinates with the WGS84 ellipsoid. A pre-slide topography was generated by using the minimum-curvature splines in tension interpolation(Smith and Wessel, 1990). The estimated volumes of evacuated sediments in the Agadir headwall area and the Central slide fairway can be obtained by subtracting the interpolated surface from the seafloor topography (Fig. 2).

3.2 2D seismic data

An 88-channel, 137.5 m long Geometrics GeoEel streamer and a standard GI-gun (primary volume of 1.7 L) were used to acquire high-resolution multichannel seismic data. In total, fifty-six two-dimensional (2D), high-resolution multi-channel seismic profiles, with an entire length of about 1500 km, were acquired during this cruise. Signal processing used the VISTA® 2D/3D Seismic Data Processing Software. Basic processing steps included binning at 12.5 m, filtering, gain recovery with increasing depth, NMO-correction, stacking and a post-stack Finite-difference (FD) migration. The IHS Kingdom® software was used to visualise and interpret the seismic data.The top (Horizon A) and bottom (Horizon B) surfaces of the Agadir Slide were interpreted along all seismic lines and gridded by using the minimum curvature gridding algorithm (Smith and Wessel, 1990). The volumes of the

Agadir Slide deposits accumulated in the Central slide fairway, Western slide fairway and Agadir Canyon were estimated by subtracting the grids created from Horizon A and B. The seismic velocity used for time-depth conversion was 1650 m/s.

3.3 Gravity cores

During cruise MSM32, 40 sediment cores were acquired in the survey area using a standard gravity corer, core recovery was generally between 5 to 10 m. Three gravity cores are used in this study (Figure 3b). Another two gravity cores (GeoB 2415-2 and GeoB4216-1) located in the immediate vicinity of the Agadir Slide were also investigated (Fig. 3b). They were obtained during the RV METEOR cruise 37/38 in 1997 (Wefer et al., 1997). All gravity cores were described in terms of sediment colour, visual grain size and sedimentary structures. Magnetic Susceptibility was measured in 2 cm-intervals using a handheld Magnetic Susceptibility Meter SM 30 from ZH Instruments. Magnetic Susceptibility measurements on cores GeoB 4215-2 and GeoB 4216-1 were obtained from Kuhlmann et al. (2004) and Freudenthal et al. (2002), respectively.

All studied cores were correlated across the study area to understand the stratigraphic framework of the Agadir Slide. We based our analysis on the Magnetic Susceptibility measurements and the identification of distinct colour changes in hemipelagic sediment, sedimentary properties and key structures. GeoB cores with already established age models (Freudenthal et al., 2002; Kuhlmann et al., 2004) facilitated the interpretation of an age model for the undisturbed sediments overlying the Agadir Slide.
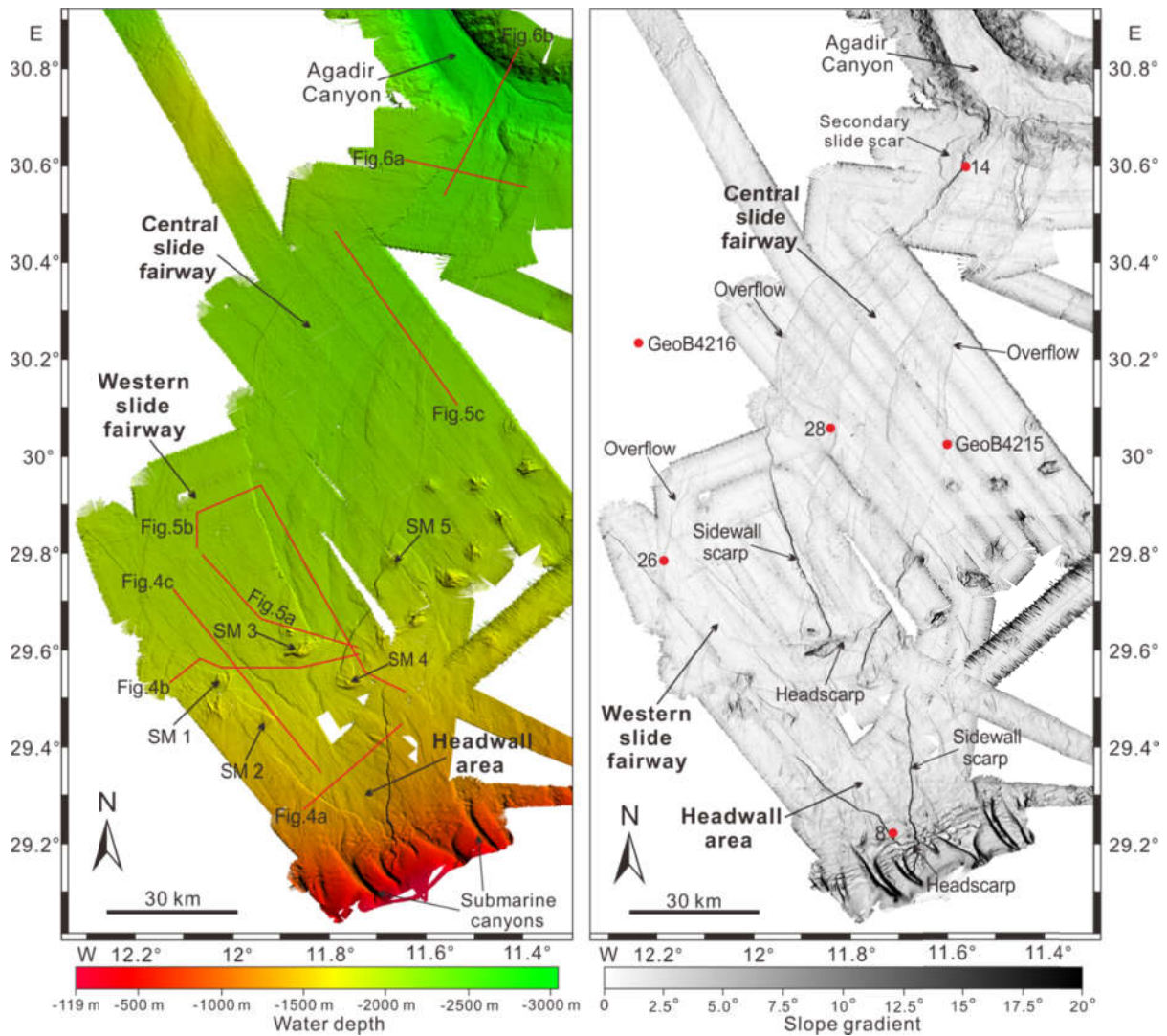
Fig.3 (a) High-resolution multibeam bathymetric map showing the detailed seafloor morphology of the Agadir Slide. The red solid lines indicate the locations of the 2D seismic lines shown in this study. Five major seamounts are also marked in the figure. (b) Slope gradient map of the Agadir Slide area revealing the pronounced headwall area and associated sidewall scarps. The red solid dots represent the location of the gravity cores described in this paper.

4 Results

4.1 Morphological description of the Agadir Slide

The acquired bathymetric data allowed a detailed morphological description of the Agadir Slide (Figs. 2 and 3a). The Agadir Slide affected an area of ~5000 km^2, extending from a water depth of 500 m to approximately 3500 m. The affected area extends over 350 km downslope (Fig. 2). The Agadir Slide is located ~200 km south of the Agadir Canyon. It is bordered to the south by a prominent sidewall cut into the continental slope (Figs. 2 and 3a). The Agadir Slide can be divided into four parts; the upper headwall area, the lower headwall area, the Western slide fairway, and the Central slide fairway (Fig. 3a and b). In addition, five seamounts, named as SM1 to 5, can be identified on the seafloor, affecting the morphology of the Agadir Slide (Fig. 2).

The upper headwall area is located at a water depth of 500 m to 1600 m (Fig. 3a). The width of the headwall area is ~2 km in the upper part and increases gradually to approximately 35 km downslope, giving the headwall area an overall V-shape in plan view (Fig. 3a).It has a length of 40 km and covers an area of approximately 560 km^2. The slope gradient within the headwall area varies between 0.6° and 4° (Fig. 3b). Seafloor morphology within the headwall area is smooth and few slide blocks can be recognised. In contrast, several submarine canyons and a field of sediment waves developed upslope of the upper headwall area of Agadir Slide. The sidewall scarp in the eastern border of the upper headwall area is ~35 km in length and shows an N-S orientation. The western sidewall scarp has a length of ~40 km and its orientation changes from NNW to NW at a water depth of 1250 m. Both sidewall scarps have a height of up to 90 m and they disappear gradually downslope (Fig. 3a). Several (minor) slide scars are identified close to the upper headwall area, and in the northwestern corner of the Central slide fairway, after analysing our bathymetric data in detail (Figs. 3a and b). The lower headwall area is located at a water depth of 1800 m to 1950 m. It is bordered by SM 3 to the west and by SM4 to the southwest, and it has a width of ~9 km. The headwall scarp in the lower headwall area has a height of ~60 m (Fig. 3a).

The Western slide fairway can be considered as the northwestern continuation of the Agadir Slide headwall at a water depth of ~1750 m (Figs. 3a and b). It is bounded by SM1 and SM 2 to the south and the western sidewall scarp of the Central slide fairway to the east. Its western border is characterised by the formation of positive relief when compared to the adjacent seafloor (Fig. 2a). It covers an area of 1250 km^2 and it has a length of ~65 km. The width of the Western slide fairway is 12 km in its upper part and increases to a maximum value of 30 km (Fig. 3a). It then decreases gradually downslope (Fig. 3a).The slope angle within the Western slide fairway also decreases from

0.6° to 0.2° downslope (Fig. 3b). The seafloor surface is smooth and only one pronounced incision surface, with a depth of ~20 m, can be identified close to the headwall area (Fig. 3a).

The Central slide fairway connects the Agadir Slide headwall area to the Agadir Canyon; it is the major pathway for slide deposits travelling into the Agadir Canyon (Fig. 3a and b). Distinctive sidewall scarps can be identified in the northern and southern parts of the Central slide fairway, with heights ranging from 30 m to 50 m. In the middle part, its orientation changes from N-S to NE-SW and seafloor morphology changes from distinctive sidewall scarps into a series of features with positive relief at water depths of 2100-2200 m. Further to the north, the Central slide fairway entered the Agadir Canyonwith a noticeable change in slope gradient from 0.5° to 1.8°, at a water depth of ~2500 m (Fig. 3b and 6b). A pronounced NW-trending slide scarp is also identified in the eastern part of the Central slide fairway (Fig. 3a).

4.2 Internal architecture of the Agadir Slide

The internal seismic character of the Agadir Slide deposits is characterised by a highly disrupted to chaotic and transparent facies bounded above, below and laterally by continuous strata (Figs. 4, 5). Two basal shear surfaces (named as BSS I and BSS II) are recognized at different stratigraphic depth in the entire study area, and each forms a continuous plane that dips parallel to the underlying strata (Figs. 4b, 5a, b and c). The BSS I extends from the headwall area to the Western slide fairway (Fig. 4c), while BSS II can only be identified in the Central slide fairway (Figs. 5b and c). Several buried MTDs are observed beneath the Agadir Slide deposits (Figs. 5c and 6a). These MTDs are cross-cut by a series of faults, some of which propagated vertically until (or were truncated by) the two basal shear surfaces (e.g. Figs. 4a and 5b). The Agadir Slide deposits are also affected by several salt diapirs (Figs. 4b, c and 5b).
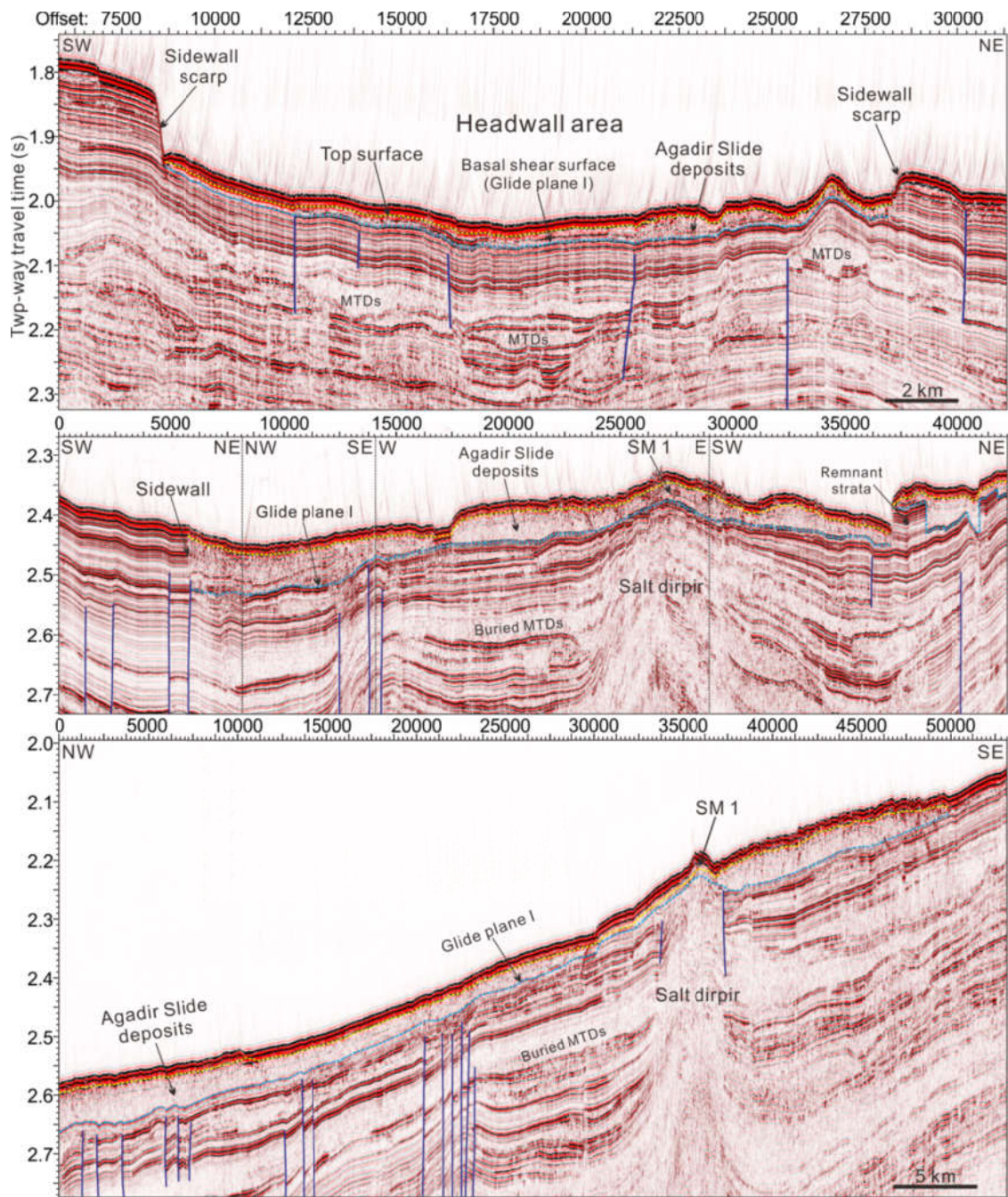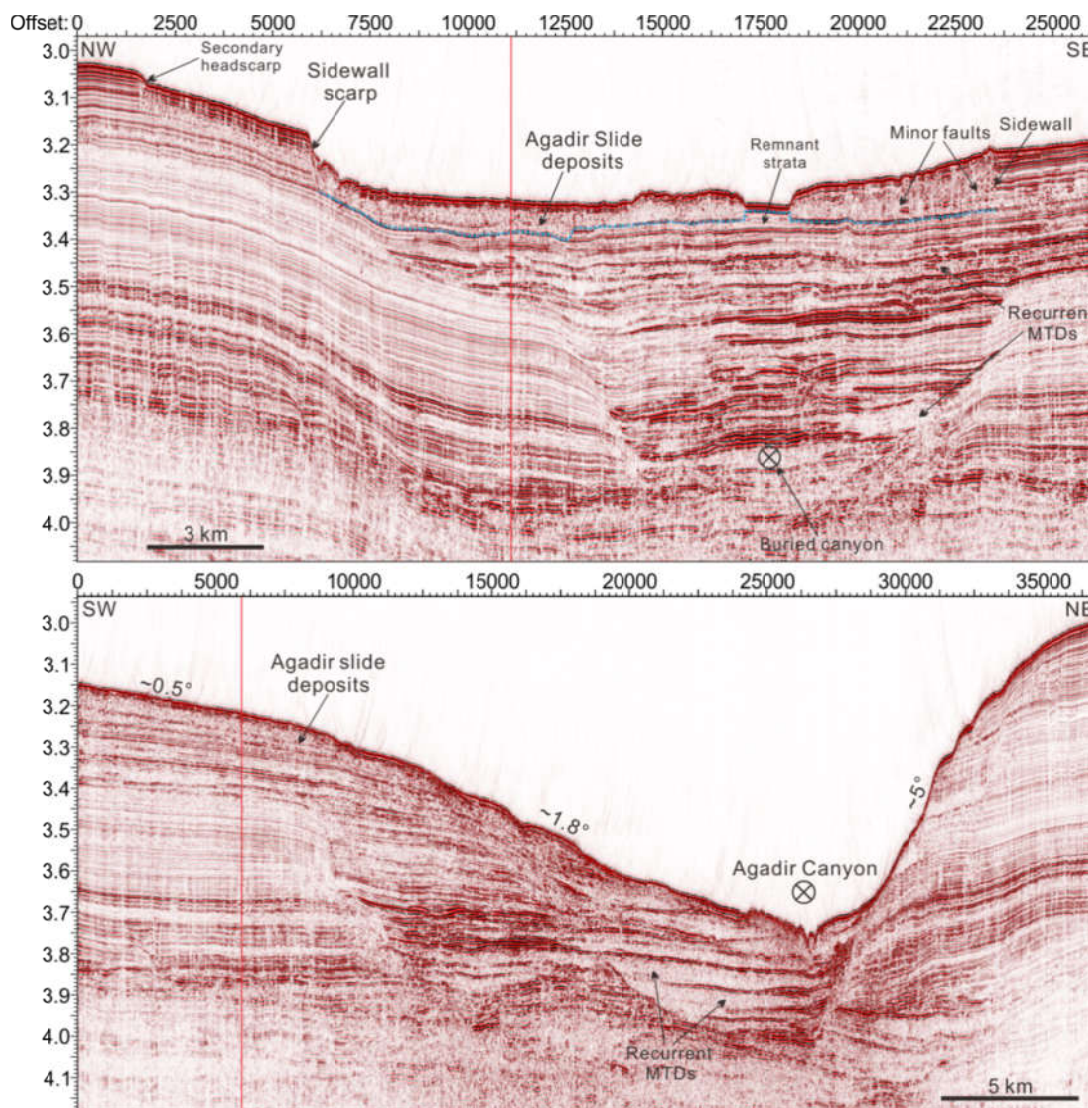
Fig.4 (a) Two-dimensional (2D) seismic profile across the headwall area of Agadir Slide showing sidewall scarps and several buried mass-transport deposits (MTDs). The blue and yellow, dashed lines indicate the base and top surface of the Agadir Slide, respectively. Note the slide deposits that remained in the headwall area are very thin, as this region was almost entirely evacuated of sediment. (b) Two-dimensional (2D) seismic profile crossing the Western slide and Central slide fairways from west to east. The profile highlights the relatively thick Agadir Slide deposits and a developed salt diapir underneath the Agadir Slide. (c) Two-dimensional (2D) seismic profile, oriented SE-NW, and crossing the headwall area and the Western slide fairway. The figure reveals how markedly the Agadir slide deposits are separated by salt diaper in parts of the headwall area.

118

Seismic lines crossing the flank of a salt dome reveal the presence of faults developed on its crest, some of which terminate at the base of the Agadir Slide (Figs. 4b and c). In the middle part of Figure 4b, the slide deposits seem to be elevated by the salt diapir. On the eastern flank of the Central slide fairway, slide material accumulated higher than the surrounding unaffected sea floor, forming a marked positive relief above the original sea bed (Fig. 5c). Significant deformational structures, and multiple small-scale faults, are identified in the toe region of the Agadir Slide deposits due to local compression (Fig. 5c).
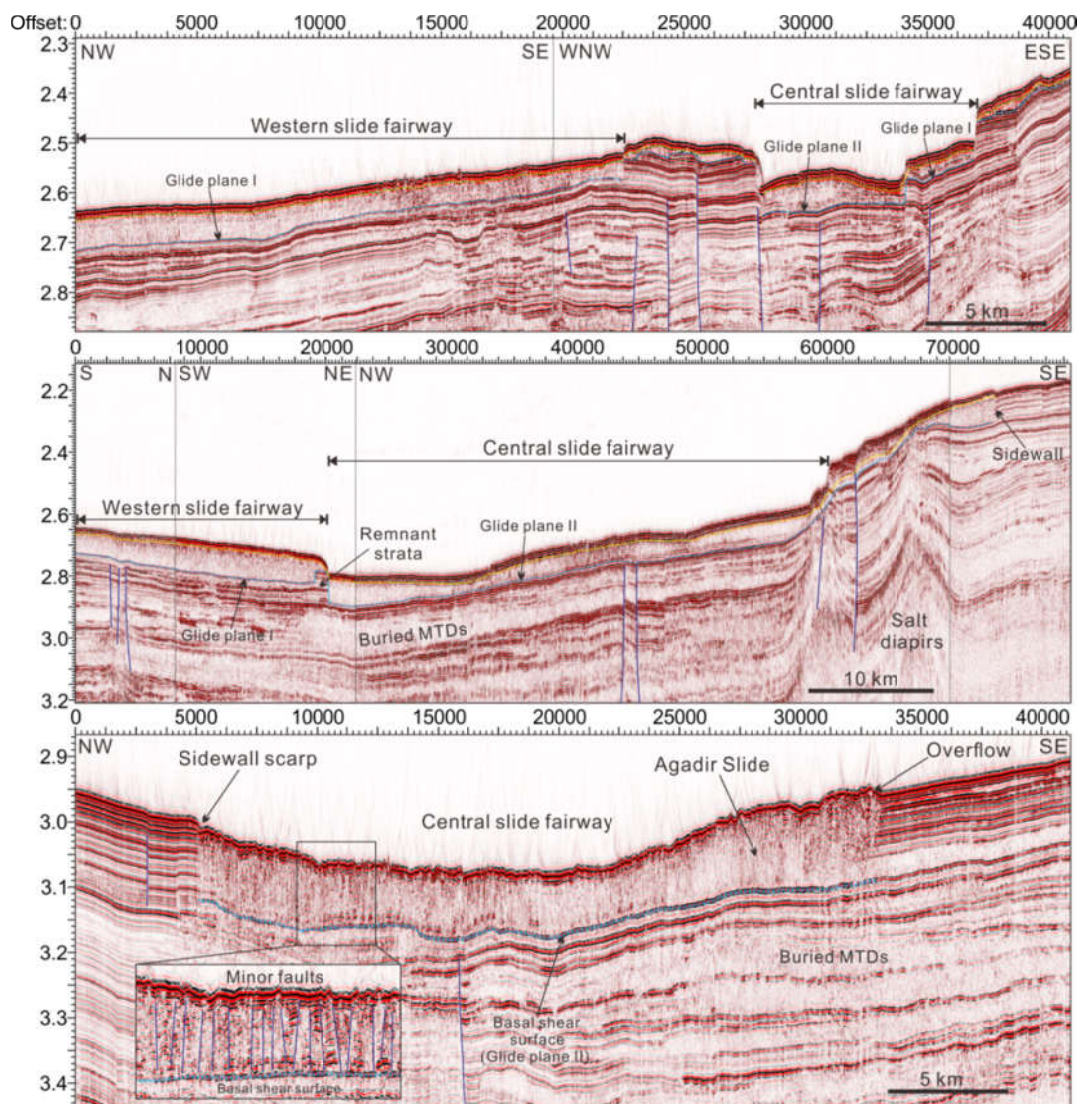
Fig.5 (a) Two-dimensional (2D) seismic profile crossing the Western slide fairway and the Central slide fairway, from northwest to southeast. This seismic profile shows the basal shear surface of Agadir Slide rooted at different stratigraphic depths. Note that numerous faults can be identified below the Agadir Slide deposits. (b) Two-dimensional (2D) seismic profile denoting thicker slide deposits in the Western slide fairway compared to those in the Central slide fairway. Note once again

the distinct stratigraphic depths of the basal shear surface in both areas and the undisturbed strata in-between the two. (c) Two-dimensional (2D) seismic profile across the Central slide fairway revealing a sidewall scarp to the northwest, and a positive overflow of slide deposits to the southeast. Several buried MTDs can be distinguished underneath the Agadir Slide deposits.


Fig.6 (a) Two-dimensional (2D) seismic profile crossing the southern part of the Central slide fairway. The profile reveals a buried submarine canyon filled by multiple MTDs, and a secondary headwall scarp to the northwest. Note that slide deposits show positive relief compared to the adjacent undisturbed strata. (b) Two-dimensional (2D) seismic profile across the southernmost part of the Central slide fairway. In this location, the Agadir Canyon shows multiple stacked MTDs in its interior. The NE flank of the Agadir Canyon is much steeper than its SW counterpart.

4.3 Volume estimation of the Agadir Slide

High-resolution multibeam bathymetry data and 2D multi-channel seismic profiles are used to estimate the volume of evacuated and accumulated Agadir Slide deposits (Fig. 3a). The pre-slide bathymetry within the Agadir Slide headwall area, and the Central slide fairway, are here reconstructed to estimate the total evacuated volume (Figs. 7a and b). A total volume of ~36 km^3 of sediment was evacuated from the Agadir Slide headwall area affecting an area of ~560 km^2(Fig. 7a). This volume and area indicate an average thickness of 65 m for the removed sediment. Strata evacuated from the Central slide fairway have a volume of 135 km^3 and a mean height of 50 m (Fig. 7b). At the western and eastern border of the Central slide fairway, 0.4 km^3 of slide deposits with a mean height of 5 m are accumulated above the pre-slide topography.
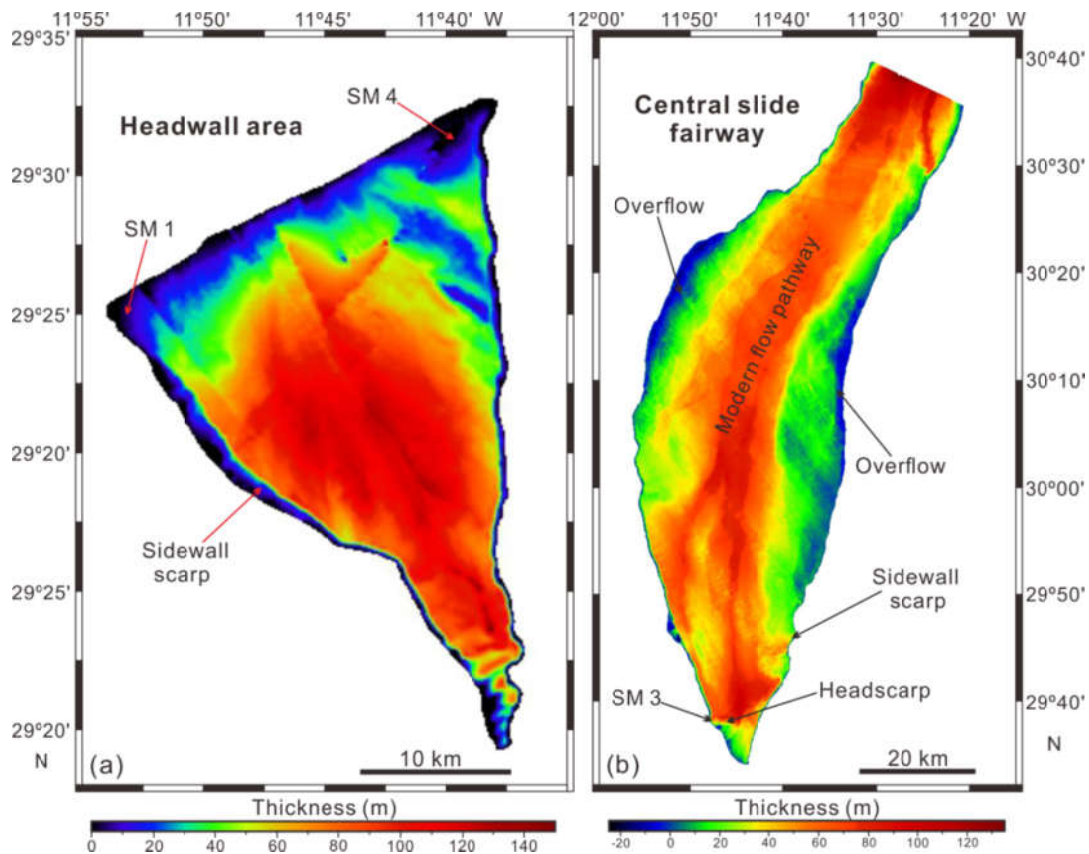

Fig.7 (a) Thickness map of the evacuated sediments in the headwall area revealing that a volume of 36 km3, and a thickness of up to 140 m of sediment, were displaced from the headwall area. (b) Thickness map of evacuated (remobilised) sediments in the Central slide fairway revealing that most of the sediments were displaced along its axis. Note the presence of an additional fairway on the western flank, connected to the main fairway. The negative values at the flanks of the Central slide fairway indicate overflow of the slide deposits.

The volume of the Agadir Slide deposits in the Central slide fairway, Western slide fairway and Agadir Canyon can be estimated based on the interpreted seismic data (Figs. 8a, b and c). In the headwall area, the thickness of the slide deposits is quite small (<25 m), indicating that erosion predominate deposition (Fig. 4a). The Agadir Slide deposits have a volume of 63 km^3 in the Western slide fairway and affect an area of ~1240 km^2 (Fig. 8a). The average thickness of the slide deposits in this area is ~51 m. In the Western slide fairway, the majority of the mobilized sediment was deposited close to its western flank and in its southern part, where the thickness of the slide deposits reaches up to 110 m (Fig. 8a). In the Central slide fairway, 206 km^3 of Agadir Slide deposits were accumulated over an area of 2970 km^2 with a mean thickness of 70 m (Fig. 8b). Most of the Agadir Slide deposits were distributed on in the eastern of the Central slide fairway (Fig. 8b). The volume and affected area of the slide deposits within the Agadir Canyon are 68 km^3 and 1686 km^2, respectively. The thickness of Agadir Slide deposits in the canyon varies greatly and it has an average thickness of 40 m. At the southern end, its thickness is less than 30 m and increases to about 40 m further north. The largest accumulation of slide deposits occurs at the northern border of the central part of the Agadir Canyon. In summary, a total volume of 170 km^3 of sediments was evacuated, while 340 km^3 of sediments were deposited by the Agadir Slide.
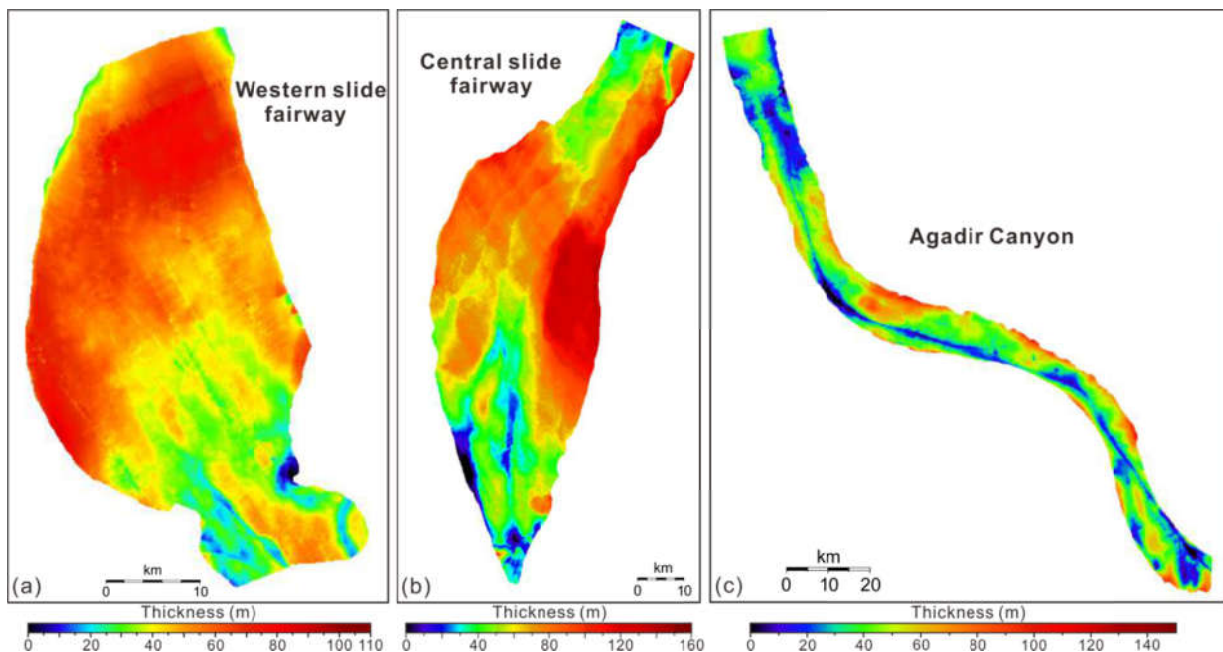
Fig.8 (a) Thickness map of the slide deposits in the Western slide fairway showing that the majority of slide deposits are located in its northern part. (b) Thickness map of the slide deposits in the Central slide fairway revealing a complex sediment distribution. Note that most of the slide deposits in this region can be identified close to the eastern and western borders of the Central slide fairway. (c) Thickness map of the slide deposits trapped within the Agadir Canyon.

4.4 Age model of the Agadir Slide
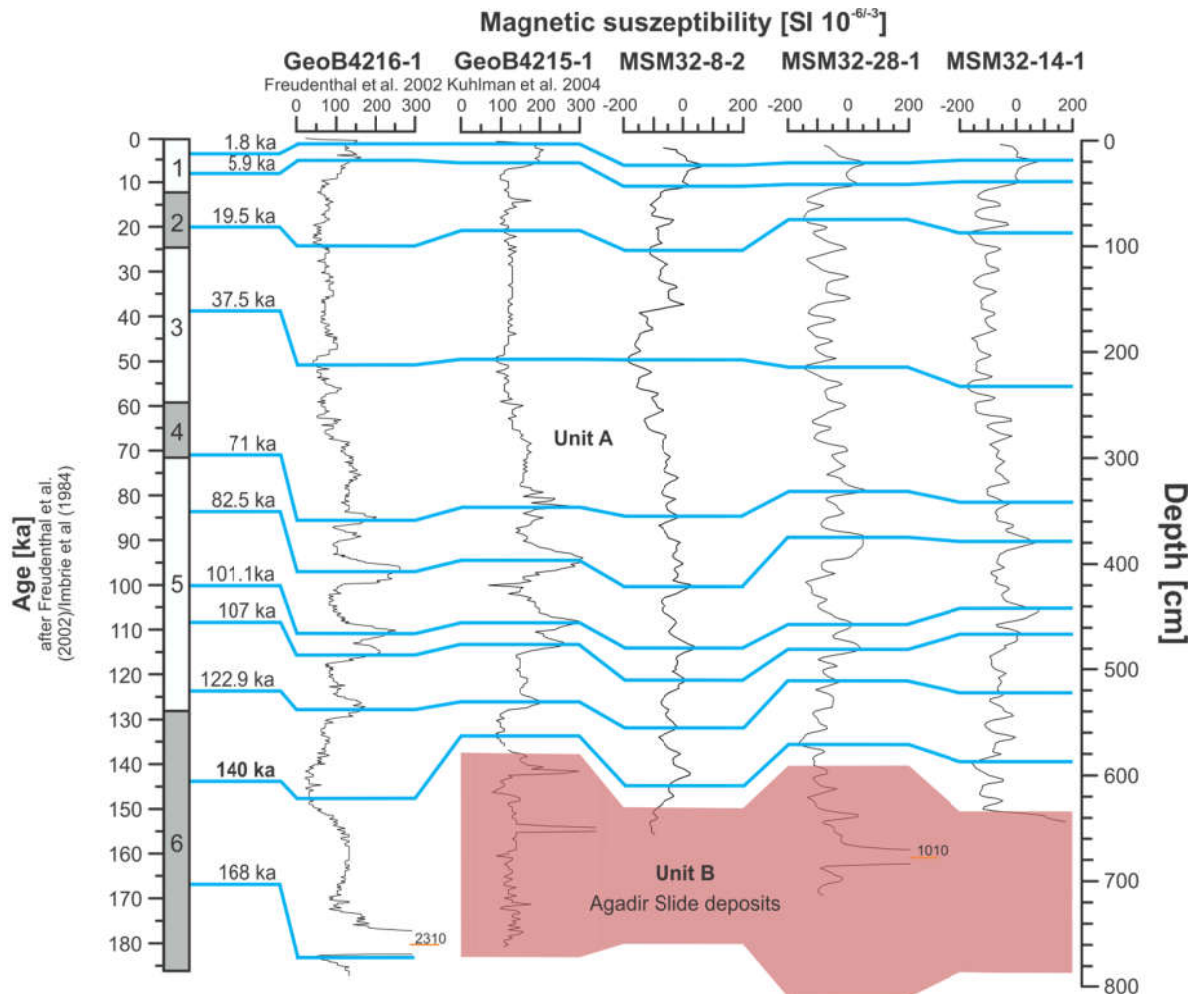
Fig.9 Sediment-core correlations across the study area of the Agadir Slide. Unit B is marked in red. Blue lines connect Magnetic Susceptibility tie-points along the full transect. The respective age for each tie-point was extracted from the datasets in Freudenthal et al. (2002) and Kuhlman et al. (2004).

Sediment sampled in the gravity cores was divided in two units; Units A and B, based on visual core descriptions (Fig. 9).Unit A, forming the upper part of the sediment cores, contains muddy carbonate-rich nannofossil ooze in various nuances of light brownish, reddish and greenish colours. Sediment grain-size in Unit A varies from mud to muddy medium-sand, and the dominant grain size is muddy silt. Microfossils, including abundant foraminifera, were identified within the sediments in Unit A. Burrows and light to moderate bioturbation are preserved in their original shapes throughout Unit A. There is no sign of sediment remobilization or hiatus. Based on these observations, Unit A is considered as a continuous succession of hemipelagic sediment comprising fine-grained biogenic and terrigenous material. Unit B is located in the lower part of the collected sediment cores and underlies Unit A (Fig. 9). Sediment in Unit B is light beige, brownish, reddish, as well as greenish,

123

foraminifera bearing, carbonate-rich nannofossil ooze. The grain size of sediments in Unit B varies from mud to muddy fine-sand. Unit B is deformed by slump folds and internal shearing. Unit B is thus be interpreted as the Agadir Slide deposits.

Core GeoB4216 is located to the west of the study area in an area not affected by the Agadir Slide (Figs. 3a and 9). The grain size ranges from silty mud to muddy fine-sand and layers are identified by varying sediment colours. Based on these observations, the whole core can be described as Unit A.

Magnetic Susceptibility was measured in Unit A to correlate the sediment-core data across the study area and to establish a stratigraphy.Magnetic Susceptibility data was not measured in Unit B as it consists of remobilized strata. Magnetic Susceptibility data in all studied cores show the same downcore trend and well discernible tie-points can be used for correlations across the study area despite the fact that only relative values were measured for the MSM32 cores (Fig. 9). This correlation was used to transfer the age model of the dated cores GeoB 4215 and 4216 (Kuhlmann et al., 2004; Freudenthal et al., 2002) to the new cores. The oldest Magnetic Susceptibility tie-point above the Agadir Slide deposits is dated at 140 ka.

The age model for Unit A enabled the calculation of sedimentation rates. The sedimentation rates for all cores are relatively constant with average sedimentation rates of 4.377 cm/ka, 3.985 cm/ka and 4.145 cm/ka for Cores MSM32-8, MSM32-28 and MSM32-14, respectively. The Magnetic Susceptibility tie-point assigned to the 140 ka age is observed 5 cm, 12 cm and 10 cm above the boundary between Unit A and Unit B in the above mentioned core. This results in an age of ~142 ka for the Agadir Slide using the average sedimentation rates mentioned above.

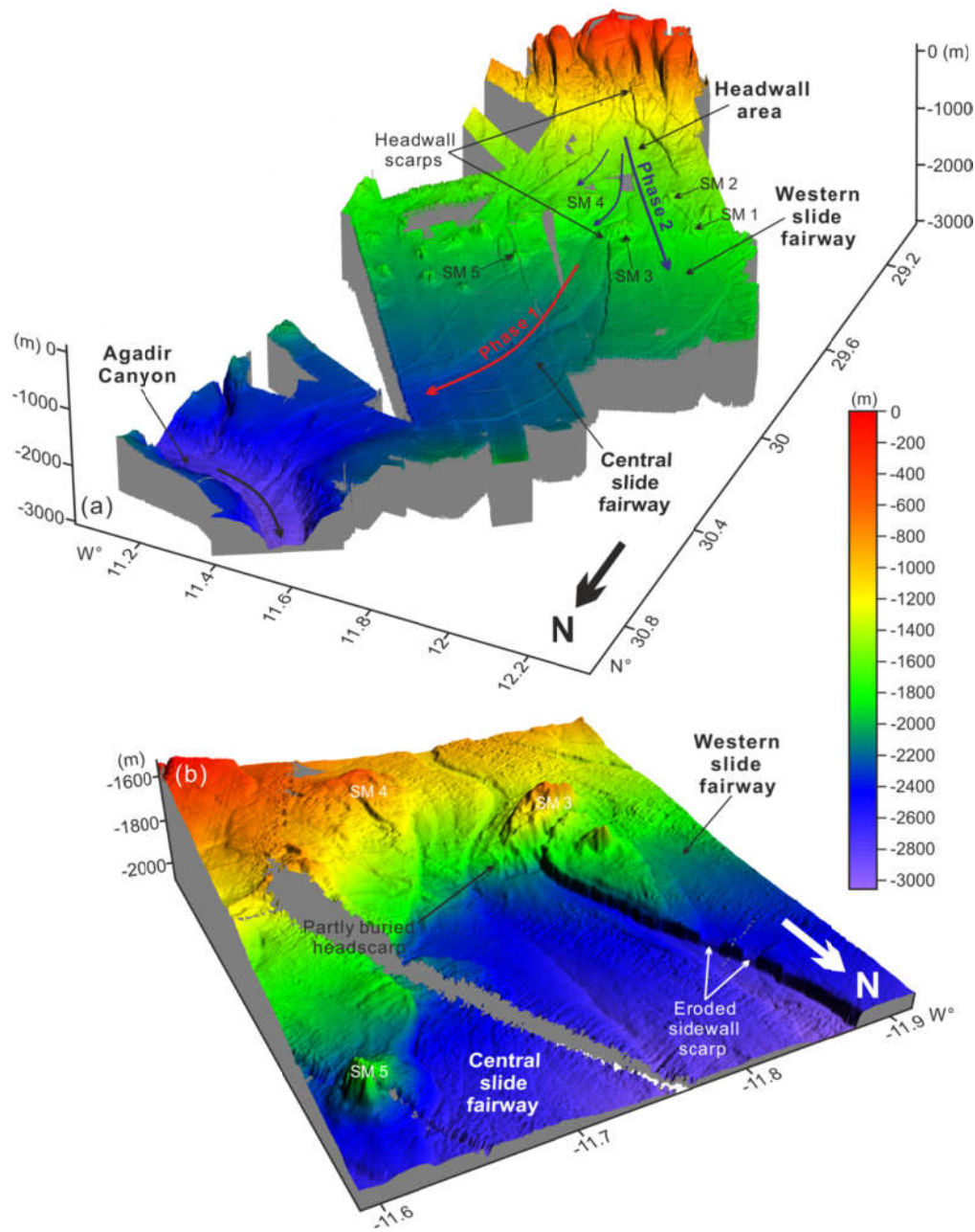# 5 Timing and emplacement processes of the Agadir Slide

The morphological features and internal architecture of the Agadir Slide, when combined with our age constraints, provide important evidence to the emplacement of the Agadir Slide. One key question is whether the Agadir Slide resulted from a single-phase event or from multiple failures. The dating of several gravity cores in the study area provides an age of ~142ka for the main slide body. However, the bathymetric data and seismic profiles of the Agadir Slide suggest three separate bodies probably reflecting three distinct instability events. In order to gain a better understanding on the emplacement processes of the Agadir Slide, the following observations and interpretations should be taken into consideration:

(a) Two obvious headwall scarps have been identified on the bathymetric and slope gradient maps (Figs. 3a, b and 10a). One is located in the headwall area and the other one is located close to SM 3 and SM 4 (Fig. 10a). Each headwall scarp may represent an individual slide event.

(b) Two basal shear surfaces (or glide planes), BSS I and BSS II, are recognized at different stratigraphic depths on all seismic profiles (Figs. 4 to 6). It is therefore reasonable to infer that two slide events occurred along two different basal shear surfaces.

(c) Basal shear surface I can be traced continuously from the upper headwall area into the Western slide fairway (Fig. 4c). This observation suggests that the slide deposits in both areas were generated during the same slide event.

Submarine landslides developed retrogressively in multiple episodes of slope failures have been documented by several case studies, e.g. the Hinlopen Slide (Vanneste et al., 2006), the Mauritania Slide Complex (Antobreh and Krastel, 2007), the Storegga Slide (Haflidason et al., 2004) and the Sahara Slide (Li et al., in press). Similar processes may take place in the case of the Agadir Slide. Based on the morphological features identified on the high-resolution bathymetric and slope gradient maps, and on the internal architecture of the Agadir Slide deposits, we interpret the Agadir Slide to have occurred in at least two phases, although the exact time interval between these two phases is difficult to determine (Figs. 10a and b).

Fig.10 (a) 3D morphological model illustrating the emplacement processes of the Agadir Slide. Red and purple arrows represent the mass movement directions of Phase 1 and 2, respectively. (b) 3D bathymetric view of the partly buried headscarp of Phase 2 slide event.

The detailed emplacement processes of the Agadir Slide are interpreted as follows (Figs. 10a and b). The first phase of the Agadir Slide was initiated in the southern part of the Central slide fairway, i.e. between SM3 and SM4. Here, a pronounced headwall scarp with a height of ~60 m was identified in the lower headwall area, but it was partly buried by the later slide deposits from the upper headwall area (Fig. 10b). The latter slide event produced the distinguished sidewall scarps of

126

the Central slide fairway and the positive topography in its western and eastern borders. Active faults and halokinesis can be considered as the plausible triggers during the first phase event (Figs. 4b and 5a). The slide deposits were further transported downslope and entered into the pre-existing fairway in the northern part (Fig. 6a). This led to the formation of pronounced sidewall scarps, which are most likely produced by enhanced erosion before the slide entered the Agadir Canyon (Fig. 10a). The increase of slope gradient from 0.5° to 1.8° at the transition from the fairway to the Agadir canyon likely promoted such an erosional of the slide (Fig. 6b).

The second slide event was triggered in the upper headwall area, and pronounced sidewall scarps were generated as a result (Fig. 10a). Approximately 36 km^3 of seafloor sediments were mobilized, leading to an almost complete evacuation of sediments in the headwall area. The mobilised sediment was transported downslope and deposition was confined by several seamounts (e.g. SM1 to SM4). Most of the slide deposits travelled between SM2 and SM4, and only a minor amount of slide deposits were transported to the west of SM2 and to the east of SM4 (Fig. 10a).The slide deposits continued beyond SM2 and SM4 and were divided into two parts downslope (Fig. 10a). The slide deposits in the western part were transported into the Western slide fairway and later spread out, leading to the generation of positive topography at its western border (Fig. 10a). The eastern part of the slide deposits were further confined when passing between SM3 and SM4, leading to increased slide velocity and erosive ability (Fig. 10b). Distinct sidewall scarps were formed close to SM3 and SM4 and almost no slide deposits were accumulated on the sea floor. After extending beyond these topographic barriers, i.e. SM3 and SM4, the slide deposits spread evenly in the middle part of the Central slide fairway (Fig. 10a).

6 Discussion

6.1 Volume discrepancy and highly erosional behavior of the Agadir Slide

The petrophysical and consolidation behaviours of MTDs have been investigated by various researchers in the past three decades (Piper et al., 1997; Sawyer et al., 2009; Dugan, 2012; Sun et al., 2017). It is a known fact that the petrophysical properties of undeformed strata can change by shear deformation triggered by submarine mass movements; MTDs commonly have higher bulk density as well as lower porosity and water content in comparison to underlying (and overlying) non-deformed strata, as documented in the Amazon Fan (Piper et al., 1997), Gulf of Mexico (Dugan, 2012), Nankai Trough (Alves et al., 2014) and the northern South China Sea (Sun et al., 2017). MTDs appear to be more consolidated than the uniaxially deformed hemipelagic sediments that bound them (Dugan, 2012) and the volume of MTDs decreases markedly after their emplacement. In this paper, volume calculations reveal that a total of ~170 km^3 of seafloor sediments evacuated from the headwall areas and the Central slide fairway depression. However, the slide material deposited across the study area involves approximately 340 km^3 of mobilized sediment. Two main reasons are proposed in this discussion to account for this volume discrepancy.

The first reason takes into account a variable sediment input from multiple minor slide events generated near the Agadir Slide's source area (Fig. 3). These slide events may have generated additional sediment, later transported into the Western slide fairway, Central slide fairway and Agadir Canyon (Fig. 3a). However, the calculated volume of these small-scale slide events does not justify a recorded volume discrepancy of ~165 km^3.

Another explanation relates to the flow behaviour of the Agadir Slide during its downslope movement (Krastel et al., 2016). A close interaction between submarine landslides and the sea floor can lead to the extensive mobilisation of pre-existing deposits on the sea bed (Georgiopoulou et al., 2010; Alves et al., 2014). Widespread erosion of subsurface sediments by debris flows, leading to an increase in the flow volume, is capable of creating a basal layer upon which the overlying gravity flows can be moved over long distances (Bull et al., 2009). We calculated a volume of 36 km^3 of sediment evacuated from the upper headwall area. However, the slide deposits in the Western slide fairway have a volume of 63 km^3. This observation reveals that ~27 km^3 of sediments have been eroded along the basal shear surface and sidewalls when the slide moved downslope. Based on the discussion above, the volume discrepancy is interpreted to result from the highly erosional behaviour of the Agadir Slide along its basal shear surfaces and sidewalls, which added volume to the mass-transported deposits as they were flowing downslope into the Agadir Canyon. As the instability

event triggering the Agadir Slide transported unconsolidated near sea-floor sediment, we do not consider volume expansion during remobilisation as justifying the discrepancy in calculated volumes.

6.2 Could the Agadir Slide be the source of the turbidite events in the Moroccan Turbidite System?

Submarine landslides and debris flows may transform to turbidity currents on both active and passive continental margins (Wynn et al., 2002; Trofimovs et al., 2008; Clare et al., 2014). Some large-volume submarine landslides (involving >100 km^3 of sediment) can rapidly disintegrate into far-travelling turbidity currents across very gentle slopes (Talling et al., 2007b). Flow transformation from debris flows to turbidity currents was reported, for instance, during the 1929 Grand Banks submarine landslide (Piper et al., 1999). The Moroccan Turbidite System offshore NW African margin has hosted numerous landslide-triggered turbidity currents over the past 200 ka (Wynn et al., 2002; Talling et al., 2007a; Hunt et al., 2013a). Most of these turbidity currents were sourced from the Moroccan margin, and were transported into the Moroccan Turbidite System via the Agadir Canyon (e.g. AB5, AB7 and AB12).

The Agadir Slide is the first identified large-scale submarine landslide in close vicinity to the Agadir Canyon (Krastel et al., 2016). So could the Agadir Slide be the source area of one of the turbidite events in the Moroccan Turbidite System? Several lines of evidence have been proposed to assess the relationship between the Agadir Slide and the turbidite events recorded in the Moroccan Turbidite System. For the past 200 ka, fourteen (14) turbidite events (AB1 to AB14) have been reported in the Moroccan Turbidite System (Wynn et al. 2002; Talling et al. 2007a; Hunt et al. 2013a). Turbidite AB12 was dated at 120 ka (early OIS5) and turbidite AB13 was deposited in the late OIS6, approximately 135 ka ago (Wynn et al. 2002; Hunt et al. 2013a). Turbidite AB14 is a volcaniclastic turbidite deposited at ~165 ka, and is commonly associated with the Icod landslide (Frenz et al. 2009; Hunt et al. 2013a). In this work, the Agadir Slide is dated as ~142 ka, and none of the turbidite events in the Moroccan Turbidite System correlates accurately with it (Fig. 9). No further slide event has been identified within Unit A of all the acquired gravity cores, providing evidence that the Agadir Slide area could not be the source area for the turbidites events in the Moroccan Turbidite System.

Submarine landslides commonly disintegrate into slide blocks of variable sizes in their toe regions (Alves, 2015). However, few slide blocks can be recognized on the bathymetric data imaging the Agadir Slide (Fig. 3a). In reality, not all submarine landslides are transformed into long run-out turbidity currents either. The Sahara Slide occurred as a relatively slow moving slab-type failure on a

low-angle slope and the high cohesiveness of the fine-grained headwall sediments likely prevented it to disintegrate into turbidity currents (Georgiopoulou et al., 2010). The fact that the Agadir Slide did not disintegrate a turbidity current indicates a slow movement downslope. Most of the slide deposits were trapped within the Central slide fairway, the Western slide fairway and the Agadir Canyon. The Agadir Slide travelled along the thalweg for another 200 km after entering the Agadir Canyon.

The absence of a distinctive turbidite event associated with the Agadir Slide in the Moroccan Turbidite System may be explained by several factors. The morphology of the Agadir Slide was largely affected by growing salt structures affecting and deforming the seafloor. We suggest these salt domes acted as topographic obstacles to the slide event and, as a result, had an impact on the slide dynamics. The Agadir Slide eroded and remobilized a large volume of strata on the continental slope, leading to a decrease of slide velocity due to friction along the basal shear surfaces and sidewalls affected by the salt topography. The height of the head scarps also played a vital role on the mobility of the slide material (Vanneste et al., 2006). The escarpment of Hinlopen Slide reaches a height of more than 1400 m, which provides a substantial potential energy for the transformation of slide material into turbidity currents with a long run-out distance. However, the height of the headwall scarps of Agadir Slide is ~60 m and, as a result, the Agadir Slide might not have gained enough speed to be transformed into a turbidity current.

In summary, the sediment transported by the Agadir Slide was: 1) almost entirely trapped in the slide fairway and Agadir Canyon, and 2) too distal to have been accelerated enough on the continental slope to form a distinct turbidite. The turbidites of the Moroccan Turbidite System must have another source. No other major landslide scars have been identified in the Agadir Canyon Region. This leaves the head region of the Agadir Canyon as the most likely source for the turbidites in the Moroccan Turbidite System despite the fact that only small failure scars (<5 km^3) can be identified in the head region of the canyon. Hence, the turbidity currents must have been highly erosive in order to mobilize large amounts of sediments, which were finally deposited in the Moroccan Turbidite System.

7 Conclusions

High-resolution multibeam bathymetry data, 2D seismic profiles and gravity cores allowed us to investigate the morphology, internal character, origin and importance of the Agadir Slide on the NW African margin. The main conclusions of this study are as follows:

(1) The Agadir Slide affected an area of 5500 km^2, displaced a volume of 340 km^3 and shows a (run-out) distance of 350 km. The Agadir Slide includes two headwall areas, Western slide fairway and Central slide fairway.

(2) The Agadir Slide was highly erosional along its basal shear surfaces and sidewalls. Discrepancies between evacuated volume and slide deposits can be attributed to its highly erosional behaviour.

(3) The Agadir Slide was emplaced retrogressively at ~142 ka in two mainphases. Seismicity and fault activity, associated with halokinesis, are considered to be the main triggers of the Agadir Slide.

(4) Salt structures affecting the seafloor have played a vital role on the morphology and evolution of the Agadir Slide. Most of the slide deposits have been trapped within the Western and Central slide fairway, and within the Agadir Canyon. As a result, the Agadir Slide is interpreted here as not being the source for any turbidites in the Moroccan Turbidite System.

References

Alves, T.M., 2015. Submarine slide blocks and associated soft-sediment deformation in deep-water basins: A review. Marine and Petroleum Geology 67, 262-285.

Alves, T.M., Strasser, M., Moore, G.F., 2014. Erosional features as indicators of thrust fault activity (Nankai Trough, Japan). Marine Geology 356, 5-18.

Antobreh, A.A., Krastel, S., 2007. Mauritania Slide Complex: morphology, seismic characterisation and processes of formation. International Journal of Earth Sciences 96, 451-472.

Bull, S., Cartwright, J., Huuse, M., 2009. A review of kinematic indicators from mass-transport complexes using 3D seismic data. Marine and Petroleum Geology 26, 1132-1151.

Clare, M.A., Talling, P.J., Challenor, P., Malgesini, G., Hunt, J., 2014. Distal turbidites reveal a common distribution for large (>0.1 km3) submarine landslide recurrence. Geology 42, 263-266.

Dugan, B., 2012. Petrophysical and consolidation behavior of mass transport deposits from the northern Gulf of Mexico, IODP Expedition 308. Marine Geology 315-318, 98-107.

Dunlap, D.B., Wood, L.J., Weisenberger, C., Jabour, H., 2010. Seismic geomorphology of offshore Morocco's east margin, Safi Haute Mer area. AAPG Bulletin 94, 615-642.

Frenz, M., Wynn, R.B., Georgiopoulou, A., Bender, V.B., Hough, G., Masson, D.G., Talling, P.J., Cronin, B.T., 2009.Provenance and pathways of late Quaternary turbidites in the deep-water Agadir Basin, northwest African margin. International Journal of Earth Sciences 98, 721-733.

Freudenthal, T., Meggers, H., Henderiks, J., Kuhlmann, H., Moreno, A., Wefer, G., 2002.Upwelling intensity and filament activity off Morocco during the last 250,000 years. Deep Sea Research Part II: Topical Studies in Oceanography 49, 3655-3674.

Frey Martinez, J., Cartwright, J., Hall, B., 2005. 3D seismic interpretation of slump complexes: examples from the continental margin of Israel. Basin Research 17, 83-108.

Gamboa, D., Alves, T., Cartwright, J., Terrinha, P., 2010. MTD distribution on a 'passive' continental margin: The Espírito Santo Basin (SE Brazil) during the Palaeogene. Marine and Petroleum Geology 27, 1311-1324.

Gee, Masson, Watts, Allen, 1999. The Saharan debris flow: an insight into the mechanics of long runout submarine debris flows. Sedimentology 46, 317-335.

Georgiopoulou, A., Masson, D.G., Wynn, R.B., Krastel, S., 2010. Sahara Slide: Age, initiation, and processes of a giant submarine slide. Geochemistry, Geophysics, Geosystems 11, 1-22.

Haflidason, H., Sejrup, H.P., Nygård, A., Mienert, J., Bryn, P., Lien, R., Forsberg, C.F., Berg, K., Masson, D., 2004. The Storegga Slide: architecture, geometry and slide development. Marine Geology 213, 201-234.

Hampton, M.A., Lee, H.J., Locat, J., 1996. Submarine landslides. Reviews of Geophysics 34, 33-59.

Harbitz, C.B., Parker, G., Elverhøi, A., Marr, J.G., Mohrig, D., Harff, P.A., 2003. Hydroplaning of subaqueous

debris flows and glide blocks: Analytical solutions and discussion. Journal of Geophysical Research: Solid Earth 108(B7).

Hühnerbach, V., Masson, D.G., 2004.Landslides in the North Atlantic and its adjacent seas: an analysis of their morphology, setting and behaviour. Marine Geology 213, 343-362.

Hunt, J.E., Wynn, R.B., Talling, P.J., Masson, D.G., 2013a. Frequency and timing of landslide-triggered turbidity currents within the Agadir Basin, offshore NW Africa: Are there associations with climate change, sea level change and slope sedimentation rates? Marine Geology 346, 274-291.

Hunt, J.E., Wynn, R.B., Talling, P.J., Masson, D.G., 2013b. Turbidite record of frequency and source of large volume (>100 km3) Canary Island landslides in the last 1.5 Ma: Implications for landslide triggers and geohazards. Geochemistry, Geophysics, Geosystems 14, 2100-2123.

Krastel, S., Behmann, J.-H., Völker, D., Stipp, M., Berndt, C., Urgeles, R., Chaytor, J., Huhn, K., Strasser, M., Harbitz, C.B., 2014. Submarine mass movements and their consequences. 6th International Symposium. Advances in Natural and Technological Research 37, pp 683.

Krastel, S., Wynn, R.B., Georgiopoulou, A., Geersen, J., Henrich, R., Meyer, M., Schwenk, T., 2012. Large-Scale Mass Wasting on the Northwest African Continental Margin: Some General Implications for Mass Wasting on Passive Continental Margins. 189-199.

Krastel, S., Wynn, R.B., Feldens, P., Schürer, A., Böttner, C., Stevenson, C., Cartigny, M.J.B., Hühnerbach, V., Unverricht, D., 2016. Flow Behaviour of a Giant Landslide and Debris Flow Entering Agadir Canyon, NW Africa, in: Lamarche, G., Mountjoy, J., Bull, S., Hubble, T., Krastel, S., Lane, E., Micallef, A., Moscardelli, L., Mueller, C., Pecher, I., Woelz, S. (Eds.), Submarine Mass Movements and their Consequences: 7th International Symposium. Springer International Publishing, Cham, pp. 145-154.

Kuhlmann, H., Freudenthal, T., Helmke, P., Meggers, H., 2004.Reconstruction of paleoceanography off NW Africa during the last 40,000 years: influence of local and regional factors on sediment accumulation. Marine Geology 207, 209-224.

Li, W., Alves, T.M., Urlaub, M., Georgiopoulou, A., Klaucke, I., Wynn, R.B., Gross, F., Meyer, M., Repschläger, J., Berndt, C., Krastel, S., Morphology, age and sediment dynamics of the upper headwall of the Sahara Slide Complex, Northwest Africa: Evidence for a large Late Holocene failure. Marine Geology, in press.

Masson, D.G., 1994. Late Quaternary turbidity current pathways to the Madeira Abyssal Plain and some constraints on turbidity current mechanisms. Basin Research 6, 17-33.

Masson, D.G., Harbitz, C.B., Wynn, R.B., Pedersen, G., Løvholt, F., 2006. Submarine landslides: processes, triggers and hazard prediction. Philosophical Transactions of the Royal Society A: Mathematical, Physical and Engineering Sciences 364, 2009-2039.

Ochoa, J., Wolak, J., Gardner, M.H., 2013. Recognition criteria for distinguishing between hemipelagic and pelagic mudrocks in the characterization of deep-water reservoir heterogeneity. AAPG Bulletin 97, 1785-1803.

Owen, M., Day, S., Long, D., Maslin, M., 2010. Investigations on the Peach 4 Debrite, a Late Pleistocene Mass Movement on the Northwest British Continental Margin, in: Mosher, D.C., Shipp, R.C., Moscardelli, L., Chaytor, J.D., Baxter, C.D.P., Lee, H.J., Urgeles, R. (Eds.), Submarine Mass Movements and Their Consequences. Springer Netherlands, Dordrecht, pp. 301-311.

Piper, D.J.W., Cochonat, P., Morrison, M.L., 1999. The sequence of events around the epicentre of the 1929 Grand Banks earthquake: initiation of debris flows and turbidity current inferred from sidescan sonar. Sedimentology 46, 79-97.

Piper, D.J.W., Pirmez, C., Manley, P.L., Long, D., Food, R.D., Normark, W.R., Showers, W., 1997. Mass-transport deposits of the Amazon Fan. In: Flood, R.D., Piper, D.J.W., Klaus, A., Peterson, L.C. (Eds.), Proceedings of the Ocean Drilling Program, Scientific Results, Vol. 155, pp. 109-146.

Rothwell, R.G., Pearce, T.J., Weaver, P.P.E., 1992. Late Quaternary evolution of the Madeira Abyssal Plain, Canary Basin, NE Atlantic. Basin Research 4, 103-131.

Sawyer, D.E., Flemings, P.B., Dugan, B., Germaine, J.T., 2009. Retrogressive failures recorded in mass transport deposits in the Ursa Basin, Northern Gulf of Mexico. Journal of Geophysical Research 114.

Seibold, E., 1982, The northwest African continental margin-An introduction, in U. Von Rad, K. Hinz, M. Sarnthein, and E. Seibold, eds., Geology of the northwest African continental margin: Berlin, Springer-Verlag, p. 215–269.

Smith, W.H.F., Wessel, P., 1990. Gridding with continuous curvature splines in tension. Geophysics 55, 293-305.

Stevenson, C.J., Talling, P.J., Sumner, E.J., Masson, D.G., Frenz, M., Wynn, R.B., 2014. On how thin submarine flows transported large volumes of sand for hundreds of kilometres across a flat basin plain without eroding the sea floor. Sedimentology 61, 1982-2019.

Sun, Q., Alves, T., Xie, X., He, J., Li, W., Ni, X., 2017. Free gas accumulations in basal shear zones of mass-transport deposits (Pearl River Mouth Basin, South China Sea): An important geohazard on continental slope basins. Marine and Petroleum Geology 81, 17-32.

Talling, P.J., Amy, L.A., Wynn, R.B., 2007a. New insight into the evolution of large-volume turbidity currents: comparison of turbidite shape and previous modelling results. Sedimentology 54, 737-769.

Talling, P.J., Wynn, R.B., Masson, D.G., Frenz, M., Cronin, B.T., Schiebel, R., Akhmetzhanov, A.M., Dallmeier-Tiessen, S., Benetti, S., Weaver, P.P., Georgiopoulou, A., Zuhlsdorff, C., Amy, L.A., 2007b. Onset of submarine debris flow deposition far from original giant landslide. Nature 450, 541-544.

Tappin, D.R., Grilli, S.T., Harris, J.C., Geller, R.J., Masterlark, T., Kirby, J.T., Shi, F., Ma, G., Thingbaijam, K.K.S., Mai, P.M., 2014. Did a submarine landslide contribute to the 2011 Tohoku tsunami? Marine Geology 357, 344-361.

Thomson, J., Weaver, P.P.E., 1994. An AMS radiocarbon method to determine the emplacement time of recent deep-sea turbidites. Sedimentary Geology 89, 1-7.

Trofimovs, J., Sparks, R.S.J., Talling, P.J., 2008. Anatomy of a submarine pyroclastic flow and associated turbidity current: July 2003 dome collapse, Soufrière Hills volcano, Montserrat, West Indies. Sedimentology 55, 617-634.

Vanneste, M., Mienert, J., Bunz, S., 2006. The Hinlopen Slide: A giant, submarine slope failure on the northern Svalbard margin, Arctic Ocean. Earth and Planetary Science Letters 245, 373-388.

Wefer, G. and cruise participants, 1997.Report and preliminary results of METEOR-Cruise M37/1, Lisbon-Las Palmas, 4.12.-23.12.1996. Berichte aus dem Fachbereich Geowissenschaften der Universität Bremen, 090. Department of Geosciences, Bremen University.

Wynn, R.B., Masson, D.G., Stow, D.A.v., Weaver, P.P.e., 2000. The Northwest African slope apron: a modern analogue for deep-water systems with complex seafloor topography. Marine and Petroleum Geology 17, 253-265.

Wien, K., Kölling, M., Schulz, H.D., 2007.Age models for the Cape Blanc Debris Flow and the Mauritania Slide Complex in the Atlantic Ocean off NW Africa. Quaternary Science Reviews 26, 2558-2573.

Wynn, R.B., Weaver, P.P.E., Masson, D.G., Stow, D.A.V., 2002. Turbidite depositional architecture across three interconnected deep-water basins on the north-west African margin. Sedimentology 49, 669-695.

5 Final conclusions and future perspectives

5.1 Conclusions

Newly acquired multibeam bathymetry, 2D seismic-acoustic data and gravity cores acquired during Cruises P395 and MSM32 allowed a detailed investigation of deep-water sedimentary systems and processes on the Northwest Africa continental margin. The main conclusions of this thesis are:

(1) Morphology, age and sediment dynamics of the upper headwall of the Sahara Slide Complex

The Sahara Slide Complex is a giant submarine landslide on the Northwest African continental margin with an affected area of 48,000 km^2. It has two major headwall scarps, namely lower and upper headwall scarps, each up to 100 m high. The upper headwall area is located at water depths between 1800 and 2100 m and it opens towards the northwest. The upper headwall area has an affected area of at least 1700 km^2 and volume calculation reveals that 150 km^3 of sediments were mobilized. The upper headwall area was almost evacuated; numerous morphological features can be identified on the modern seafloor, such as slide scarps, glide planes, plateaus, lobes and slide blocks. Three glide planes are widespread in the headwall area and have been observed approximately 100 m, 50 m and 20 m below the seafloor. These glide planes are interpreted as weak layers, which is considered as one of the most important preconditioning factors for the formation of the slope failures in the upper headwall area. The slide events in the upper headwall area mainly occurred in two different modes retrogressively: translational sliding and spreading. Dating of gravity cores reveals an age of ~2 ka BP of the failure, which is a time of a stable sea-level high stand. The young age is an important contribution to the ongoing debate on potential relationships between sea-level and landslide frequency, as it shows that very large landslide do occur during times of a stable sea level high stand. The large volume and young age of the slide events in the upper headwall area and the presence of crown cracks in the upslope unfailed strata calls for a reassessment of slope instabilities during times of a stable sea level along the margin offshore Northwest Africa and other passive continental margins. Such an assessment needs to include better estimates of the tsunamigenic potential of observed and potential future slope failures.

136

(2) Origin, evolution and paleoceanographic implications of giant buried sediment mounds on the Western Saharan margin (NW Africa).

Newly acquired seismic data allowed the discovery of three giant sediment mounds buried beneath the upper headwall area of Sahara Slide Complex on the Western Sahara margin off NW Africa. These large-scale sediment mounds show lengths from 25 to 37 km and widths from 10 to 15 km. They strike in a SE-NW direction perpendicular to the continental margin. Sediment waves are widespread within the sediment mounds, revealing the importance of bottom currents for the formation of the mounds. The flanks of the sediment mounds were quite unstable and recurrent slope failures occurred, leading to the formation of numerous slide scarps on their flanks. A seismic stratigraphy in the study area was established in order to constrain the formation processes of these sediment mounds. The sediment mounds began to develop in the Middle Eocene on an unconformity (H1) and halted at the Middle-Late Miocene boundary (H4). They mainly developed in three stages: a) initial growth stage during the Middle Eocene, b) main growth stage during the Early Miocene and, c) maintenance stage during Middle Miocene. The formation of these sediment mounds was controlled by the combined effects of turbidity currents and contour currents. The sediment that forms the sediment mounds mainly originated from the fine-grained components of turbidity currents flowing on the continental slope through submarine canyons; contour currents were responsible for the redistribution ofthe fine-grained sediment on the mounds. The sediment mounds are promising records for the initiation,intensification,and evolution of bottom currentsalong the Western Saharan margin and detailed investigation of their development processes could improve our understanding of the sedimentary evolution of the Western Saharan margin. The sediment mounds halted to develop at the Middle/Late Miocene boundary, indicating a major paleoceanographic change that occurred at this time.Since Late Miocene a new depositional pattern was established along the NW Africa margin.

(3) Morphology, age model, evolution and implications of a newly discovered submarine slide (Agadir Slide) on the Moroccan margin offshore NW Africa.

The Agadir Slide is a mega-slide on the Moroccan continental margin offshore NW Africa. It affected an area of 5500 km^2 and displaced 340 km^3 of sediments. High-resolution bathymetry data reveal that the morphology of the Agadir Slide is very complex. The Agadir Slide can be divided into four parts: two headwall areas, the Western slide fairway and the Central slide fairway. Salt structures on the seafloor may have played a vital role for the transport dynamics and

sediment-dispersal patterns of the Agadir Slide. Volume estimations show that the volume of the accumulated slide deposits is twice as large as the volume evacuated from the source areas of the Agadir Slide. This discrepancy is mainly caused by the highly erosional behavior of the Agadir Slide along its basal shear surfaces and sidewalls. Detailed investigations of the seismic data illustrate the presence of two basal shear surfaces at different stratigraphic depth. The Agadir Slide occurred at ~142 ka. It was emplaced retrogressively in two main phases. Local seismicity and fault activity related to halokinesis played an important role for the formation and triggering of the Agadir Slide. The age model and internal character of the Agadir Slide indicate that the Agadir Slide did not contribute to the sedimentary succession of the Moroccan Turbidite System. The Agadir Slide entered the Agadir Canyons but did not transform in a turbidity current. This suggests that the source area of the siliciclastic turbidites of the Moroccan Turbidite Systemis located in the upper reaches of the Agadir Canyon.

(4) General implications of the deep-water sedimentary processes on the continental margin offshore NW Africa

The deep-water sedimentary processes affecting the continental margin offshore NW Africa includes gravity-driven, downslope processes (submarine landslides and turbidity currents) and along-slope processes (bottom currents). They are of great importance for the construction and erosion of the NW African continental margin, which may become a hot region for hydrocarbon exploration in the future. This thesis improved the understanding of the deep-water sedimentary process on the NW African margin by investigating the Sahara Slide, giant sediment mounds beneath the Sahara Slide, and the Agadir Slide. The internal architecture of the headwall area of the Sahara Slide and the Agadir Slide illustrate that the widespread occurrence of weak layers is one of the most important preconditioning factors for the submarine landslides on the NW Africa margin. Weak layers have reduced shear strength and play a vital role in the initiation of submarine landslides. The formation processes of the giant sediment mounds imply that the interaction of downslope and along-slope sedimentary processes is a widespread phenomenon on the NW African margin and other deep-water margin settings worldwide. The NW African margin has been affected by along-slope processes at least since the Middle Eocene. The deposition of thick and widespread contourites is important for hydrocarbon exploration as contourites usually include large volume sand bodies, which may act as reservoir rock. In addition, contourites are prone to slope failure and increase the risk of slope instabilities. The resulting submarine landslides and turbidity currents are potentially hazardous for hydrocarbon production, seafloor infrastructures and coastal communities.

It is interesting to note that the upper headwall area of the Sahara Slide Complex is exactly located in the area of the giant sediment mounds. However, it remains unclear if the sediment mounds have played a vital role in controlling the location of the upper headwall area of the Sahara Slide Complex.

5.2 Outlook

This PhD thesis provides a detailed investigation of the upper headwall area of the Sahara Slide Complex, the giant sediment mounds buried beneath the upper headwall and the Agadir Slide. The results contribute to a better understanding of the deep-water sedimentary processes (downslope and alongslope processes) along the northwest African continental margin. However, there are still several scientific questions to be addressed in future work.

In **Chapter 2**, we use two gravity cores to constrain the ages of the slide events in the upper headwall area of the Sahara Slide Complex and the results reveal a young (~2 ka) age. However, the chronology of the slide events in the upper headwall area could not be reconstructed due to the distribution of gravity cores. In future, it would be advisable to acquire more cores in this area in order to build a compressive age model for the slide events in the upper headwall and better understanding of the sediment dynamics. It would be critical that these cores include undisturbed surface sediments due to the young age of the Sahara Slide. Surface sediments may be lost during gravity coring. Hence Multicorer and/or Giant Box Corer need to complement gravity coring. Furthermore, the three glide planes (weak layers) were not penetrated by the gravity cores in the upslope undeformed area and the composition of the weak layers remain unknown. Future acquisition of longer sediment cores penetrating the weak layers would allow us to investigate the geotechnical properties of weak layers and thus improve our knowledge on the preconditioning factors for the slide events in the upper headwall area.

In **Chapter 3**, we discovered three giant sediment mounds on the Western Saharan margin, which were formed in the framework of the Central Atlantic paleoceanographic evolution. However, the extent of this mound is still not known and more sediment mounds may exist further to the north or south of the study area. A more regional set of seismic profiles would help to gain better insights into the evolution and controlling factors of these sediment mounds. Additional work should also be focused on the potential relationship between the locations of the headwall area of Sahara Slide Complex and the giant sediment mounds, as the crests of these sediment mounds are corresponding to the sidewall scarps in the upper headwall area.

In **Chapter 4**, we have established the age model for the Agadir Slide and excluded the possibility that the Agadir Slide is one source of the turbidite beds recorded in the Moroccan Turbidite System. Therefore, the source area of the turbidites in the Moroccan Turbidite Systems remains unclear. The most likely source area for the turbidites is the upper reach of the Agadir Canyon, which is not fully surveyed yet. A targeted survey of the head region of the canyon with hydroacoustics and coring would be the preferred approach for identifying the source area of the

turbidites. The factors controlling flow dynamics and flow transformation of sedimentary gravity flows is still poorly understood. It remains unclear why some landslides fully disintegrate while others not. The Agadir Canyon may be a key region for addressing this question.

6 Acknowledgement

7 Curriculum Vitae

Wei Li

Date of Birth: April 17th, 1987

Place of Birth: Zibo, Shandong, P.R. China

Address: Olshausenstr. 73, Room 4410, 24118 Kiel

Email: li@geophysik.uni-kiel.de

Education

Since 2014.10

> PhD student in University of Kiel, Germany
> Supervisors: Prof. Sebastian Krastel, Prof. Christian Berndt and Dr. Tiago Alves, Dr. Morelia Urlaub

Since 2013.9-2014.9

> PhD student in University of Bremen, Germany
> Supervisors: Prof. Achim Kopf and Dr. David Voelker

2010.9-2013.7

> Master in Science, Marine Geology and Geophysics, Institute of Oceanology, Chinese Academy of Sciences, Qingdao, China
> Supervisors: Prof. Xiujuan Wang and Prof. Shiguo Wu.

2006.9-2010.6

> Bachelor of Geo-exploration and Information Technology, Ocean University of China, Qingdao, China.